

# University of Cincinnati

Date: 10/27/2017

**I, Nathan A Eberhardt, hereby submit this original work as part of the requirements for the degree of Doctor of Philosophy in Chemistry.**

It is entitled:

**Synthesis and Reactivity of Nickel POCOP Pincer Complexes for the Reduction of Carbon Dioxide and Related Compounds**

Student's name: **Nathan A Eberhardt**

This work and its defense approved by:

Committee chair: Hairong Guan, Ph.D.

Committee member: William Connick, Ph.D.

Committee member: Allan Pinhas, Ph.D.



27952

**Synthesis and Reactivity of Nickel POCOP Pincer Complexes for  
the Reduction of Carbon Dioxide and Related Compounds**

A dissertation submitted to the Graduate School  
of the University of Cincinnati in partial fulfillment of the  
requirements for the degree of

**Doctor of Philosophy (Ph.D.)**

In the Department of Chemistry  
of McMicken College of Arts and Sciences by

Nathan Andrew Eberhardt

Bachelor of Arts (B.A.), Chemistry  
Transylvania University, Lexington, KY 2012

Committee Chair: Hairong Guan, Ph.D.

# **Synthesis and Reactivity of Nickel POCOP Pincer Complexes for the Reduction of Carbon Dioxide and Related Compounds**

## **Abstract**

The development of new catalysts for the reduction of carbon dioxide is of utmost importance to both limit the harmful greenhouse gas as well as to provide usable C1 feedstock chemicals. One method to reduce this CO<sub>2</sub> is through the use of a metal hydride complex. Of these metal complexes, nickel POCOP pincer hydride complexes have been highly successful at catalyzing the reduction of carbonyl functionalities. Although these catalysts are effective at catalyzing this reduction, there are few processes to make these hydrides. Additionally, not much is known about which factors will improve catalytic reduction or what other reactions they can catalyze.

Nickel chloride complexes bearing POCOP pincer ligands were easily synthesized using a microwave reactor. Through this methodology nickel POCOP pincer chloride complexes can be made in as little as 5 minutes in very high purities and yields. Nickel complexes with <sup>i</sup>Pr, <sup>o</sup>Pe, Cy, Ph, and <sup>t</sup>Bu substituents on the phosphorous atoms can all be synthesized using this method. Additionally, palladium chloride complexes bearing isopropyl substituted POCOP ligands can be made. This method was also found to greatly limit the solvent needed to make these complexes.

Alternative routes to synthesize nickel hydride complexes is an important problem due to the harsh methods used to synthesize them. To explore an additional method for hydride synthesis, nickel fluoride complexes bearing POCOP pincer ligands were synthesized. These complexes can be easily converted to hydride complexes using silanes or boranes.

The factors that influence a metal hydrides ability to reduce CO<sub>2</sub> were investigated. To determine which factors had an impact on the reduction of CO<sub>2</sub> to formate complex, a series of nickel hydride and formate complexes were synthesized. The complexes were tested to determine the relative thermodynamic favorability for the reduction of CO<sub>2</sub> to formate. Complexes bearing more electron donating ligands were found to be better at reducing CO<sub>2</sub> to formate. Additionally, complexes with more sterically accessible nickel centers were found to be far better at reducing CO<sub>2</sub>. Also, nickel was found to be better than palladium for this reduction.

Nickel hydride complexes were also found catalyze the oxidative esterification of aldehydes and alcohols. The process was found to be very efficient at this process with a number of alcohols and aldehydes. The mechanism proceeds through a reduction of an aldehyde to form an alkoxide complex followed by an exchange with an alcohol. The nickel alkoxide then reacts with an additional aldehyde to form a hemiacetal complex. Beta hydride elimination then forms the ester product. Alternative entry into the catalytic cycle using benchtop stable nickel chloride complex and nucleophilic base was achieved. Water, oxidation, and protonation of nickel hydride were identified as deactivation pathways. The products of deactivation were independently synthesized.



## Preface

Parts of this thesis have been adapted from articles co-written by the author. The following articles were reproduced in part with permission from the American Chemical Society and Elsevier

1) Eberhardt, N. A.; Guan, H. Reduction of CO<sub>2</sub> Mediated or Catalyzed by Pincer Complexes. In *The Chemistry of Pincer Compounds*; 2nd ed.; Morales-Morales, D., Ed.; Elsevier, Amsterdam, **2018**; Chapter 4.

2) Eberhardt, N. A.; Guan, H. "Nickel Hydride Complexes." *Chemical Reviews* **2016**, *116*, 8373-8426.

3) Li H.; Meng, W.; Adhikary, A.; Li, S.; Ma, N. Zhao, Q.; Yang, Q.; Eberhardt, N. A.; Leahy, K. M.; Krause, J. A.; Zhang, J.; Chen, X.; Guan, H. "Metathesis Reactivity of Bis(phosphinite) Pincer Ligated Nickel Chloride, Isothiocyanate and Azide Complexes." *Journal of Organometallic Chemistry*, **2016**, *804*, 132-141.

## Acknowledgements

I would like to thank the University of Cincinnati for providing me the opportunity to undergo my Ph. D. studies and for providing me the opportunity to work for Dr. Hairong Guan. I would especially like to thank Hairong for taking me in and teaching me how to be a better scientist. Hairong has relentlessly worked to help me improve my scientific knowledge, thought process, and especially my organization. I am sincerely grateful for everything he has provided for me.

I would also like to thank the faculty members who have worked with me over the years. My committee members Dr. Allan Pinhas and Dr. Bill Connick have been very helpful in getting me to where I am today. They constantly give great feedback and always have great suggestions for my research and thought process. Dr. Jeanette Krause has both taught me crystallography and solved most of my crystal structures. I have enjoyed all of my conversations with them and would not be here without them.

I would also like to thank all of my group members for the support and help they have provided me. My former group members Dr. Sumit Chakraborty, Dr. Sanjeewa Rodrigo, Dr. Papri Bhattacharya, Dr. Anubendu Adhikary, Dr. Gleason Wilson, Dr. Arundhoti Chakraborty, Dr. Aaron Bailey, and Dr. Nadeesha Wellala have all provided guidance for my research. I would especially like to thank Gleason and Sanjeewa for all of their help. Sanjeewa first taught me about the lab and helped me to learn new techniques. When my projects changed, Gleason taught me everything I needed to know about how to make organometallic nickel complexes. I also would like to thank Gleason for being a great friend.

I would like to thank my current group members Yingze Li, Huiguang Dai, Becca Haley, Joel Collett, Dewmi Ekanayake, Evan Lydon, and Conghui Yue. I would like to thank them for all of their support as well as for putting up with all of my group meeting questions. I have truly enjoyed my time working with all of these people in the lab and for that I am grateful.

I would like to thank my family and friends. My parents Bill and Karen Eberhardt, and my brothers and sister Henry, Adam, and Adelle have provided constant love and support. I also need to thank my wife Celine. She has been so supportive of me and has helped me so much during this process.



## **CHAPTER 1**

---

<b>INTRODUCTION</b>	<b>1</b>
<b>1.1 CATALYTIC CO<sub>2</sub> REDUCTION USING NICKEL Pincer COMPLEXES</b>	<b>2</b>
<b>1.2 CATALYTIC ALDEHYDE REDUCTION USING NICKEL HYDRIDE COMPLEXES</b>	<b>10</b>
<b>1.3 RESEARCH OBJECTIVES</b>	<b>14</b>
<b>1.4 REFERENCES CITED</b>	<b>17</b>

## **CHAPTER 2**

---

<b><u>SYNTHESIS OF POCOP NICKEL CHLORIDE COMPLEXES USING A MICROWAVE REACTOR</u></b>	<b>21</b>
<b>2.1 INTRODUCTION</b>	<b>22</b>
<b>2.2 ONE-POT SYNTHESIS OF NICKEL POCOP COMPLEXES USING A MICROWAVE REACTOR</b>	<b>25</b>
<b>2.3 EXPERIMENTAL SECTION</b>	<b>31</b>
<b>2.4 REFERENCES CITED</b>	<b>32</b>

## **CHAPTER 3**

---

<b><u>NICKEL POCOP Pincer FLUORIDE COMPLEXES AS PRECURSORS FOR THE SYNTHESIS OF NICKEL HYDRIDE COMPLEXES</u></b>	<b>34</b>
<b>3.1 INTRODUCTION</b>	<b>35</b>
<b>3.2 SYNTHESIS OF NICKEL FLUORIDE COMPLEXES</b>	<b>37</b>
<b>3.3 REACTIONS OF NICKEL FLUORIDE COMPLEXES WITH BORANES AND SILANES AS A MEANS TO GENERATE NICKEL HYDRIDE COMPLEXES</b>	<b>40</b>
<b>3.4 CONCLUSIONS</b>	<b>42</b>
<b>3.5 EXPERIMENTAL SECTION</b>	<b>42</b>
<b>3.6 REFERENCES CITED</b>	<b>44</b>

## **CHAPTER 4**

---

<b><u>RELATIVE THERMODYNAMIC FAVORABILITY OF CO<sub>2</sub> REDUCTION BY NICKEL HYDRIDE COMPLEXES</u></b>	<b>46</b>
<b>4.1 INTRODUCTION</b>	<b>47</b>
<b>4.2 SYNTHESIS OF <sup>t</sup>BuPOCOP NICKEL Pincer HYDRIDE AND FORMATE COMPLEXES BEARING DIFFERENT PARA-SUBSTITUENTS</b>	<b>50</b>
<b>4.3 EFFECTS OF PARA-SUBSTITUENTS ON THE RELATIVE THERMODYNAMICS FOR THE REDUCTION OF CO<sub>2</sub> BY POCOP NICKEL Pincer HYDRIDE COMPLEXES</b>	<b>63</b>

<b>4.4 EFFECTS OF P-SUBSTITUENTS ON THE RELATIVE THERMODYNAMICS FOR THE REDUCTION OF CO<sub>2</sub> BY POCOP NICKEL Pincer HYDRIDE COMPLEXES</b>	<b>66</b>
<b>4.5 COMPARISON OF NICKEL AND PALLADIUM COMPLEXES</b>	<b>69</b>
<b>4.6 CONCLUSIONS</b>	<b>70</b>
<b>4.7 EXPERIMENTAL SECTION</b>	<b>70</b>
<b>4.8 REFERENCES CITED</b>	<b>78</b>

## **CHAPTER 5**

---

### **OXIDATIVE ESTERIFICATION OF ALDEHYDES WITH ALCOHOLS CATALYZED BY A POCOP Pincer HYDRIDE COMPLEX**

---

<b>5.1 INTRODUCTION</b>	<b>81</b>
<b>5.2 OPTIMIZATION OF CATALYTIC OXIDATIVE ESTERIFICATION OF BENZALDEHYDE WITH SHORT-CHAIN ALCOHOLS</b>	<b>83</b>
<b>5.3 REACTION PROFILE AND MECHANISTIC ELUCIDATION</b>	<b>86</b>
<b>5.4 SUBSTRATE SCOPE</b>	<b>89</b>
<b>5.5 AN ALTERNATIVE WAY TO ENTER INTO THE CATALYTIC CYCLE USING NICKEL CHLORIDE COMPLEXES</b>	<b>92</b>
<b>5.6 STUDIES OF CATALYST DECOMPOSITION PATHWAYS</b>	<b>94</b>
<b>5.7 CONCLUSIONS</b>	<b>98</b>
<b>5.8 EXPERIMENTAL SECTION</b>	<b>98</b>
<b>5.9 REFERENCES CITED</b>	<b>100</b>



# Synthesis and Reactivity of Nickel POCOP Pincer Complexes for the Reduction of Carbon Dioxide and Related Compounds

## List of Figures

### Chapter 1: Introduction

Figure 1.1. General framework of pincer complexes 3

Figure 1.2 Nickel-based catalysts for the hydrosilylation of aldehydes and ketones 11

### Chapter 2: Synthesis of POCOP Nickel Chloride Complexes Using a Microwave Reactor

Figure 2.1 ORTEP drawing of  $[2,6-(\text{Cy}_2\text{PO})_2\text{C}_6\text{H}_3]\text{NiCl}$  27

### Chapter 3: Nickel POCOP Pincer Fluoride Complexes as Precursors for the Synthesis of Nickel Hydride Complexes

Figure 3.1. ORTEP drawing of  $[2,6-(^t\text{Bu}_2\text{PO})_2\text{C}_6\text{H}_3]\text{NiF}$  39

Figure 3.2. ORTEP drawing of  $[2,6-(\text{Ph}_2\text{PO})_2\text{C}_6\text{H}_3]\text{NiF}$  40

### Chapter 4: Relative Thermodynamic Favorability of CO<sub>2</sub> Reduction by Nickel Hydride Complexes

Figure 4.1 ORTEP drawing of  $[2,6-(^t\text{Bu}_2\text{PO})_2\text{C}_6\text{H}_2\text{NMe}_2]\text{NiCl}$  53

Figure 4.2 ORTEP drawing of  $[2,6-(^t\text{Bu}_2\text{PO})_2\text{C}_6\text{H}_2\text{F}]\text{NiCl}$  54

Figure 4.3 ORTEP drawing of  $[2,6-(^t\text{Bu}_2\text{PO})_2\text{C}_6\text{H}_2\text{NMe}_2]\text{NiH}$  56

Figure 4.4 ORTEP drawing of  $[2,6-(^t\text{Bu}_2\text{PO})_2\text{C}_6\text{H}_2\text{F}]\text{NiOCOH}$  58

Figure 4.5 ORTEP drawing of  $[2,6-(^t\text{Bu}_2\text{PO})_2\text{C}_6\text{H}_2\text{OMe}]\text{NiOCOH}$  59

Figure 4.6 ORTEP drawing of  $[2,6-(^t\text{Bu}_2\text{PO})_2\text{C}_6\text{H}_2\text{NMe}_2]\text{NiOCOH}$  60

Figure 4.7 ORTEP drawing of  $[2,6-(^t\text{Bu}_2\text{PO})_2\text{C}_6\text{H}_2\text{NMe}_2]\text{NiOCOH}$  62

Figure 4.8 ORTEP drawing of [ $\{2,6\text{-}(\text{tBu}_2\text{PO})_2\text{C}_6\text{H}_2\text{COOMe}\}\text{Ni}(\text{H}_2\text{O})\text{]OTf}\cdot\text{H}_2\text{O}$  76

**Chapter 5: Oxidative Esterification of Aldehydes with Alcohols Catalyzed by a POCOP  
Pincer Hydride Complex**

Figure 5.1. Reaction profile for the oxidative esterification of benzaldehyde and ethanol 87

# Synthesis and Reactivity of Nickel POCOP Pincer Complexes for the Reduction of Carbon Dioxide and Related Compounds

## List of Tables

### **Chapter 2: Synthesis of POCOP Nickel Chloride Complexes Using a Microwave Reactor**

Table 2.1 Synthesis of POCOP Nickel Chloride Complexes 26

Table 2.2 Solvents used in microwave reactions 30

### **Chapter 4: Relative Thermodynamic Favorability of CO<sub>2</sub> Reduction by Nickel Hydride Complexes**

Table 4.1 Relative thermodynamic measurements of POCOP complexes 65

### **Chapter 5: Oxidative Esterification of Aldehydes with Alcohols Catalyzed by a POCOP Pincer Hydride Complex**

Table 5.1. Optimization of the oxidative esterification of benzaldehyde 85

Table 5.2. Oxidative esterification of benzaldehyde and alcohols catalyzed by complex **2** 89

Table 5.3. Oxidative esterification of various *para*-substituted benzaldehydes with methanol 90

Table 5.4 Oxidative esterification of various *para*-substituted benzaldehydes with methanol stopped at 1 h 91

Table 5.5 Oxidative esterification of benzaldehyde and alcohols using pre-catalyst (**4**) 94

Table 5.6. Catalyst deactivation through the addition of common substrate impurities 97



# **Chapter 1**

## **Introduction**



## 1.1 Catalytic CO<sub>2</sub> Reduction Using Nickel Pincer Complexes

The utilization of renewable feedstocks for chemical synthesis is one of the most important challenges that face chemists today. While much effort has been devoted to advancing the technology of converting bio-based feedstocks to chemicals, developing strategies to convert CO<sub>2</sub> to chemicals has also been a recent research focus. Not only is CO<sub>2</sub> renewable but also accumulating in the atmosphere due to the fact that the emission outpaces the sequestration. From the economic point of view, CO<sub>2</sub> is an inexpensive C1 feedstock, making it very attractive for the production of chemicals and fuels.<sup>1</sup> For CO<sub>2</sub> to be converted to value-added chemicals including energy storage materials, a reduction process is often required. It has been long known that Grignard reagents and reactive metal hydrides reduce CO<sub>2</sub> stoichiometrically; however, making these reagents requires significantly high input of energy. Much research has thus been conducted in the development of catalysts that can promote the reduction of CO<sub>2</sub> with milder reducing agents such as boranes,<sup>2</sup> silanes,<sup>2b</sup> dihydrogen,<sup>3</sup> and electrons,<sup>4</sup> or with photons.<sup>5</sup>

Pincer complexes have provided a new avenue for catalytic reduction of CO<sub>2</sub> to useful chemicals and fuels. Pincer ligands are defined as tridentate monoanionic ligands that can bind to a metal in a coplanar fashion (Figure 1.1). Because of the relatively high rigidity and modularity of the pincer scaffold, many of these complexes have exhibited unique reactivity that is unavailable in non-pincer systems.<sup>6</sup> Pincer complexes of iridium, platinum, rhenium, tungsten, ruthenium, rhodium, palladium, molybdenum, iron, cobalt, and nickel have been known to reduce CO<sub>2</sub>. Nickel is one of the more desirable metal sources due to its low cost relative to the analogous second and third row transition metals.<sup>7</sup>

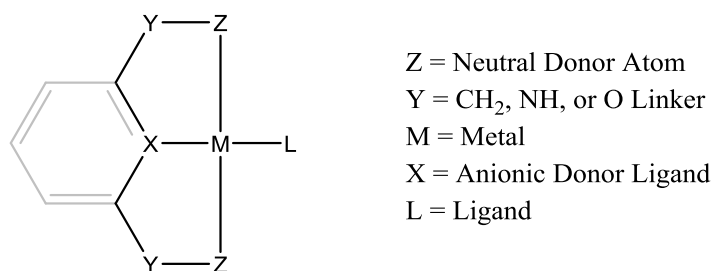
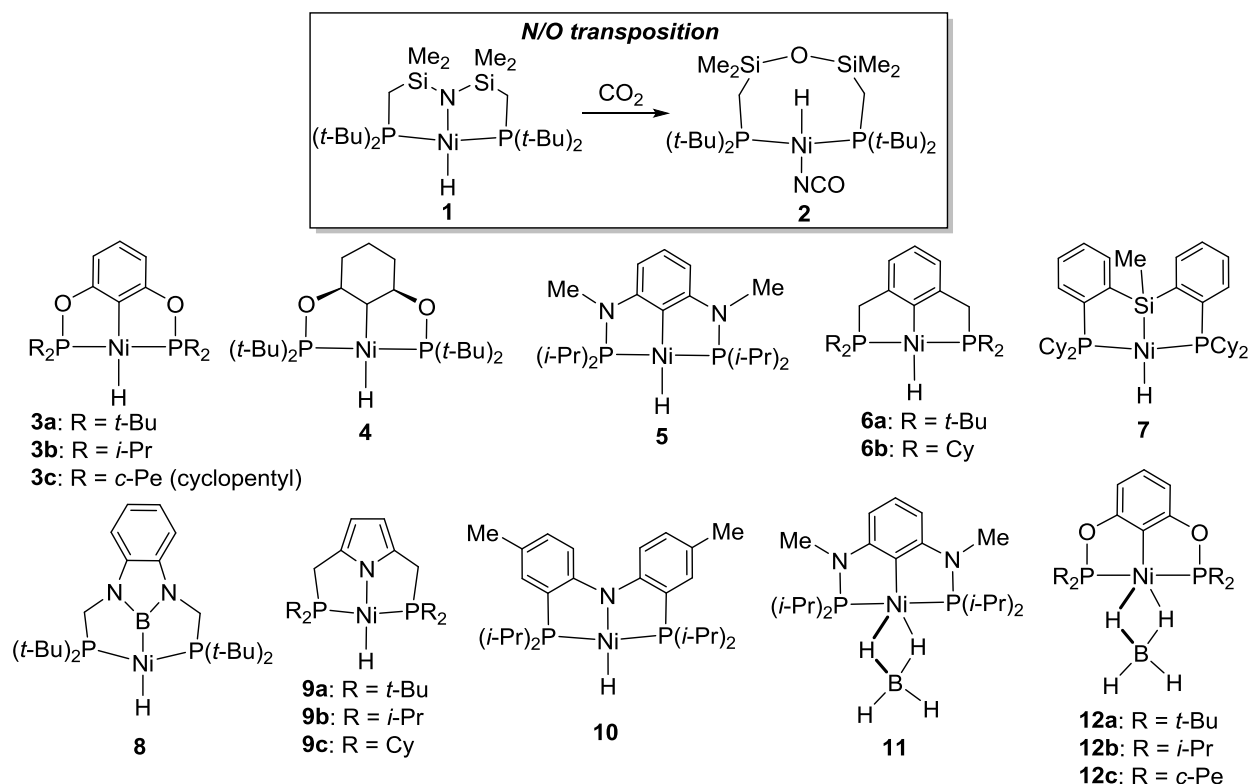


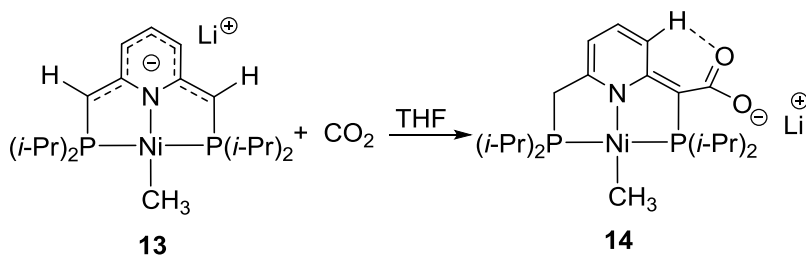
**Figure 1.1.** General framework of pincer complexes

A wide variety of nickel pincer hydride complexes have been studied for the reduction of CO<sub>2</sub> (Scheme 1.1).<sup>8</sup> Nickel formate complexes are typically isolated as the reduction products except in the case of the PNP pincer complex **1**, which gives rise to a hydrido-nickel cyanate complex via N/O atom transposition.<sup>9</sup> DFT calculations suggest that the rate of CO<sub>2</sub> insertion into the Ni–H bond is highly dependent on the *trans* effect of the donor group situated opposite to the hydride.<sup>10</sup> Consistent with the *trans*-influence argument, those containing POCOP,<sup>11</sup> PNCNP,<sup>12</sup> PCP,<sup>10,13</sup> PSiP,<sup>10</sup> and PBP pincer ligands<sup>14</sup> all react with CO<sub>2</sub> (1 atm) rapidly at room temperature. In contrast, nickel hydrides bearing a less *trans*-influencing central donor such as nitrogen (i.e., complexes **9a-c** and **10**) undergo CO<sub>2</sub> insertion sluggishly.<sup>15</sup> In particular, the reaction of **9a** with CO<sub>2</sub> requires heating at 80 °C and 5 bar of CO<sub>2</sub> pressure.<sup>15c</sup> The borohydride complexes **11** and **12a** also react with CO<sub>2</sub> to give the corresponding formate complexes.<sup>12,16</sup> Compared to **3a**, the reaction of **12a** with CO<sub>2</sub> is substantially slower due to the need to dissociate BH<sub>3</sub> first. The less sterically hindered complexes **12b** and **12c** are more reluctant to release BH<sub>3</sub>, showing little reactivity toward CO<sub>2</sub> even heated at 60 °C for 48 h.<sup>16</sup>



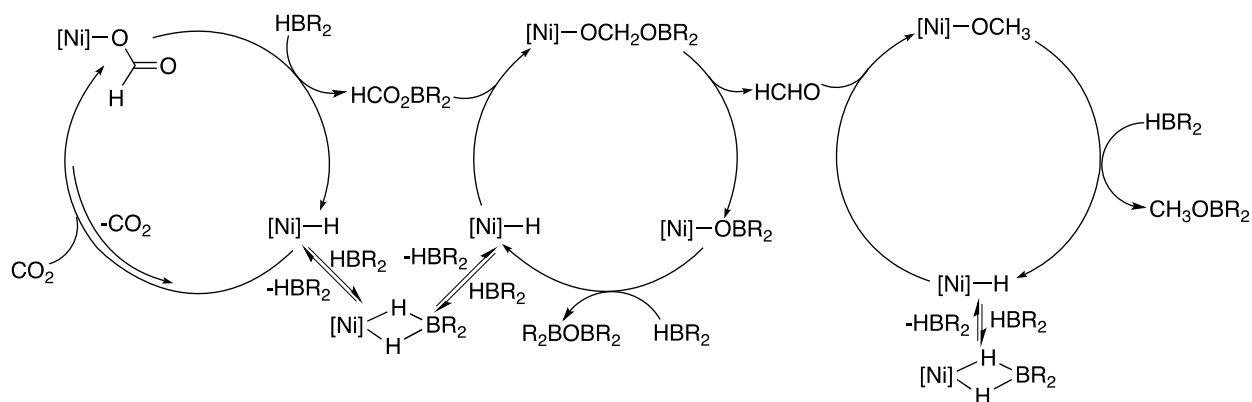
**Scheme 1.1** Nickel pincer hydride complexes studied for the reduction of CO<sub>2</sub>

In addition to nickel hydrides, nickel methyl and allyl complexes, especially those supported by a PCP or POCOP pincer ligand, can also undergo CO<sub>2</sub> insertion to give nickel carboxylate complexes, a process that formally reduces CO<sub>2</sub>. With the same pincer ligand, the kinetic barrier for CO<sub>2</sub> insertion is the lowest for the hydride complexes followed by the allyl complexes,<sup>13</sup> which is analogous to the palladium system.<sup>17</sup> The methyl complexes are the slowest to react, often requiring elevated temperatures and extended reaction times.<sup>11c,13</sup> A very unusual case involving a doubly deprotonated PNP pincer ligand (i.e., complex **13**) shows that CO<sub>2</sub> does not insert into the nickel methyl bond but adds to its pincer arm to form a carboxylate **14** (Scheme 1.2).<sup>18</sup> Unlike the ruthenium systems, nickel pincer complexes bearing a singly deprotonated PNP pincer ligand does not react with CO<sub>2</sub> at all.



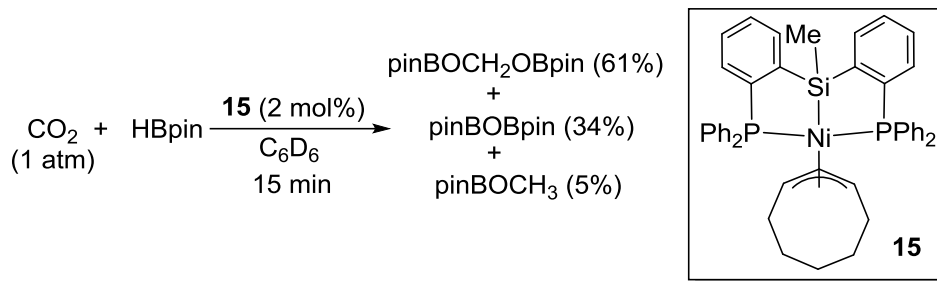
**Scheme 1.2** Reaction of an anionic nickel methyl complex with CO<sub>2</sub>

Some of the nickel hydrides illustrated in Scheme 1.1 have been investigated as catalysts for the reduction of CO<sub>2</sub> with boranes. For example, in the presence of catecholborane (HBcat), the POCOP pincer complex **3a** promotes the conversion of CO<sub>2</sub> to CH<sub>3</sub>OBcat along with catBOBcat. The catalytic system is efficient at room temperature under 1 atm of CO<sub>2</sub> pressure, providing CH<sub>3</sub>OBcat with a TON of 495 (based on B–H bond) in 1 h.<sup>11a</sup> The reaction proceeds via three consecutive catalytic cycles that reduce CO<sub>2</sub> sequentially to HCO<sub>2</sub>Bcat, HCHO, and CH<sub>3</sub>OBcat (Scheme 1.3). Each catalytic cycle features the insertion of a C=O bond into the nickel hydride followed by the regeneration of the hydride. DFT calculations suggest that the insertion of HCO<sub>2</sub>Bcat crosses the highest kinetic barrier in the entire process.<sup>19</sup> Further studies show that the less bulky hydrides **3b** and **3c** are less active catalysts, mainly due to their higher tendency to be trapped by the borane to form the off-cycle dihydridoborate complexes.<sup>16</sup> Additionally, the *tert*-butyl groups in **3a** provide a better protection of the P–O bonds against the attack by the borane, which is the deactivation pathway for the catalysts.



**Scheme 1.3** Catalytic cycles for nickel-catalyzed reduction of CO<sub>2</sub> with boranes

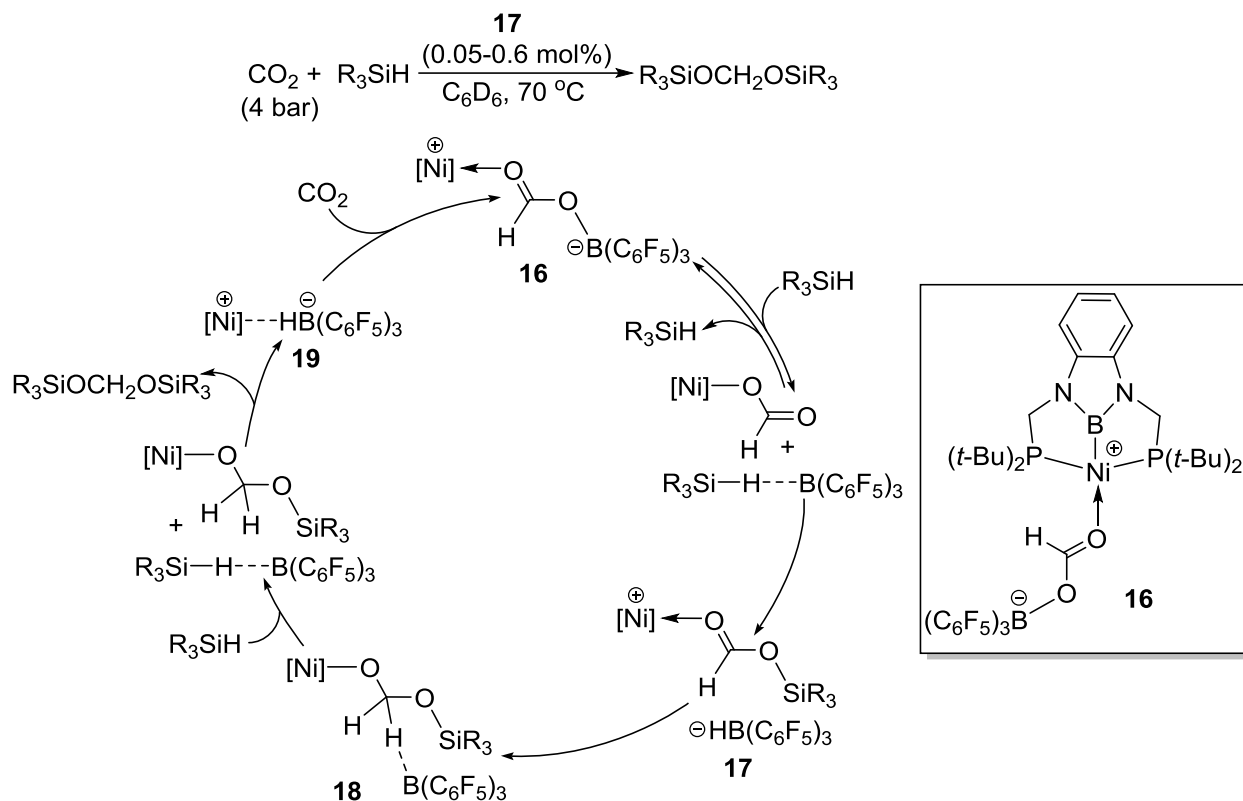
The choices of boranes and pincer ligands are critical to the efficiency and selectivity for the catalytic reaction. Replacing HBcat with BH<sub>3</sub> traps the hydrides **3a-c** as borohydride complexes **12a-c**, which are catalytically inactive.<sup>16</sup> Using **3a** as the catalyst, 9-borabicyclo[3.3.1]nonane (9-BBN) follows the similar reaction pattern as HBcat whereas HBpin only reduces CO<sub>2</sub> to HCO<sub>2</sub>Bpin, suggesting that it stops after the first catalytic cycle in Scheme 1.3.<sup>11b</sup> When changing the POCOP pincer hydride complexes to a PSiP  $\eta^3$ -cyclooctenyl complex **15**, HBpin can reduce CO<sub>2</sub> further to pinBOCH<sub>2</sub>OBpin, pinBOBpin, and pinBOCH<sub>3</sub> in as short as 15 min (Scheme 1.4).<sup>20</sup> Extending the reaction time to 12 h gives a mixture of pinBOBpin (85%), pinBOCH<sub>3</sub> (13%), HCHO, and some unidentified products. The reduction is presumably initiated by the elimination of 1,3-cyclooctadiene from **15** to generate a nickel hydride species, which may enter into catalytic cycles analogous to those shown in Scheme 1.3. The same reaction catalyzed by a palladium pincer hydride generates HCO<sub>2</sub>Bpin selectively, highlighting the roles that both the metal and the pincer ligand play on the selectivity of the process.



**Scheme 1.4** Reduction of CO<sub>2</sub> with HBpin catalyzed by a PSiP nickel pincer complex

The oxophilic and electrophilic nature of boranes is the key to their ability to reduce CO<sub>2</sub> in the presence of a nickel catalyst. While silicon is oxophilic too, most silanes are not nearly as electrophilic as boranes. Thus, it is not too surprising that silanes such as PhSiH<sub>3</sub> do not react with POCOP nickel pincer formate complexes as needed to turn over the catalytic cycle.<sup>11b</sup> Similarly, Et<sub>3</sub>SiH shows no reactivity towards the nickel formate complex derived from the PBP pincer hydride **8**.<sup>21</sup> However, at 70 °C in the presence of B(C<sub>6</sub>F<sub>5</sub>)<sub>3</sub>, reduction of the nickel formate complex with Et<sub>3</sub>SiH takes place, giving Et<sub>3</sub>SiOCH<sub>2</sub>OSiEt<sub>3</sub> as the reduced product. Similar to the PSiP palladium and platinum pincer systems,<sup>22</sup> B(C<sub>6</sub>F<sub>5</sub>)<sub>3</sub> reacts with the nickel formate complex to generate a formatoborate complex **16**, which can be employed directly as a catalyst for the reduction of CO<sub>2</sub> with Et<sub>3</sub>SiH (Scheme 1.5). The catalytic reaction operates at 70 °C under 4 bar of H<sub>2</sub> pressure, providing Et<sub>3</sub>SiOCH<sub>2</sub>OSiEt<sub>3</sub> with TONs and TOFs up to 1200 and 55.8 h<sup>-1</sup>, respectively. Other silanes such as Ph<sub>2</sub>MeSiH and PhMe<sub>2</sub>SiH can be used as well, although in the latter case methyl silyl ether (8%) and methane (14%) are also observed as the reduction products. Given that B(C<sub>6</sub>F<sub>5</sub>)<sub>3</sub>-catalyzed cleavage of C–O bonds with silanes is a well-established process,<sup>23</sup> the selectivity for R<sub>3</sub>SiOCH<sub>2</sub>OSiR<sub>3</sub> observed by this catalytic system is particularly notable. The proposed mechanism (Scheme 1.5), as supported experimentally and computationally,<sup>24</sup> involves abstraction of B(C<sub>6</sub>F<sub>5</sub>)<sub>3</sub> from **16** by the silane to yield [R<sub>3</sub>Si–H···B(C<sub>6</sub>F<sub>5</sub>)<sub>3</sub>], which delivers R<sub>3</sub>Si<sup>+</sup>

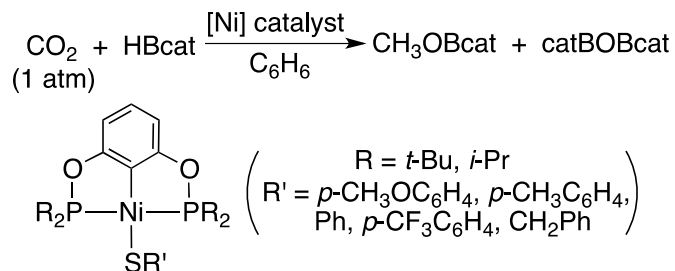
and  $\text{H}^-$  in a stepwise fashion to the nickel formate to give **18**. Activation of the second silane by  $\text{B}(\text{C}_6\text{F}_5)_3$  followed by  $\text{R}_3\text{Si}^+$  transfer releases the bis(silyl)acetal product while generating complex **19** to close the catalytic cycle through its reaction with  $\text{CO}_2$ . During the catalytic process,  $\text{B}(\text{C}_6\text{F}_5)_3$  is likely to be trapped in nickel complexes **16**, **18**, and **19**, preventing it from reducing  $\text{R}_3\text{SiOCH}_2\text{OSiR}_3$  further to  $\text{CH}_3\text{OSiR}_3$  and  $\text{CH}_4$ .



**Scheme 1.5** Reduction of  $\text{CO}_2$  with silanes catalyzed by a nickel formatoborate complex

Nickel thiolate complexes supported by a POCOP pincer ligand are remarkable catalysts for the reduction of  $\text{CO}_2$  to a methanol derivative using HBcat as the reducing agent (Scheme 1.6).<sup>25</sup> This catalytic system is more efficient than the analogous palladium thiolate system<sup>26</sup> as well as the nickel hydride system.<sup>11a</sup> Among the ten catalysts tested, the most active one bears isopropyl groups on the phosphorus donors and the  $p\text{-CH}_3\text{OC}_6\text{H}_4$  group on the sulfur, which gives

a TOF of 2400 h<sup>-1</sup> at room temperature. Although some of these thiolate complexes do react with HBcat to form the nickel hydrides species, under the catalytic conditions a number of other nickel complexes produced are likely to be more active than the hydrides. Furthermore, in contrast to the hydride system, the *tert*-butyl-substituted pincer complexes are less effective catalysts than their isopropyl derivatives.



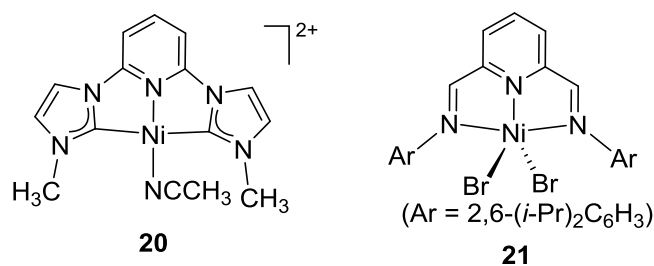
**Scheme 1.6** Reduction of CO<sub>2</sub> with HBcat catalyzed by nickel thiolate complexes

Despite the facile CO<sub>2</sub> insertion observed with many nickel pincer hydride complexes, catalytic hydrogenation of CO<sub>2</sub> with these hydrides or related complexes has not been accomplished to date. The closest example to this process is the hydrogenation of sodium bicarbonate to formate catalyzed by the PCP pincer hydride **6a**.<sup>27</sup> A TON of 3038 over 20 h is obtained when the hydrogenation reaction is carried out at 150 °C under 55 bar of H<sub>2</sub> pressure. This hydride also catalyzes the reverse process, decomposition of formic acid to H<sub>2</sub> and CO<sub>2</sub> under basic conditions.

Several nickel pincer complexes have been studied as catalysts for electrochemical reduction of CO<sub>2</sub> (Scheme 1.7). In comparison to the cyclic voltammogram obtained under N<sub>2</sub>, the bis(carbene)-based pincer complex **20** under CO<sub>2</sub> displays a substantial enhancement of the cathodic current.<sup>28</sup> Analyzing the gaseous products from controlled potential electrolysis of **20** in CO<sub>2</sub>-saturated CH<sub>3</sub>CN solution confirms CO as the main product with no detectable amount of H<sub>2</sub>.



The high selectivity for CO over H<sub>2</sub> is preserved even in the presence of water. The bis(aldimino)pyridine-based pincer complex **21** also shows current enhancement when CO<sub>2</sub> is introduced.<sup>29</sup> However, analysis of the products suggests that CO is generated with a low Faradaic efficiency (<3%). In this case, the main product is H<sub>2</sub> with a 89% Faradaic yield.



**Scheme 1.7** Nickel pincer complexes studied as electrocatalysts for CO<sub>2</sub> reduction

## 1.2 Catalytic Aldehyde Reduction Using Nickel Hydride Complexes

Catalytic reductions of aldehydes are of interest as both models for the reduction of CO<sub>2</sub> and as a means to produce alcohols. Nickel-catalyzed hydrosilylation of aldehydes and ketones has received a great deal of attention in recent years. Many of these catalytic systems employ nickel hydrides directly as the catalysts while others use catalyst precursors that are converted to nickel hydrides under the catalytic conditions (Figure 1.2). The dinickel complex  $\{(\text{PN}^{\text{iPr}_3})\text{Ni}(\mu\text{-Br})\}_2$  (**22**), when mixed with 2 equiv of KO<sup>t</sup>Bu, is an excellent catalyst for the hydrosilylation of aldehydes with Et<sub>3</sub>SiH.<sup>30</sup> At 100 °C, aldehydes bearing different functional groups including F, Cl, and Me<sub>2</sub>N are reduced to their silyl ethers with TONs up to 50 and TOFs up to 287 h<sup>-1</sup>. The TONs are lower (25-35) for the hydrosilylation of bulky aldehydes such as 2,6-dimethylbenzaldehyde or ketones such as cyclohexanone and benzophenone. According to the NMR studies, complex **22** reacts with KO<sup>t</sup>Bu and Et<sub>3</sub>SiH to form  $\{(\text{PN}^{\text{iPr}_3})\text{Ni}(\mu\text{-H})\}_2$ , which is likely to dissociate into monomeric (PN<sup>iPr<sub>3</sub></sup>)NiH. Insertion of aldehydes into the 3-coordinate

nickel hydride leads to nickel alkoxide complexes, which undergo metathesis reaction with  $\text{Et}_3\text{SiH}$  to release the silyl ether products and regenerate  $(\text{PN}^{\text{iPr}_3})\text{NiH}$ . Aldehydes such as 3-thiophenecarboxaldehyde and 2-pyridinecarboxaldehyde are not viable substrates for this catalytic system. Presumably, the heterocyclic rings could coordinate to the nickel center and prevent carbonyl insertion.

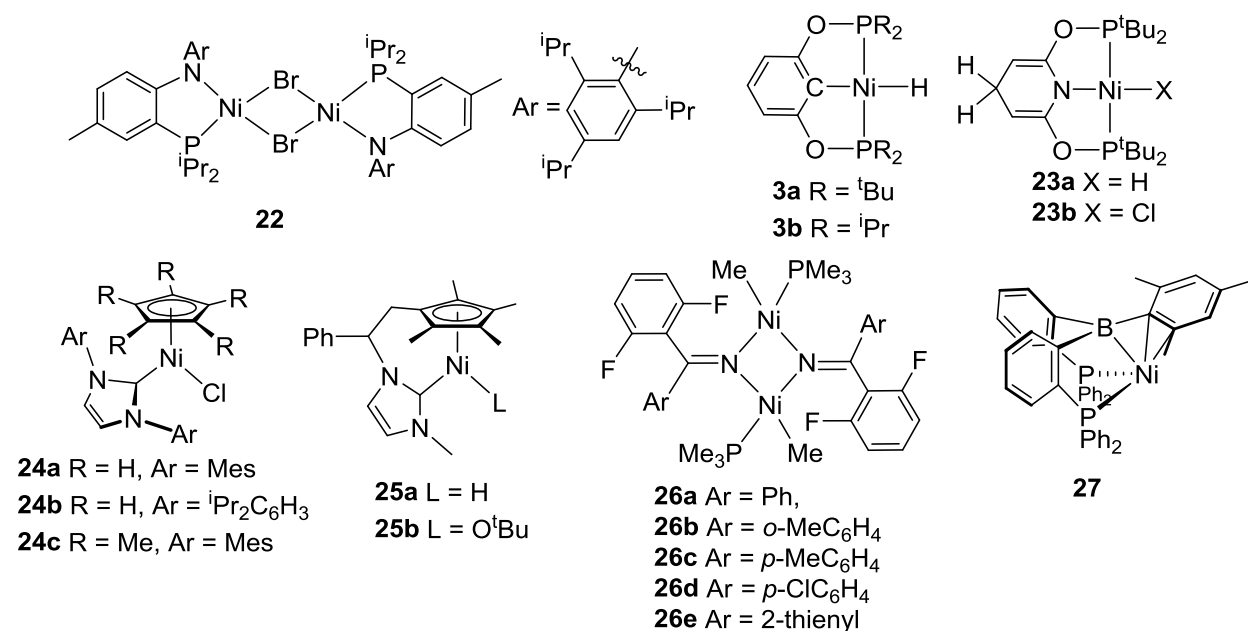


**Figure 1.2** Nickel-based catalysts for the hydrosilylation of aldehydes and ketones

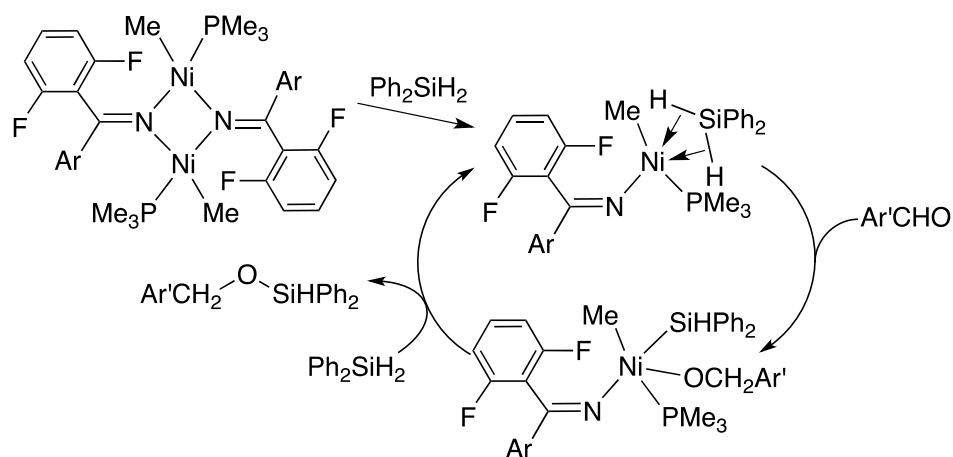
The bis(phosphinite)-based nickel hydride **3b** is a more active hydrosilylation catalyst. With a catalyst loading as low as 0.2 mol%, a variety of aldehydes including those with pyridine and thiophene rings can be reduced by  $\text{PhSiH}_3$  or  $\text{Ph}_2\text{SiH}_2$  at room temperature (TONs up to 500).<sup>31</sup> As with the  $\{(\text{PN}^{\text{iPr}_3})\text{Ni}(\mu\text{-Br})\}_2$  system, ketones such as cyclohexanone, acetophenone, and benzophenone are less reactive, giving TONs of 6-60 at 70 °C. Replacing the isopropyl groups of the catalyst with *tert*-butyl groups (**3a**) results in a less active catalyst, which is attributed to more

sluggish insertion of aldehydes. The reaction mechanism is consisted of two steps: carbonyl insertion and metathesis with silanes. Each step has been verified by NMR experiments. Other nickel pincer hydrides have been explored for catalytic hydrosilylation of aldehydes. The reduction of PhCHO with PhSiH<sub>3</sub> is catalyzed by 8.3 mol% of (<sup>t</sup>BuP<sup>O</sup>N<sup>O</sup>P<sup>t</sup>Bu-H)NiH (**23a**) at room temperature.<sup>32</sup> The chloride complex (<sup>t</sup>BuP<sup>O</sup>N<sup>O</sup>P<sup>t</sup>Bu-H)NiCl (**23b**) shows some catalytic activity; however, the time needed to fully convert PhCHO is much longer (2 d vs. 10 h). A stoichiometric reaction between complex **23a** and PhCHO surprisingly gives no insertion product but PhCH(OH)COPh as a result of benzoin condensation.

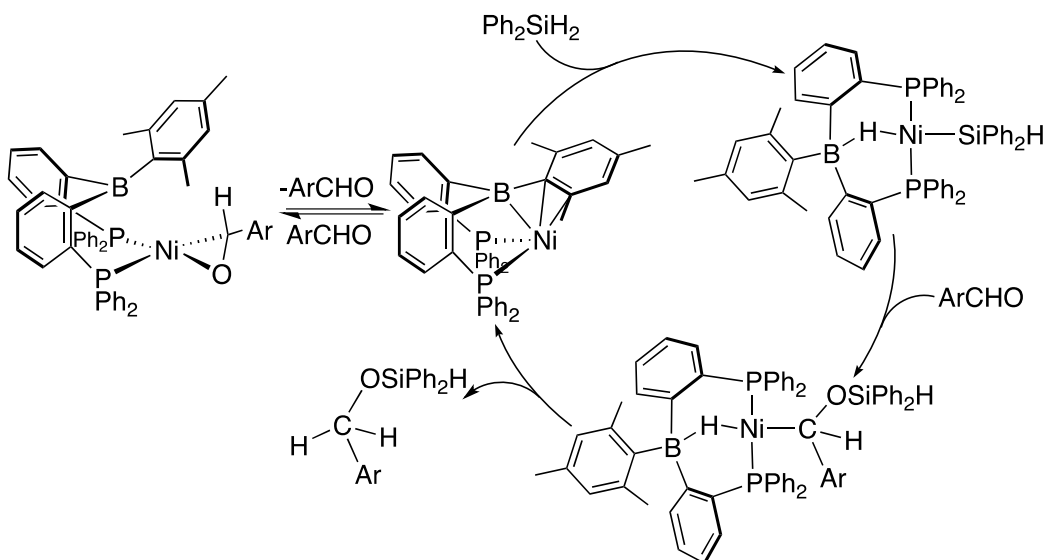
Several half-sandwich nickel complexes have been studied as hydrosilylation catalysts. For the reduction of PhCHO with Ph<sub>2</sub>SiH<sub>2</sub>, CpNi(IMes)Cl (**24a**) (5 mol%) is effective at 70 °C, resulting in >97% conversion of the substrates in 22 h.<sup>33</sup> The catalytic performance is significantly enhanced with the addition of NaEt<sub>3</sub>BH, which is shown to convert CpNi(IMes)Cl to CpNi(IMes)H. Using the *in-situ* generated nickel hydride, the catalyst loading can be reduced to 0.5 mol%, the reaction time can be shortened to 1 h, and the temperature can be lowered to 25 °C. Compared to complex **24a**, catalytic activities of Cp\*Ni(IMes)H (**24c**) and CpNi(IPr)H (**24b**) are lower. With 1 mol% of CpNi(IMes)H, a wide range of aldehydes (except those with OH and Br groups) are reduced to the corresponding alcohols in high yields following basic hydrolysis of the silyl ether products. Furthermore, in the presence of 5 mol% of **24a**, various ketones are readily reduced by Ph<sub>2</sub>SiH<sub>2</sub> at 25 °C. The mechanism for this catalytic system is not well understood. The nickel hydride does not react with PhCHO or Ph<sub>2</sub>SiH<sub>2</sub>. In contrast, a closely related system using an NHC ligand tethered to the cyclopentadienyl ring shows insertion of aldehydes into (Cp\*-NHC)NiH (**25a**).<sup>34</sup> However, mixing PhCHO, Ph<sub>2</sub>SiD<sub>2</sub>, and (Cp\*-NHC)NiH in 1 : 1 : 1 ratio gives PhCHD–OSiDPh<sub>2</sub> with no deuterium incorporated into the nickel hydride, suggesting that the

hydride is a spectator ligand. For convenience, the *tert*-butoxide complex (Cp\*-NHC)NiO<sup>t</sup>Bu (**25b**) is used as the catalyst for the hydrosilylation reactions as it is readily converted to **25a** by the silane. The hydrosilylation of aldehydes with PhSiH<sub>3</sub> is typically completed within 5 min with 1 mol% of **25a**. The hydrosilylation of ketones, however, require a higher temperature (100 °C) and longer reaction time (2-24 h).

Hydrosilylation of aldehydes catalyzed by {(Me<sub>3</sub>P)(Me)Ni( $\mu$ -imine)}<sub>2</sub> (**26**) and (<sup>Mes</sup>DPB<sup>Ph</sup>)Ni (**27**) appears to follow a mechanism without the involvement of a terminal hydride. The reaction of **26** with Ph<sub>2</sub>SiH<sub>2</sub> gives a mononuclear species with the silane  $\sigma$ -bonded to nickel (Scheme 1.8).<sup>35</sup> Insertion of aldehydes into the Si–H bond and reductive elimination of the silyl ethers complete the catalytic cycle. Among the dinickel complexes screened, the one with an *ortho*-methyl substituted phenyl group (**26b**) shows the best activity. With a 0.6 mol% catalyst loading at 45 °C, hydrosilylation of aldehydes with Ph<sub>2</sub>SiH<sub>2</sub> is complete within 7 h. Functional groups such as F, Cl, MeO, furyl and C=C bond are tolerated under the catalytic conditions. Complex **27** reacts with Ph<sub>2</sub>SiH<sub>2</sub> and PhCHO individually to give (<sup>Mes</sup>DPB<sup>Ph</sup>-H)Ni(SiPh<sub>2</sub>H) and (<sup>Mes</sup>DPB<sup>Ph</sup>)Ni( $\eta^2$ -PhCHO), respectively.<sup>14b</sup> Monitoring the catalytic reaction, however, reveals a new species that is more consistent with a siloxyalkyl complex. Thus, hydrosilylation of aldehydes catalyzed by **27** is more likely to proceed via a mechanism featuring insertion of aldehydes into the Ni–Si bond (Scheme 1.9). With 5 mol% of **27** at room temperature, hydrosilylation of benzaldehyde derivatives with Ph<sub>2</sub>SiH<sub>2</sub> is complete within one hour or a few days, depending on the substituents on the benzene ring. The reaction is faster for those bearing an electron-donating group such as Me<sub>2</sub>N, MeO, and Me.



**Scheme 1.8** Mechanism for the hydrosilylation of aldehydes catalyzed by  $\{(\text{Me}_3\text{P})(\text{Me})\text{Ni}(\mu\text{-imine})\}_2$  (**26**)



**Scheme 1.9** Mechanism for the hydrosilylation of aldehydes catalyzed by  $(^{\text{Mes}}\text{DPB}^{\text{Ph}})\text{Ni}$  (**27**)

### 1.3 Research Objectives

The study of nickel hydride complexes for the reduction of  $\text{CO}_2$  to formates and the related compounds is of great interest to the organometallic chemistry community. The previous success with nickel hydride complexes for reduction processes has led to increased interest in the development of new catalysts as well as the development of improved synthetic methods to access

these complexes. This dissertation will first focus on new methods of synthesizing both nickel chloride and fluoride complexes that can serve as precursors to nickel hydride complexes. New nickel hydride and formate complexes will subsequently be discussed, especially in the context of CO<sub>2</sub> reduction for a better understanding of structure-reactivity relationships. Also discussed will be the oxidative esterification of aldehydes with alcohols, a catalytic process further highlighting the broad range of reactivity that these complexes have.

The current method of choice to synthesize nickel pincer chloride complexes involves the reaction of the isolated pincer ligand with nickel chloride salts performed under high temperatures for long periods of time. This process requires large amounts of solvent as well as lengthy workup procedures in order to obtain pure products. One alternative approach to the traditional method is through the use of a microwave reactor. Microwave reactors have been known to provide more even heating at high temperatures (often beyond the boiling point of the solvent used) as well as to shorten the reaction time. In Chapter 2, a new method for the synthesis of POCOP nickel pincer chloride complexes will be discussed. Our study shows that nickel pincer chloride complexes can be synthesized in microwave reactors in short periods of time and using much less solvent. This research can potentially be extended to other metal systems as a more efficient way to prepare POCOP pincer and related complexes.

New avenues for the synthesis of nickel hydride complexes are of synthetic interest. Many existing methods use highly reactive reagents such as LiAlH<sub>4</sub> or LiHBET<sub>3</sub> (super hydride). Other methods start from air sensitive starting materials such as Ni(COD)<sub>2</sub> (COD = 1,5-cyclooctadiene). A less explored method for the synthesis of nickel hydrides is through the reaction of nickel fluoride complexes with silanes or boranes. In Chapter 3, a brief story of our endeavor into the synthesis and isolation of nickel fluoride complexes will be discussed. Nickel fluoride complexes

were synthesized and readily converted to the corresponding nickel hydride complexes; however, these nickel fluoride complexes were found to be too sensitive to be fully characterized. Nonetheless, X-ray crystallographic and NMR spectral studies of these nickel fluoride complexes support their formation, although the crystal structures often display decomposition products along with the desired fluoride complexes.

The reduction of CO<sub>2</sub> to formate, as previously discussed, is an important process for energy storage and the manufacturing of value-added chemicals. Many nickel hydride complexes have been known to perform this reaction; however, there are limited studies on what factors make this process more favorable. Experimental studies have been limited to the observation (or the lack of observation) of complexes reducing CO<sub>2</sub> with no quantitative data on both kinetics and thermodynamics of these processes. In Chapter 4, the synthesis of a series of nickel hydride complexes and their reactivity towards CO<sub>2</sub> reduction will be discussed. A variety of nickel POCOP pincer complexes were compared for a better understanding of what factors affect the thermodynamic preference for the reduction of CO<sub>2</sub>. Also compared in this study were nickel hydride complexes supported by other type pincer ligands as well as the analogous palladium POCOP pincer complexes.

Nickel hydride complexes bearing a POCOP pincer ligand have been known to catalyze a number of reactions. Among these reactions are catalytic hydroboration of CO<sub>2</sub>, hydrosilylation of aldehydes and ketones, and cyanomethylation of aldehydes. The catalytic reduction of carbonyl functionalities by this series of complexes is diverse and efficient. In Chapter 5, the oxidative esterification of aldehydes with alcohols catalyzed by nickel hydride complexes will be discussed. The reduction of an aldehyde is paired with the oxidation of another aldehyde in a formally disproportionation process. After optimization of the reaction conditions, various hetero-esters

can be synthesized through this method. Additionally, catalyst deactivation pathways were identified, which will provide guidelines for the future improvement of the catalytic reaction.

#### 1.4 References Cited

- (a) Arakawa, H.; Aresta, M.; Armor, J. N.; Barteau, M. A.; Beckman, E. J.; Bell, A. T.; Bercaw, J. E.; Creutz, C.; Dinjus, E.; Dixon, D. A.; Domen, K.; DuBois, D. L.; Eckert, J.; Fujita, E.; Gibson, D. H.; Goddard, W. A.; Goodman, D. W.; Keller, J.; Kubas, G. J.; Kung, H. H.; Lyons, J. E.; Manzer, L. E.; Marks, T. J.; Morokuma, K.; Nicholas, K. M.; Periana, R.; Que, L.; Rostrup-Nielson, J.; Sachtler, W. M. H.; Schmidt, L. D.; Sen, A.; Somorjai, G. A.; Stair, P. C.; Stults, B. R.; Tumas, W., Catalysis Research of Relevance to Carbon Management: Progress, Challenges, and Opportunities. *Chemical Reviews* **2001**, *101* (4), 953-996; (b) Aresta, M.; Dibenedetto, A., Utilisation of CO<sub>2</sub> as a Chemical Feedstock: Opportunities and Challenges. *Dalton Transactions* **2007**, (28), 2975-2992; (c) Sakakura, T.; Choi, J.-C.; Yasuda, H., Transformation of Carbon Dioxide. *Chemical Reviews* **2007**, *107* (6), 2365-2387; (d) Appel, A. M.; Bercaw, J. E.; Bocarsly, A. B.; Dobbek, H.; DuBois, D. L.; Dupuis, M.; Ferry, J. G.; Fujita, E.; Hille, R.; Kenis, P. J. A.; Kerfeld, C. A.; Morris, R. H.; Peden, C. H. F.; Portis, A. R.; Ragsdale, S. W.; Rauchfuss, T. B.; Reek, J. N. H.; Seefeldt, L. C.; Thauer, R. K.; Waldrop, G. L., Frontiers, Opportunities, and Challenges in Biochemical and Chemical Catalysis of CO<sub>2</sub> Fixation. *Chemical Reviews* **2013**, *113* (8), 6621-6658; (e) Aresta, M.; Dibenedetto, A.; Angelini, A., Catalysis for the Valorization of Exhaust Carbon: from CO<sub>2</sub> to Chemicals, Materials, and Fuels. Technological Use of CO<sub>2</sub>. *Chemical Reviews* **2014**, *114* (3), 1709-1742.
- (a) Bontemps, S., Boron-Mediated Activation of Carbon Dioxide. *Coordination Chemistry Reviews* **2016**, *308* (Part 2), 117-130; (b) Chauvier, C.; Cantat, T., A Viewpoint on Chemical Reductions of Carbon–Oxygen Bonds in Renewable Feedstocks Including CO<sub>2</sub> and Biomass. *ACS Catalysis* **2017**, *7* (3), 2107-2115.
- (a) Jessop, P. G.; Ikariya, T.; Noyori, R., Homogeneous Hydrogenation of Carbon Dioxide. *Chemical Reviews* **1995**, *95* (2), 259-272; (b) Leitner, W., Carbon Dioxide as a Raw Material: The Synthesis of Formic Acid and Its Derivatives from CO<sub>2</sub>. *Angewandte Chemie International Edition* **1995**, *34* (20), 2207-2221; (c) Wang, W.-H.; Himeda, Y.; Muckerman, J. T.; Manbeck, G. F.; Fujita, E., CO<sub>2</sub> Hydrogenation to Formate and Methanol as an Alternative to Photo- and Electrochemical CO<sub>2</sub> Reduction. *Chemical Reviews* **2015**, *115* (23), 12936-12973.
- (a) Benson, E. E.; Kubiak, C. P.; Sathrum, A. J.; Smieja, J. M., Electrocatalytic and Homogeneous Approaches to Conversion of CO<sub>2</sub> to Liquid Fuels. *Chemical Society Reviews* **2009**, *38* (1), 89-99; (b) Finn, C.; Schnittger, S.; Yellowlees, L. J.; Love, J. B., Molecular Approaches to the Electrochemical Reduction of Carbon Dioxide. *Chemical Communications* **2012**, *48* (10), 1392-1399; (c) Costentin, C.; Robert, M.; Saveant, J.-M., Catalysis of the Electrochemical Reduction of Carbon Dioxide. *Chemical Society Reviews* **2013**, *42* (6), 2423-2436; (d) Qiao, J.; Liu, Y.; Hong, F.; Zhang, J., A Review of Catalysts for the Electroreduction of Carbon Dioxide to Produce Low-Carbon Fuels. *Chemical Society Reviews* **2014**, *43* (2), 631-675; (e) Taheri, A.; Berben, L. A., Making C-H Bonds with CO<sub>2</sub>: Production of Formate by Molecular Electrocatalysts. *Chemical Communications* **2016**, *52* (9), 1768-1777.
- (a) Morris, A. J.; Meyer, G. J.; Fujita, E., Molecular Approaches to the Photocatalytic Reduction of Carbon Dioxide for Solar Fuels. *Accounts of Chemical Research* **2009**, *42* (12), 1983-



- 1994; (b) Roy, S. C.; Varghese, O. K.; Paulose, M.; Grimes, C. A., Toward Solar Fuels: Photocatalytic Conversion of Carbon Dioxide to Hydrocarbons. *ACS Nano* **2010**, *4* (3), 1259-1278.
6. (a) Albrecht, M.; van koten, G., *Platinum Group Organometallics Based on "Pincer" Complexes: Sensors, Switches, and Catalysts*. 2001; Vol. 40, p 3750-3781; (b) van der Boom, M. E.; Milstein, D., Cyclometalated Phosphine-Based Pincer Complexes: Mechanistic Insight in Catalysis, Coordination, and Bond Activation. *Chemical Reviews* **2003**, *103* (5), 1759-1792.
7. Prices taken from <http://www.infomine.com/investment/metal-prices/>
8. Eberhardt, N. A.; Guan, H., Nickel Hydride Complexes. *Chemical Reviews* **2016**, *116* (15), 8373-8426.
9. Laird, M. F.; Pink, M.; Tsvetkov, N. P.; Fan, H.; Caulton, K. G., Unusual Selectivity of a (pincer)Ni-Hydride Reacting with CO<sub>2</sub>. *Dalton Transactions* **2009**, (8), 1283-1285.
10. Suh, H.-W.; Schmeier, T. J.; Hazari, N.; Kemp, R. A.; Takase, M. K., Experimental and Computational Studies of the Reaction of Carbon Dioxide with Pincer-Supported Nickel and Palladium Hydrides. *Organometallics* **2012**, *31* (23), 8225-8236.
11. (a) Chakraborty, S.; Zhang, J.; Krause, J. A.; Guan, H., An Efficient Nickel Catalyst for the Reduction of Carbon Dioxide with a Borane. *Journal of the American Chemical Society* **2010**, *132* (26), 8872-8873; (b) Chakraborty, S.; Patel, Y. J.; Krause, J. A.; Guan, H., Catalytic Properties of Nickel Bis(phosphinite) Pincer Complexes in the Reduction of CO<sub>2</sub> to Methanol Derivatives. *Polyhedron* **2012**, *32* (1), 30-34; (c) Jonasson, K. J.; Wendt, O. F., Synthesis and Characterization of a Family of POCOP Pincer Complexes with Nickel: Reactivity Towards CO<sub>2</sub> and Phenylacetylene. *Chemistry – A European Journal* **2014**, *20* (37), 11894-11902.
12. Murugesan, S.; Stöger, B.; Weil, M.; Veiros, L. F.; Kirchner, K., Synthesis, Structure, and Reactivity of Co(II) and Ni(II) PCP Pincer Borohydride Complexes. *Organometallics* **2015**, *34* (7), 1364-1372.
13. Schmeier, T. J.; Hazari, N.; Incarvito, C. D.; Raskatov, J. A., Exploring the Reactions of CO<sub>2</sub> with PCP Supported Nickel Complexes. *Chemical Communications* **2011**, *47* (6), 1824-1826.
14. (a) Lin, T.-P.; Peters, J. C., Boryl–Metal Bonds Facilitate Cobalt/Nickel-Catalyzed Olefin Hydrogenation. *Journal of the American Chemical Society* **2014**, *136* (39), 13672-13683; (b) MacMillan, S. N.; Hill Harman, W.; Peters, J. C., Facile Si-H Bond Activation and Hydrosilylation Catalysis Mediated by a Nickel-Borane Complex. *Chemical Science* **2014**, *5* (2), 590-597.
15. (a) Venkanna, G. T.; Tammineni, S.; Arman, H. D.; Tonzetich, Z. J., Synthesis, Characterization, and Catalytic Activity of Nickel(II) Alkyl Complexes Supported by Pyrrole–Diphosphine Ligands. *Organometallics* **2013**, *32* (16), 4656-4663; (b) Yoo, C.; Kim, J.; Lee, Y., Synthesis and Reactivity of Nickel(II) Hydroxycarbonyl Species, NiCOOH-κC. *Organometallics* **2013**, *32* (23), 7195-7203; (c) Kreye, M.; Freytag, M.; Jones, P. G.; Williard, P. G.; Bernskoetter, W. H.; Walter, M. D., Homolytic H<sub>2</sub> Cleavage by a Mercury-Bridged Ni(I) Pincer Complex [{(PNP)Ni}<sub>2</sub>{μ-Hg}]. *Chemical Communications* **2015**, *51* (14), 2946-2949.
16. Chakraborty, S.; Zhang, J.; Patel, Y. J.; Krause, J. A.; Guan, H., Pincer-Ligated Nickel Hydridoborate Complexes: the Dormant Species in Catalytic Reduction of Carbon Dioxide with Boranes. *Inorganic Chemistry* **2013**, *52* (1), 37-47.
17. Johnson, M. T.; Johansson, R.; Kondrashov, M. V.; Steyl, G.; Ahlquist, M. S. G.; Roodt, A.; Wendt, O. F., Mechanisms of the CO<sub>2</sub> Insertion into (PCP) Palladium Allyl and Methyl σ-Bonds. A Kinetic and Computational Study. *Organometallics* **2010**, *29* (16), 3521-3529.
18. Vogt, M.; Rivada-Wheelaghan, O.; Iron, M. A.; Leitus, G.; Diskin-Posner, Y.; Shimon, L. J. W.; Ben-David, Y.; Milstein, D., Anionic Nickel(II) Complexes with Doubly Deprotonated PNP Pincer-Type Ligands and Their Reactivity toward CO<sub>2</sub>. *Organometallics* **2013**, *32* (1), 300-308.

19. Huang, F.; Zhang, C.; Jiang, J.; Wang, Z.-X.; Guan, H., How Does the Nickel Pincer Complex Catalyze the Conversion of CO<sub>2</sub> to a Methanol Derivative? A Computational Mechanistic Study. *Inorganic Chemistry* **2011**, *50* (8), 3816-3825.
20. Suh, H.-W.; Guard, L. M.; Hazari, N., Synthesis and Reactivity of a Masked P*Si*P Pincer Supported Nickel Hydride. *Polyhedron* **2014**, *84*, 37-43.
21. Rios, P.; Curado, N.; Lopez-Serrano, J.; Rodriguez, A., Selective Reduction of Carbon Dioxide to Bis(silyl)acetal Catalyzed by a PBP-Supported Nickel Complex. *Chemical Communications* **2016**, *52* (10), 2114-2117.
22. Mitton, S. J.; Turculet, L., Mild Reduction of Carbon Dioxide to Methane with Tertiary Silanes Catalyzed by Platinum and Palladium Silyl Pincer Complexes. *Chemistry – A European Journal* **2012**, *18* (48), 15258-15262.
23. Parks, D. J.; Blackwell, J. M.; Piers, W. E., Studies on the Mechanism of B(C<sub>6</sub>F<sub>5</sub>)<sub>3</sub>-Catalyzed Hydrosilylation of Carbonyl Functions. *The Journal of Organic Chemistry* **2000**, *65* (10), 3090-3098.
24. Ríos, P.; Rodríguez, A.; López-Serrano, J., Mechanistic Studies on the Selective Reduction of CO<sub>2</sub> to the Aldehyde Level by a Bis(phosphino)boryl (PBP)-Supported Nickel Complex. *ACS Catalysis* **2016**, *6* (9), 5715-5723.
25. Liu, T.; Meng, W.; Ma, Q.-Q.; Zhang, J.; Li, H.; Li, S.; Zhao, Q.; Chen, X., Hydroboration of CO<sub>2</sub> Catalyzed by Bis(phosphinite) Pincer Ligated Nickel Thiolate Complexes. *Dalton Transactions* **2017**, *46* (14), 4504-4509.
26. Ma, Q.-Q.; Liu, T.; Li, S.; Zhang, J.; Chen, X.; Guan, H., Highly Efficient Reduction of Carbon Dioxide with a Borane Catalyzed by Bis(phosphinite) Pincer Ligated Palladium Thiolate Complexes. *Chemical Communications* **2016**, *52*(99), 14262-14265
27. Enthaler, S.; Brück, A.; Kammer, A.; Junge, H.; Irran, E.; Güllak, S., Exploring the Reactivity of Nickel Pincer Complexes in the Decomposition of Formic Acid to CO<sub>2</sub>/H<sub>2</sub> and the Hydrogenation of NaHCO<sub>3</sub> to HCOONa. *ChemCatChem* **2015**, *7* (1), 65-69.
28. Sheng, M.; Jiang, N.; Gustafson, S.; You, B.; Ess, D. H.; Sun, Y., A Nickel Complex with a Biscarbene Pincer-Type Ligand Shows High Electrocatalytic Reduction of CO<sub>2</sub> over H<sub>2</sub>O. *Dalton Transactions* **2015**, *44* (37), 16247-16250.
29. Narayanan, R.; McKinnon, M.; Reed, B. R.; Ngo, K. T.; Groysman, S.; Rochford, J., Ambiguous Electrocatalytic CO<sub>2</sub> Reduction Behaviour of a Nickel Bis(aldimino)pyridine Pincer Complex. *Dalton Transactions* **2016**, *45* (39), 15285-15289.
30. Tran, B. L.; Pink, M.; Mendiola, D. J., Catalytic Hydrosilylation of the Carbonyl Functionality via a Transient Nickel Hydride Complex. *Organometallics* **2009**, *28* (7), 2234-2243.
31. Chakraborty, S.; Krause, J. A.; Guan, H., Hydrosilylation of Aldehydes and Ketones Catalyzed by Nickel PCP-Pincer Hydride Complexes. *Organometallics* **2009**, *28* (2), 582-586.
32. Kundu, S.; Brennessel, W. W.; Jones, W. D., Synthesis and Reactivity of New Ni, Pd, and Pt 2,6-Bis(di-*tert*-butylphosphinito)pyridine Pincer Complexes. *Inorganic Chemistry* **2011**, *50* (19), 9443-9453.
33. Bheeter, L. P.; Henrion, M.; Brelot, L.; Darcel, C.; Chetcuti, M. J.; Sortais, J.-B.; Ritleng, V., Hydrosilylation of Aldehydes and Ketones Catalyzed by an *N*-Heterocyclic Carbene-Nickel Hydride Complex under Mild Conditions. *Advanced Synthesis & Catalysis* **2012**, *354* (14-15), 2619-2624.
34. Postigo, L.; Royo, B., *N*-Heterocyclic Carbene Complexes of Nickel as Efficient Catalysts for Hydrosilylation of Carbonyl Derivatives. *Advanced Synthesis & Catalysis* **2012**, *354* (14-15), 2613-2618.

35. Wang, L.; Sun, H.; Li, X., Imine Nitrogen Bridged Binuclear Nickel Complexes via N–H Bond Activation: Synthesis, Characterization, Unexpected C,N-Coupling Reaction, and Their Catalytic Application in Hydrosilylation of Aldehydes. *Organometallics* **2015**, *34* (20), 5175-5182.

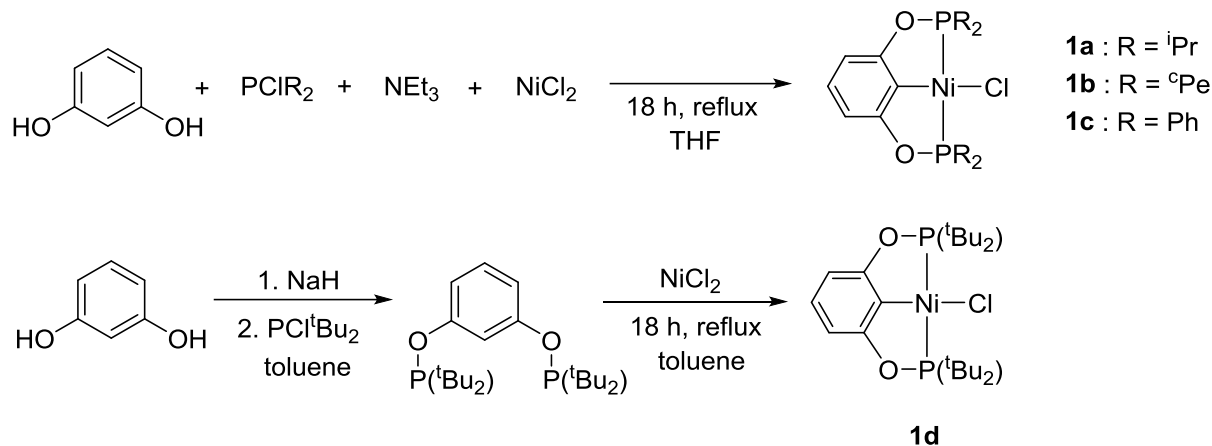
## **Chapter 2**

# **Synthesis of POCOP Nickel Chloride Complexes Using a Microwave Reactor**

## 2.1 Introduction

The development of new homogeneous catalysts is a large field in organometallic chemistry. One area of this research involves organometallic complexes bearing pincer type ligands, which are often defined as tridentate monoanionic ligands that bind metals in a coplanar fashion. Pincer type complexes are highly desirable for their high thermal stability and a broad range of catalytic reactions that they can perform. Of these complexes, bis-phosphinite or POCOP type pincer ligands are particularly attractive for their relatively low cost and a large range of catalytic applications.<sup>1</sup>

Typically, POCOP pincer type complexes of nickel are formed through the refluxing of the pre-synthesized POCOP ligands and nickel halide (Scheme 2.1).<sup>2</sup> Often the synthesis of the ligands requires strong or harmful bases (NaH, DMAP, etc). There has also been progress in developing one pot synthetic methods for these complexes.<sup>2a</sup> However, these synthetic methods always require large amounts of organic solvents (80-100 mL) and long reaction times (18-24 h). Additionally, there are usually extensive workup procedures including washing and/or column chromatography needed for the purification of these complexes. Progress has been made in limiting by-products of these reactions; however, the synthesis remains time-consuming.<sup>3</sup> One potential approach in improving both the time and the selectivity of this process is through microwave synthesis.

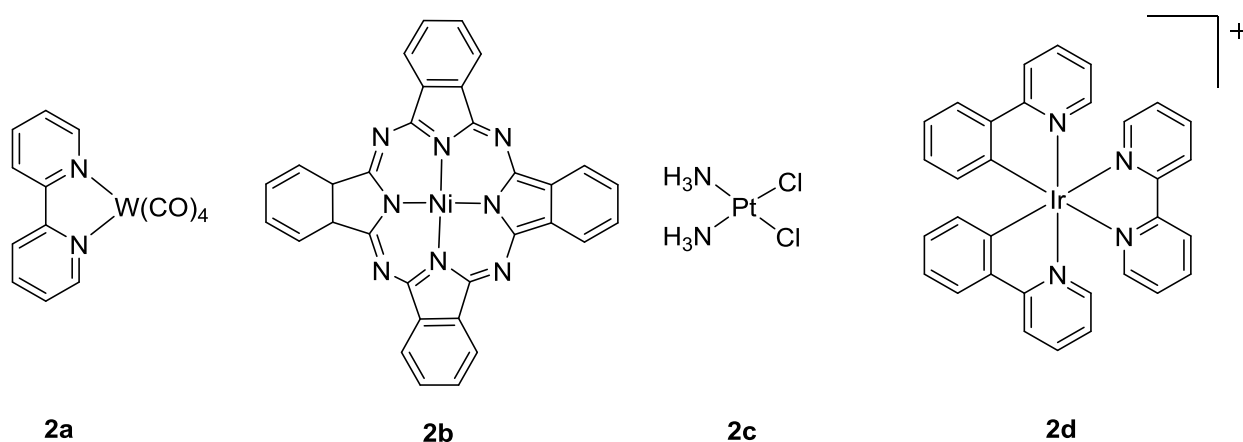


**Scheme 2.1.** Traditional synthesis of POCOP pincer nickel chloride complexes

Microwave synthesis has long been used for the preparation of inorganic and organic molecules.<sup>4</sup> The increasing availability of microwave reactors has led to an uptick in microwave-assisted synthesis published in the literature. Attractive attributes of microwave synthesis include the even dielectric heating of the reaction vessel leading to no local heating, which in turn results in less by-products and minimal decomposition.<sup>5</sup> Using a closed system, heating a solvent well above its boiling point also becomes available due to no direct heating of the microwave vessel. Additionally, the “specific microwave effect” can lead to increased rates, as demonstrated in several reactions.<sup>6</sup>

Although microwave-assisted synthesis of organic and inorganic molecules has been explored thoroughly, synthesis of organometallic complexes using microwave remains far less explored (Scheme 2.2). Organometallic complexes containing chromium, molybdenum, and tungsten (**2a**) can be made through displacement of carbonyl moieties with bidentate ligands such as bipy and dppe using microwave synthesis.<sup>7</sup> The synthesis of phthalocyanine type complexes (**2b**) can also be improved through microwave synthesis.<sup>8</sup> So can the synthesis of the organometallic anticancer drug cisplatin (**2c**).<sup>9</sup> Recently, microwave methodology has been used

for the efficient synthesis of iridium bipyridyl type organometallic complexes (**2d**).<sup>10</sup> Through the use of a microwave reactor, the reaction time was decreased from 48 h to just 1 h and 20 min. This study highlights the utility of microwave synthesis of organometallic complexes. To our knowledge, this is the only report of an organometallic *catalyst* known to be synthesized in a microwave reactor.



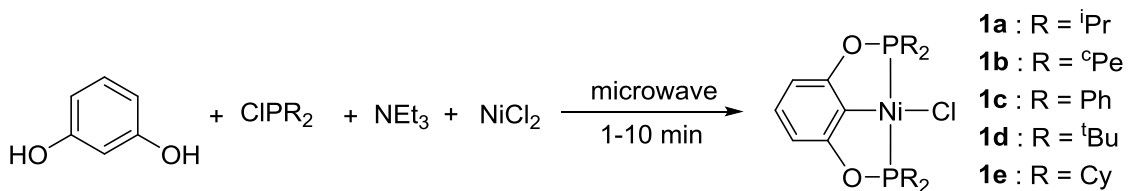
**Scheme 2.2.** Organometallic complexes synthesized using a microwave reactor

In this study, we demonstrate the utility of a microwave reactor for the synthesis of POCOP pincer nickel and palladium chloride complexes. For these reactions, traditional microwave solvents such as water and alcohols are not compatible with the chlorophosphines due to their nucleophilic nature. Instead, less absorbing microwave solvents such as THF must be used. Through the use of microwave synthesis, the reaction time was lowered from 18-36 h to just 5 min. In fact, this new method provides POCOP type pincer complexes in the most expedited fashion. In addition, this method uses a lesser amount of solvent and generates the desired products more cleanly, thus requiring less workup than the traditional method without using microwave.

## 2.2 One-Pot Synthesis of Nickel POCOP Complexes Using a Microwave Reactor

Bisphosphinite-based POCOP pincer complexes were chosen for initial studies due to their utility as precursors to several catalysts. This family of complexes is typically synthesized through refluxing the mixture of the ligand, nickel halide, and a base for extended periods of time (Scheme 2.1). With less sterically bulky *P*-substituents, the ligand can be generated in situ, providing the opportunity to conduct one-pot synthesis of the metal complexes from ligand precursors. Nickel chloride complex supported by the isopropyl-substituted POCOP ligand (**1a**) was chosen for optimization due to its relatively simple synthesis.<sup>2a</sup> After initial studies, <sup>31</sup>P{<sup>1</sup>H}NMR of the crude products show that the chlorophosphine is fully consumed in as short as 5 min. Additionally, the only phosphorous-containing product observed corresponds with the POCOP nickel pincer chloride complex **1a** (Table 2.1, entry 1).



**Table 2.1** Synthesis of POCOP Nickel Chloride Complexes

Entry	Phosphine	Purity	isolated yield	other species present
1	<i>i</i> Pr	>99%	91%	
2	<sup>c</sup> Pe	>99%	63%	
3	Cy	>99%	98%	
4	<sup>t</sup> Bu	45%	20%	36% ClP <sup>t</sup> Bu <sub>2</sub>
5 <sup>a</sup>	<sup>t</sup> Bu	90%	70%	decomposition
6	Ph	54%	30%	10% Ligand
7 <sup>b</sup>	Ph	36%	-	46% Ligand
8 <sup>c</sup>	<i>i</i> Pr	60%	31%	33% Ligand, 7% ClP <sup>i</sup> Pr <sub>2</sub>

Purity is measured through in situ <sup>31</sup>P{<sup>1</sup>H} NMR before workup.

All reactions are on a 1.1 mmol scale, 10 min, 180°C.

<sup>a</sup>Reaction performed at 220°C. <sup>b</sup>reaction only ran for 1 min. <sup>c</sup> reaction performed in 180°C oil bath.

Following the initial success in the synthesis of isopropyl-substituted POCOP complex, synthesis of other POCOP pincer complexes was pursued. The initial expansion to sterically similar <sup>c</sup>Pe (**1b**) and Cy (**1e**) derivatives proceeded without any setbacks achieving >99% conversion based on in situ <sup>31</sup>P{<sup>1</sup>H} NMR spectroscopy. Complex **1e** being a new compound was fully characterized. The analytically pure material yielded <sup>1</sup>H, <sup>31</sup>P{<sup>1</sup>H}, and <sup>13</sup>C{<sup>1</sup>H} NMR spectra

similar to the other POCOP nickel chloride complexes (**1a-d**). Additionally, the structure of the complex was studied by X-ray crystallography (Figure 2.1). The bulkier <sup>t</sup>Bu substituted compound (**1d**) did not proceed as efficiently as the previously stated compounds only showing 45% conversion under the standard conditions. The analysis of the crude material suggests that the second phosphorylation reaction required to make the pincer ligand is not fast enough for this reaction to go to completion. Under further optimization, a simple increase in temperature helps the reaction to proceed up to 90% completion.

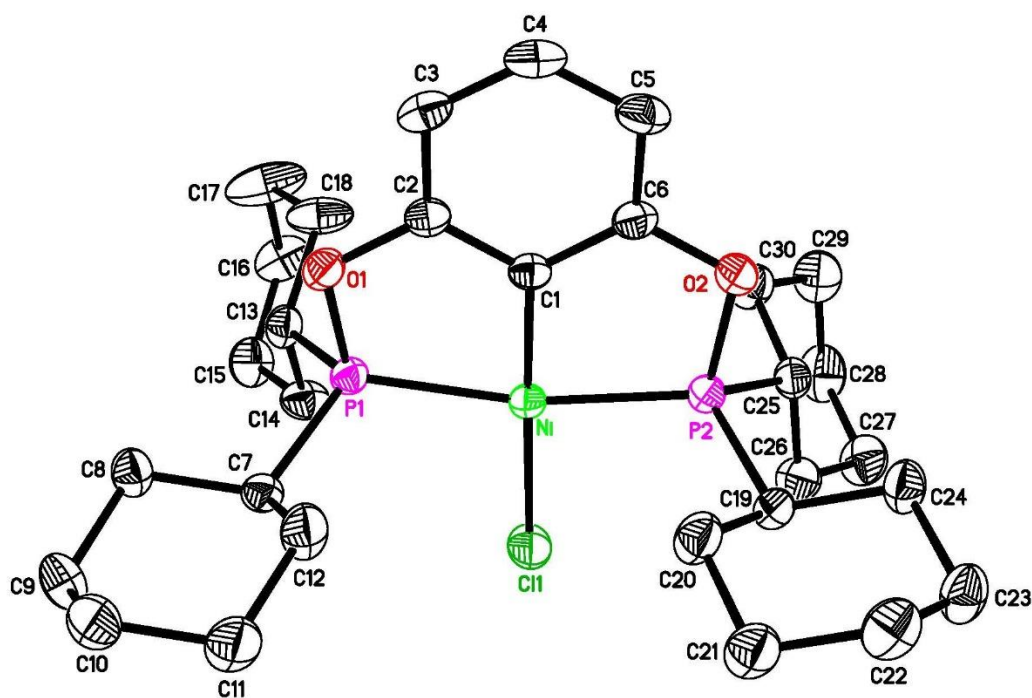
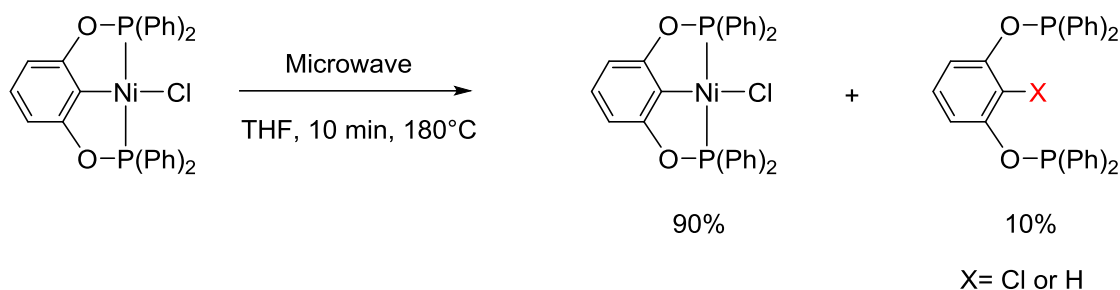


**Figure 2.1** ORTEP drawing of [2,6-(Cy<sub>2</sub>PO)<sub>2</sub>C<sub>6</sub>H<sub>3</sub>]NiCl (**1e**) at the 50 % probability level.

Selected bond lengths (Å) and angles (°): Ni–C (1) 1.8775(15), Ni–Cl(1) 2.1829(5), Ni–P(1) 2.1625(5), Ni–P(2) 2.1529(5), P(1)–Ni–P(2) 164.522(19), C(1)–Ni–Cl(1) 176.62(5).

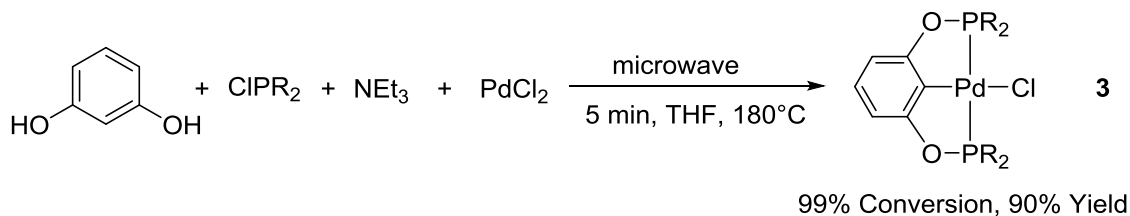
The phenyl-substituted compound **1c** also exhibits some issues only showing 54% purity under the standard conditions. Unlike the reaction for the *tert*-butyl derivative, there appears to be no remaining chlorophosphine in the crude reaction mixture. Additionally, there was a large amount of black precipitates observed in the reaction mixture. This suggests that there is a decomposition pathway involving reductive elimination of the ligand to form nickel(0). To test this hypothesis, pure phenyl-substituted POCOP complex **1c** was placed in the microwave reactor (Scheme 2.3). Interestingly there was observed decomposition of the complex yielding a black precipitate and what appeared to be the POCOP ligand or a chlorinated POCOP ligand. In an attempt to limit the decomposition of the complex, the reaction time was limited to 1 min; however, this led to only 36% conversion to the expected complex.



**Scheme 2.3.** Decomposition of complex **1c** under microwave conditions

In addition to the POCOP nickel chloride complexes made, the synthesis of palladium complexes of this ligand type was explored. After initial screening, the isopropyl-substituted complex (**3**) was synthesized using the same procedure developed for the nickel analog. This

reaction also took only 5 min to complete and resulted in a very clean product. This is notable because the literature procedure for the synthesis of complex **3** requires refluxing for at least 36 h.<sup>11</sup> This reaction also demonstrates that the utility of microwave synthesis is not limited to nickel complexes. Additionally flow microwave reactors could lead to one-pot synthesis of catalyst followed by cross-coupling reactions which are also known to be enhanced by using microwave reactors.<sup>12</sup>

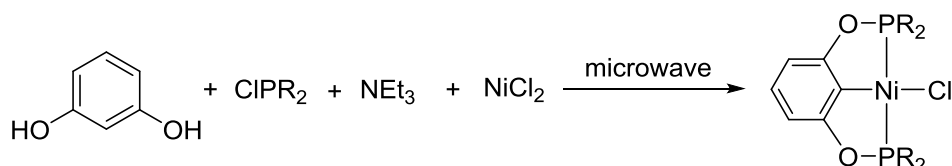


**Scheme 2.4** Synthesis of POCOP palladium chloride complex **3**

From the green chemistry point of view, using the microwave reactor also led to a decrease in the amount of solvent needed in both carrying out the reaction and during the workup. The microwave reactions only need 1.5 mL of THF to run the reaction and an additional 1 mL to help extract the product. This is far less than the experiment using traditional heating, which typically uses about 50 mL of solvent. The high purity of the crude mixtures also led to our pursuit of simplification of the purification procedures. The literature procedures for the synthesis of POCOP complexes typically require column chromatography or extensive washing to further purify the crude material; both steps demand the use of large amounts of solvents. For the microwave synthesis, we were also able to develop a procedure where only a separation of Et<sub>3</sub>N•HCl via filtration was all that was needed to produce analytically pure complex **1a**. The purification of the <sup>n</sup>Pe, Cy, and <sup>t</sup>Bu-substituted complexes required washing with a total of 0.5 mL

of methanol to yield an analytically pure product. By comparison, our control reaction using the traditional method required 30 mL of methanol during the washing step for purification, suggesting that the microwave reaction is less solvent demanding due to reduced amounts of byproducts.

**Table 2.2** Solvents used in microwave reactions



Entry	Phosphine	Reaction Solvent	Workup Solvents
1	<i>i</i> Pr	1.5 mL THF	1 mL THF
2	<sup>o</sup> Pe	1.5 mL THF	1mL THF, 0.5mL MeOH
3	Cy	1.5 mL THF	1mL THF, 0.5mL MeOH
4	<sup>t</sup> Bu	1.5 mL THF	1mL THF, 5mL MeOH
5	Ph	1.5 mL THF	1mL THF, 10mL MeOH
6 <sup>a</sup>	<i>i</i> Pr	1.5 mL THF	1mL THF, 30mL MeOH

THF in workup is for extraction of product, MeOH is for washing of product.

<sup>a</sup>oil bath control experiment.

The mechanism by which the microwave helps the reaction remains unknown. A control solution reaction was run in a microwave vial using a 180°C oil bath behind a blast shield (Table 2.1 entry 8, Table 2.2 entry 6). The control reaction's solution composition contains both unreacted chlorophosphine and the unreacted ligand. This suggests that the microwave reactor helps with both the nucleophilic substitution reaction on the phosphorus to form the ligand as well as the C–H bond activation to form the final complex. This hypothesis was supported by the

synthesis of *tert*-butyl derivative (**1d**) which typically requires stronger bases to form the ligand. Additionally, the literature suggests that much longer times are needed for the C–H bond activation reaction.

In conclusion, a series of POCOP complexes have been synthesized using a microwave reactor. The reactions proceed rapidly, resulting in products with high yield and purity. The reactions also limit the amount of solvent needed for the reaction as well as the solvent needed for the purification procedures. Synthesis of other related complexes is currently being explored.

### 2.3 Experimental Section

**Materials and methods.** Unless otherwise mentioned, all the compounds were prepared and handled under an argon atmosphere using Schlenk and glovebox techniques. All chemicals were purchased from Sigma Aldrich and were used without further purification. Dry and oxygen-free solvents (THF and toluene) were collected from an Innovative Technology solvent purification system. All microwave reactions were carried out using a Biotage microwave synthesizer with an automated sampler equipped with temperature and pressure probes. All reactions were carried out in sealed 2-5 mL Biotage microwave vials.  $^1\text{H}$  and  $^{31}\text{P}\{^1\text{H}\}$  NMR spectra were recorded on a Bruker Avance-400 MHz spectrometer. Chemical shifts in  $^1\text{H}$  NMR were referenced to residual solvents.  $^{31}\text{P}\{^1\text{H}\}$  NMR spectrum were referenced externally to 85%  $\text{H}_3\text{PO}_4$  (0 ppm).

**General Procedure for the Synthesis of Compounds in a Microwave.** A mixture of resorcinol (2.3 mmol), chlorophosphine (4.7 mmol), nickel chloride (2.3 mmol), and triethylamine (8 mmol) was added to a Biotage microwave vial. 1.5 mL of solvent was then added to bring the mixture volume between the necessary volume fill lines on the microwave vial. The vial was then sealed and placed in the microwave reactor. The reaction was pre-stirred and brought to the desired temperature. As soon as the microwave reaction was done, a small aliquot was withdrawn for in

situ  $^{31}\text{P}\{^1\text{H}\}$  NMR analysis. The reaction mixture was then gravity filtered. The remaining solid was then washed with additional solvent to extract any residual product. The combined solutions were evaporated to dryness to yield the complexes as powders. If needed, the solids were washed with chilled (0 °C) MeOH to achieve high purity.

**Synthesis of [2,6-(Cy<sub>2</sub>PO)<sub>2</sub>C<sub>6</sub>H<sub>3</sub>]NiCl.** The above procedure was repeated using ClPCy<sub>2</sub> as the chlorophosphine. The product was isolated in 98% yield (1.339g). Single crystals were grown from slow evaporation of a THF solution.  $^1\text{H}$  NMR (400 MHz, CDCl<sub>3</sub>,  $\delta$ ): 1.28-1.36 (m, CH<sub>2</sub>, 12H), 1.82-1.94 (m, CH<sub>2</sub>, 24H), 2.14-2.25 (m, CH, CH<sub>2</sub>, 8H), 6.38 (d,  $J_{\text{P-H}} = 8$  Hz, Ar, 2H), 6.93 (t,  $J_{\text{P-H}} = 8$  Hz, ArH, 1H).  $^{13}\text{C}\{^1\text{H}\}$  NMR (101 MHz, CDCl<sub>3</sub>,  $\delta$ ): 25.95 (s, CH<sub>2</sub>), 26.48-26.67 (m, CH<sub>2</sub>), 26.77 (s, CH<sub>2</sub>), 27.15 (s, CH<sub>2</sub>), 36.82 (t,  $J_{\text{P-C}} = 11.1$  Hz, CH), 104.99 (t,  $J_{\text{P-C}} = 6.1$  Hz,  $C_{\text{meta}}$ ), 125.36 (t,  $J_{\text{P-C}} = 21.2$  Hz,  $C_{\text{ipso}}$ ), 128.50 (s,  $C_{\text{para}}$ ), 168.86 (t,  $J_{\text{P-C}} = 10.1$  Hz,  $C_{\text{ortho}}$ ).  $^{31}\text{P}\{^1\text{H}\}$  NMR (162 MHz, CDCl<sub>3</sub>,  $\delta$ ): 177.75 (s). Anal. Calcd for C<sub>30</sub>H<sub>47</sub>O<sub>2</sub>P<sub>2</sub>NiCl: C, 60.48; H, 7.95. Found C, 59.70; H, 7.92.

## 2.4 References Cited

1. Göttker-Schnetmann, I.; White, P.; Brookhart, M., Iridium Bis(phosphinite) p-XPCP Pincer Complexes: Highly Active Catalysts for the Transfer Dehydrogenation of Alkanes. *Journal of the American Chemical Society* **2004**, *126* (6), 1804-1811.
2. (a) Chakraborty, S.; Krause, J. A.; Guan, H., Hydrosilylation of Aldehydes and Ketones Catalyzed by Nickel PCP-Pincer Hydride Complexes. *Organometallics* **2009**, *28* (2), 582-586; (b) Pandarus, V.; Zargarian, D., New Pincer-Type Diphosphinito (POCOP) Complexes of Nickel. *Organometallics* **2007**, *26* (17), 4321-4334; (c) Lapointe, S.; Vabre, B.; Zargarian, D., POCOP-Type Pincer Complexes of Nickel: Synthesis, Characterization, and Ligand Exchange Reactivities of New Cationic Acetonitrile Adducts. *Organometallics* **2015**, *34* (14), 3520-3531; (d) Adhikary, A.; Krause, J. A.; Guan, H., Configurational Stability and Stereochemistry of P-Stereogenic Nickel POCOP-Pincer Complexes. *Organometallics* **2015**, *34* (14), 3603-3610.
3. Vabre, B.; Lindeperg, F.; Zargarian, D., Direct, one-pot synthesis of POCOP-type pincer complexes from metallic nickel. *Green Chemistry* **2013**, *15* (11), 3188-3194.

4. Lidström, P.; Tierney, J.; Wathey, B.; Westman, J., Microwave assisted organic synthesis—a review. *Tetrahedron* **2001**, *57* (45), 9225-9283.
5. Gabriel, C.; Gabriel, S.; H. Grant, E.; H. Grant, E.; S. J. Halstead, B.; Michael P. Mingos, D., Dielectric parameters relevant to microwave dielectric heating. *Chemical Society Reviews* **1998**, *27* (3), 213-224.
6. Langa, F.; de la Cruz, P.; de la Hoz, A.; Diaz-Ortiz, A.; Diez-Barra, E., Microwave irradiation: more than just a method for accelerating reactions. *Contemporary Organic Synthesis* **1997**, *4* (5), 373-386.
7. VanAtta, S. L.; Duclos, B. A.; Green, D. B., Microwave-Assisted Synthesis of Group 6 (Cr, Mo, W) Zerovalent Organometallic Carbonyl Compounds. *Organometallics* **2000**, *19* (12), 2397-2399.
8. (a) Shaabani, A., Synthesis of Metallophthalocyanines under Solvent-free Conditions using Microwave Irradiation. *Journal of Chemical Research, Synopses* **1998**, (10), 672-673; (b) Ungurenasu, C., Improved Synthesis of Octaalkoxymetalphthalocyanines (MCl<sub>2</sub>, M = Si, Ge, Sn) Under Microwave Conditions. *Synthesis* **1999**, *1999* (10), 1729-1730.
9. (a) Petruzzella, E.; Chiroasca, C. V.; Heidenga, C. S.; Hoeschele, J. D., Microwave-assisted synthesis of the anticancer drug cisplatin, cis-[Pt(NH<sub>3</sub>)<sub>2</sub>Cl<sub>2</sub>]. *Dalton Transactions* **2015**, *44* (7), 3384-3392; (b) Pedrick, E. A.; Leadbeater, N. E., Preparation of cisplatin using microwave heating and continuous-flow processing as tools. *Inorganic Chemistry Communications* **2011**, *14* (3), 481-483.
10. Monos, T. M.; Sun, A. C.; McAtee, R. C.; Devery, J. J.; Stephenson, C. R. J., Microwave-Assisted Synthesis of Heteroleptic Ir(III)+ Polypyridyl Complexes. *The Journal of Organic Chemistry* **2016**, *81* (16), 6988-6994.
11. Adhikary, A.; Schwartz, J. R.; Meadows, L. M.; Krause, J. A.; Guan, H., Interaction of Alkynes with Palladium POCOP-Pincer Hydride Complexes and its Unexpected Relation to Palladium-Catalyzed Hydrogenation of Alkynes. *Inorganic Chemistry Frontiers* **2014**, *1* (1), 71-82.
12. Larhed, M.; Moberg, C.; Hallberg, A., Microwave-Accelerated Homogeneous Catalysis in Organic Chemistry. *Accounts of Chemical Research* **2002**, *35* (9), 717-727.



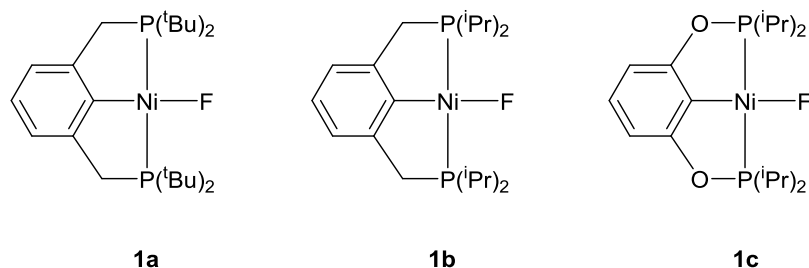
## **Chapter 3**

# **Nickel POCOP Pincer Fluoride Complexes as Precursors for the Synthesis of Nickel Hydride Complexes**

### 3.1 Introduction

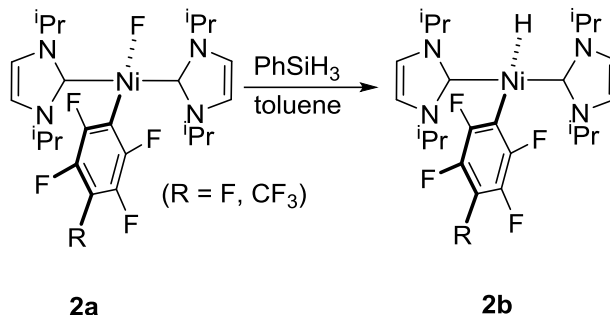
Synthesis of fluorine-containing organic molecules is an important chemical process. These fluorinated molecules are of particular interest to the pharmaceutical and agricultural industries due to their increased stability in biological systems compared to the non-fluorinated molecules.<sup>1</sup> Common fluorination methods include nucleophilic  $F^-$  reagents<sup>2</sup> as well as electrophilic  $F^+$  reagents<sup>3</sup> although these reagents are often expensive or difficult to make. One method to circumvent using these fluorination reagents is through the use of transition metal catalysts. In most of these transition metal catalyzed fluorination reactions, metal fluoride complexes are either proposed or isolated as key intermediates.<sup>4</sup> Studies of these metal fluoride complexes are of importance for both the understanding of how to improve the catalytic cycles and the understanding of the properties of these metal fluoride complexes.

Although organometallic complexes containing fluoride ligands have been identified as catalysts for fluorination reactions, the knowledge base for these types of complexes remains relatively limited. Most metal based fluorination catalysts are derived from copper,<sup>5</sup> silver,<sup>6</sup> rhodium<sup>7</sup> or palladium.<sup>4b</sup> Many of these fluoride complexes are notoriously difficult to make due to their high reactivity towards common ligands such as phosphines or etherated solvents. Additionally, when these complexes decompose, they tend to generate HF, which is a quite dangerous byproduct. Several palladium fluoride complexes have been well characterized and shown to reductively eliminate C–F bonds under catalytic conditions.<sup>8</sup> In contrast, nickel fluoride complexes are relatively unexplored.



**Scheme 3.1** Reported nickel pincer fluoride complexes

Several nickel fluoride complexes have been previously reported in the literature (Scheme 3.1). Although these complexes have not exhibited the desired catalytic activity for fluorination chemistry observed by other transition metal analogues, study of these complexes remains of fundamental interest. Peruzinni et al. studied the ability of a <sup>t</sup>BuPCP pincer ligated nickel fluoride complex **1a** to undergo fluorine scrambling with BF<sub>3</sub>.<sup>9</sup> Campora et al. examined the electron donation effects that fluoride has on pπ-dπ-pπ ligand-metal interactions relative to other anionic donor ligands in PCP ligated pincer complexes.<sup>10</sup> Zargarian et al. investigated the transformation of a POCOP pincer nickel fluoride complex **1c** for the conversion to nickel trifluoromethyl derivatives.<sup>11</sup> Also studied by Zargarian was the ability of the nickel fluoride complex to catalytically fluorinate benzyl halides using silver fluoride. The catalytic transformation is inefficient with a TON of 6.5. Additionally, nickel (0) complexes have been known to undergo oxidative addition with polyfluoro aromatics to generate nickel fluoride complexes (**2a**).<sup>12</sup> These nickel fluoride complexes can then be treated with PhSiH<sub>3</sub> to generate nickel hydride complexes **2b** (Scheme 3.2), a transformation that was particularly of interest to us.



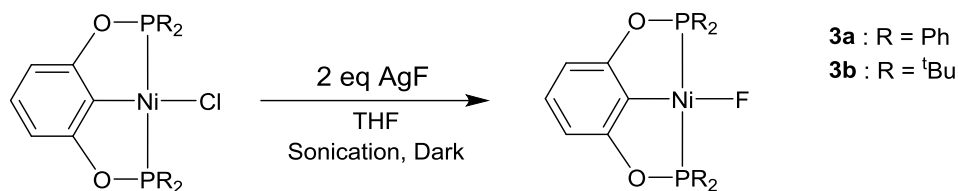
**Scheme 3.2** Hydride generation from nickel fluoride complex

This chapter will discuss the synthesis of new nickel fluoride complexes supported by a POCOP pincer ligand. These nickel fluoride complexes were characterized as well as they could be before decomposition. The <sup>t</sup>BuPOCOP nickel pincer fluoride complex was then treated with silanes and boranes to generate the corresponding nickel hydride complex. This transformation is of particular interest because many reduction reactions with these nickel hydride complexes require silanes or boranes. This method thus provides an alternative route to access the catalytic cycles.

### 3.2 Synthesis of Nickel Fluoride Complexes

Synthesis of nickel fluoride complexes was accomplished following literature procedures for related compounds.<sup>9-11</sup> Nickel chloride complexes with <sup>t</sup>Bu and Ph substituents on the phosphorous donors were synthesized first as precursors to the fluoride complexes. Unfortunately we were unable to achieve the same success that Zargarian and co-workers had for the isopropyl derivative **1c**; no reaction occurred when simply stirring silver fluoride with the nickel chloride complexes in the dark.<sup>11</sup> An alternative approach was also pursued using the high-speed ball mill (HSBM) to mechanically grind silver fluoride and a nickel chloride complex. This process was

abandoned due to low isolated yields (10-15%) and difficulty in scaling up beyond 200 mg. A more practical synthesis involved sonication of the mixture of the nickel chloride complexes and silver fluoride in the dark (Scheme 3.3). The reaction takes 4-36 h to reach completion.



**Scheme 3.3** Synthesis of nickel fluoride complexes

The existence of a fluoride ligand was confirmed by the characteristic doublet observed in the  $^{31}\text{P}\{^1\text{H}\}$  NMR spectrum due to phosphorus-fluorine coupling. Their  $^{31}\text{P}$  chemical shifts appear downfield of those for the corresponding chloride complex, a trend also observed with other pincer fluoride complexes reported in the literature.<sup>10-11</sup> These new fluoride complexes have also been studied by X-ray crystallography. The *tert*-butyl derivative (**3b**) co-crystalizes with resorcinol, suggesting that the synthesis of the complex leads to the decomposition of the ligand backbone (Figure 3.1). The phenyl-substituted complex is hydrogen bonded to a water molecule implying the possibility for this complex to generate HF, which could be another decomposition pathway (Figure 3.2). Unfortunately, solubility and stability issues have prevented the observation of a quartet as expected for the *ipso* carbon resonance with similar  $J_{\text{C-P}}$  and  $J_{\text{C-F}}$  coupling constants. The limited stability has also prevented satisfactory combustion analysis to further confirm the formula of the complexes. Various solvents including water and  $\text{Et}_2\text{O}$  could lead to the decomposition of these complexes. The complexes also decompose slowly in the presence of THF, which was the solvent used for its synthesis. Exposure to residual  $\text{H}_2\text{O}$  leads to the generation of a black precipitate, unidentified products, and HF as evidenced by the etching of the glassware used.

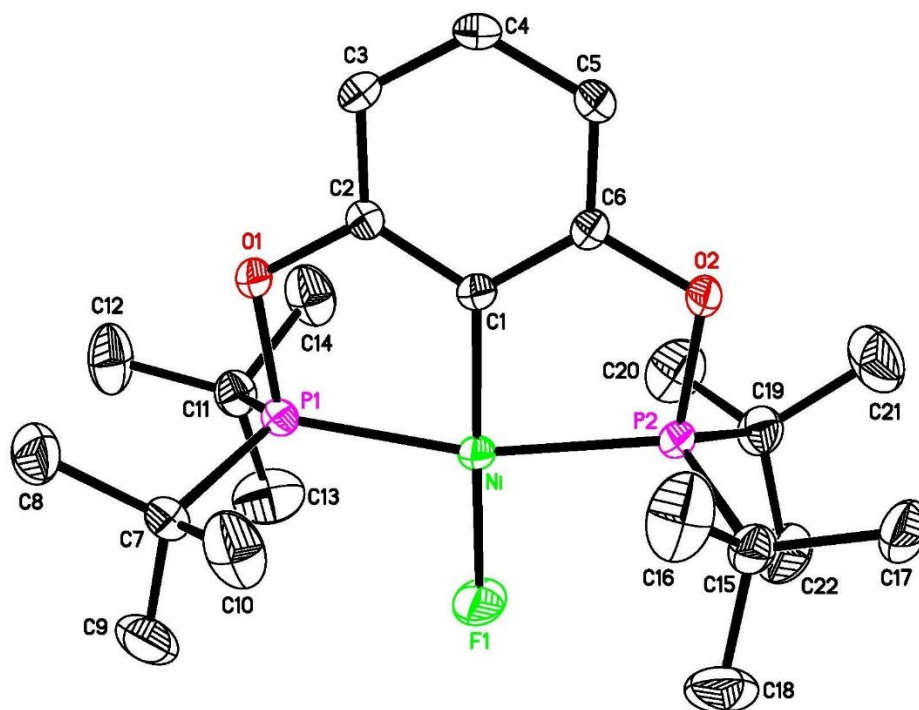


**Figure 3.1.** ORTEP drawing of  $[2,6-(t\text{Bu}_2\text{PO})_2\text{C}_6\text{H}_3]\text{NiF}$  (**3b**) at the 50 % probability level. The molecule co-crystalizes with resorcinol from the decomposed ligand. Selected bond lengths (Å) and angles (°): Ni–C (1) 1.8762(16), Ni–F(1) 1.8620(11), Ni–P(1) 2.1865(5), Ni–P(2) 2.1825(5), P(1)–Ni–P(2) 164.540(19), C(1)–Ni–F(1) 178.53(7).

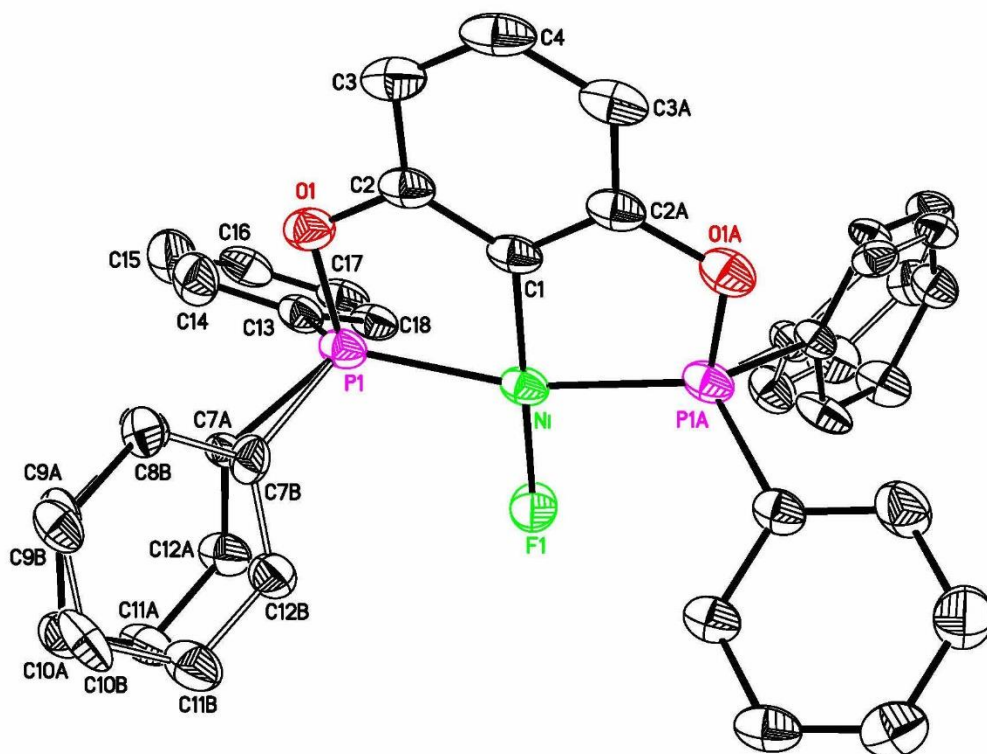


**Figure 3.2.** ORTEP drawing of [2,6-(Ph<sub>2</sub>PO)<sub>2</sub>C<sub>6</sub>H<sub>3</sub>]NiF (**3a**) at the 50 % probability level.

Selected bond lengths (Å) and angles (°): Ni–C (1) 1.878(3), Ni–F(1) 1.8776(18), Ni–P(1) 2.1692(7), Ni–P(2) 2.1692(7), P(1)–Ni–P(2) 163.48(3), C(1)–Ni–F(1) 180.000(1).

### 3.3 Reactions of Nickel Fluoride Complexes with Boranes and Silanes as a Means to Generate Nickel Hydride Complexes

To demonstrate the utility of these complexes, synthesis of *tert*-butyl-substituted hydride complexes from the fluoride complexes was attempted. Due to the high affinity of fluoride for silicon and boron, silanes and boranes were chosen as hydride donors for these complexes. In a typical experiment, nickel fluoride complex **3b** was mixed with a stoichiometric amount of silane

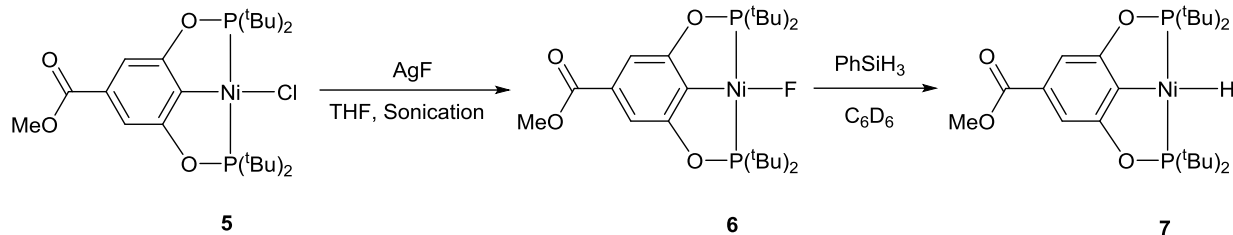
or borane. A complete conversion to the hydride complex **4** was observed in >10 min as judged by  $^1\text{H}$  and  $^{31}\text{P}\{^1\text{H}\}$  NMR spectroscopy. Also observed was an immediate color change from orange to pale yellow, characteristic of the formation of hydride complexes. The reactions using silanes evolve gas vigorously, which could be  $\text{Si}_2\text{F}_6$  resulted from disproportionation of the initially formed alkyl fluoro silanes.



**Scheme 3.4.** Synthesis of nickel hydride complex **4** from **3b** using silanes or boranes

Due to the instability of the fluoride complexes, synthesis of hydrides via this fluoride-to-hydride transformation offers limited advantages. Nickel hydride complexes are more routinely made using powerful hydride donors such as  $\text{LiAlH}_4$  or  $\text{NaHBEt}_3$ ; however, these reactive hydrides are incompatible with many functional groups. To illustrate the synthetic utility of the fluoride complexes, the ester-substituted POCOP pincer fluoride complex (**6**) was made. The synthesis proceeds seamlessly through sonication of silver fluoride and the nickel chloride complex in THF. The resulting fluoride complex shows characteristic  $J_{\text{P-F}}$  coupling in the  $^{31}\text{P}\{^1\text{H}\}$  NMR spectrum as well as a chemical shift further downfield from its chloride complex. The  $^{13}\text{C}\{^1\text{H}\}$  NMR spectrum exhibits a quartet for the  $\text{C}_{\text{ipso}}$  resonance, further confirming the composition of this complex. Low stability has prevented this complex from growing X-ray quality crystals or obtaining satisfactory combustion analysis. When mixed with phenylsilane, complex **6** is fully converted to the hydride species **7**, which otherwise could not be isolated from the  $\text{LiAlH}_4$  or  $\text{NaHBEt}_3$  route.





**Scheme 3.5.** Synthesis of nickel hydride **7** using nickel fluoride complex **6**

### 3.4 Conclusions

Though no complexes were fully characterized, the synthesis of short-lived nickel fluoride complexes was achieved through sonication of nickel chloride complexes with silver fluoride. There is evidence that these nickel fluoride complexes are made; however, low stability prevents these molecules being isolated in a pure form. The complexes can be fully converted to the hydride complexes in the presence of boranes or silanes, providing an alternative route to these hydride complexes. Further study of these nickel fluoride complexes is hampered by their facile decomposition.

### 3.5 Experimental Section

**Materials and Methods.** Unless otherwise mentioned, all the organometallic compounds were prepared and handled under an argon atmosphere using Schlenk and glovebox techniques. All chemicals were purchased from commercial sources and used without further purification. Dry and oxygen-free THF was collected from an Innovative Technology solvent purification system. Nickel chloride complexes were prepared according to the literature procedures.<sup>13</sup>  $^1\text{H}$ ,  $^{13}\text{C}\{^1\text{H}\}$  and  $^{31}\text{P}\{^1\text{H}\}$  NMR spectra were recorded on a Bruker Avance-400 MHz spectrometer. Chemical shifts in NMR were referenced to residual solvents.  $^{31}\text{P}\{^1\text{H}\}$  NMR spectrum were referenced externally to 85%  $\text{H}_3\text{PO}_4$  (0 ppm).

**Synthesis of [2,6-(<sup>t</sup>Bu<sub>2</sub>PO)<sub>2</sub>C<sub>6</sub>H<sub>3</sub>]NiF (3b).** A solution of nickel chloride complex (0.200 g, 0.41 mmol) was prepared in 25 mL of THF. Silver fluoride (0.086 g, 0.41 mmol) was added under dark conditions. The reaction mixture was then sonicated for 8 h. The suspension was filtered over Celite and pumped to dryness to yield an orange powder (0.172 g, 87% yield). <sup>1</sup>H NMR (400 MHz, C<sub>6</sub>D<sub>6</sub>, δ): 1.44 (vt, *J*<sub>P-H</sub> = 8 Hz, CH<sub>3</sub>, 36H), 6.50 (d, *J*<sub>H-H</sub> = 8 Hz, CH<sub>meta</sub>, 2H), 6.52 (t, *J*<sub>H-H</sub> = 8 Hz, CH<sub>para</sub>, 1H). <sup>31</sup>P{<sup>1</sup>H} NMR (162 MHz, C<sub>6</sub>D<sub>6</sub>, δ): 180.66 (d, *J*<sub>F-P</sub> = 26 Hz).

**Synthesis of [2,6-(Ph<sub>2</sub>PO)<sub>2</sub>C<sub>6</sub>H<sub>3</sub>]NiF (3a).** A solution of nickel chloride complex (0.200 g, 0.35 mmol) was prepared in 25 mL of THF. Silver fluoride (0.0466 g, 0.36 mmol) was added under dark conditions. The reaction mixture was then sonicated for 8 h. The suspension was filtered over Celite and pumped to dryness to yield an orange-brown powder (0.163 g, 84% yield). <sup>1</sup>H NMR (400 MHz, C<sub>6</sub>D<sub>6</sub>, δ): 6.65(d, *J*<sub>H-H</sub> = 8 Hz, ArH, 2H), 6.89 (t, *J*<sub>H-H</sub> = 8 Hz, ArH, 2H), 6.97-6.92 (m, ArH, 12H), 8.0-8.22 (m, ArH, 8H). <sup>31</sup>P{<sup>1</sup>H} NMR (162 MHz, C<sub>6</sub>D<sub>6</sub>, δ): 134.58 (d, *J*<sub>F-P</sub> = 22 Hz).

**Synthesis of [2,6-(<sup>t</sup>Bu<sub>2</sub>PO)<sub>2</sub>C<sub>6</sub>H<sub>2</sub>COOMe]NiF (6).** A solution of nickel chloride complex (0.400 g, 0.73 mmol) was prepared in 25 mL of THF. Silver fluoride (0.092 g, 0.73 mmol) was added under dark conditions. The reaction mixture was then sonicated for 8 h. The suspension was filtered over Celite and pumped to dryness to yield a bright orange powder (0.301 g, 76% yield). <sup>1</sup>H NMR (400 MHz, C<sub>6</sub>D<sub>6</sub>, δ): 1.46 (vt, *J*<sub>P-H</sub> = 8 Hz, CH<sub>3</sub>, 36H), 3.49 (s, CH<sub>3</sub>, 3H), 7.78 (s, ArH, 2H). <sup>13</sup>C{<sup>1</sup>H} NMR (101 MHz, C<sub>6</sub>D<sub>6</sub>, δ): 27.30 (t, *J*<sub>P-C</sub> = 3.0 Hz, CCH<sub>3</sub>), 38.23 (t, *J*<sub>P-C</sub> = 7.1 Hz, CCH<sub>3</sub>), 51.34 (s, COOCH<sub>3</sub>), 106.50 (t, *J*<sub>P-C</sub> = 6.1 Hz, C<sub>meta</sub>) 131.27 (q, *J*<sub>P-C</sub> = *J*<sub>F-C</sub> = 20.2 Hz, C<sub>ipso</sub>), 130.85 (s, C<sub>para</sub>), 166.54 (s, COOMe), 170.18 (t, *J*<sub>P-C</sub> = 10.1 Hz, C<sub>ortho</sub>). <sup>31</sup>P{<sup>1</sup>H} NMR (162 MHz, C<sub>6</sub>D<sub>6</sub>, δ): 179.50 (d, *J*<sub>F-P</sub> = 22 Hz).

### General Procedure for the Generation of Hydride Complexes. Nickel fluoride complex (0.010

g) was dissolved in C<sub>6</sub>D<sub>6</sub> in a screwcap NMR tube. Silane or borane (1 equiv) was then injected into the tube via a syringe. The solution immediately started to bubble and turned pale in color.

<sup>1</sup>H and <sup>31</sup>P {<sup>1</sup>H} NMR spectra were recorded to confirm the formation of the hydride species.

### 3.6 References Cited

1. (a) Jeschke, P., The Unique Role of Fluorine in the Design of Active Ingredients for Modern Crop Protection. *ChemBioChem* **2004**, *5* (5), 570-589; (b) Müller, K.; Faeh, C.; Diederich, F., Fluorine in Pharmaceuticals: Looking Beyond Intuition. *Science* **2007**, *317* (5846), 1881-1886; (c) Kirsch, P., Applications of Organofluorine Compounds. In *Modern Fluoroorganic Chemistry*, Wiley-VCH Verlag GmbH & Co. KGaA: 2005; pp 203-277.
2. (a) Middleton, W. J., New Fluorinating Reagents. Dialkylaminosulfur Fluorides. *The Journal of Organic Chemistry* **1975**, *40* (5), 574-578; (b) Akio, T.; Hiroshi, I.; Nobuo, I., F-Propene-Dialkylamine Reaction Products as Fluorinating Agents. *Bulletin of the Chemical Society of Japan* **1979**, *52* (11), 3377-3380; (c) Tang, P.; Wang, W.; Ritter, T., Deoxyfluorination of Phenols. *Journal of the American Chemical Society* **2011**, *133* (30), 11482-11484; (d) Lal, G. S.; Pez, G. P.; Pesaresi, R. J.; Prozonic, F. M.; Cheng, H., Bis(2-methoxyethyl)aminosulfur Trifluoride: A New Broad-Spectrum Deoxyfluorinating Agent with Enhanced Thermal Stability. *The Journal of Organic Chemistry* **1999**, *64* (19), 7048-7054; (e) Hayashi, H.; Sonoda, H.; Fukumura, K.; Nagata, T., 2,2-Difluoro-1,3-dimethylimidazolidine (DFI). A New Fluorinating Agent. *Chemical Communications* **2002**, (15), 1618-1619.
3. (a) Kirsch, P., Synthesis of Complex Organofluorine Compounds. In *Modern Fluoroorganic Chemistry*, Wiley-VCH Verlag GmbH & Co. KGaA: 2005; pp 25-169; (b) Landelle, G.; Bergeron, M.; Turcotte-Savard, M.-O.; Paquin, J.-F., Synthetic Approaches to Monofluoroalkenes. *Chemical Society Reviews* **2011**, *40* (5), 2867-2908; (c) Umemoto, T.; Kawada, K.; Tomita, K., N-Fluoropyridinium Triflate and its Derivatives: Useful Fluorinating Agents. *Tetrahedron Letters* **1986**, *27* (37), 4465-4468.
4. (a) Liang, T.; Neumann, C. N.; Ritter, T., Introduction of Fluorine and Fluorine-Containing Functional Groups. *Angewandte Chemie International Edition* **2013**, *52* (32), 8214-8264; (b) Grushin, V. V., The Organometallic Fluorine Chemistry of Palladium and Rhodium: Studies toward Aromatic Fluorination. *Accounts of Chemical Research* **2010**, *43* (1), 160-171.
5. (a) Ye, Y.; Sanford, M. S., Mild Copper-Mediated Fluorination of Aryl Stannanes and Aryl Trifluoroborates. *Journal of the American Chemical Society* **2013**, *135* (12), 4648-4651; (b) Subramanian, M. A.; Manzer, L. E., A "Greener" Synthetic Route for Fluoroaromatics via Copper (II) Fluoride. *Science* **2002**, *297* (5587), 1665-1665; (c) Fier, P. S.; Hartwig, J. F., Copper-Mediated Fluorination of Aryl Iodides. *Journal of the American Chemical Society* **2012**, *134* (26), 10795-10798; (d) Truong, T.; Klimovica, K.; Daugulis, O., Copper-Catalyzed, Directing Group-Assisted Fluorination of Arene and Heteroarene C-H Bonds. *Journal of the American Chemical Society* **2013**, *135* (25), 9342-9345; (e) Fier, P. S.; Luo, J.; Hartwig, J. F., Copper-Mediated Fluorination of Arylboronate Esters. Identification of a Copper(III) Fluoride Complex. *Journal of the American Chemical Society* **2013**, *135* (7), 2552-2559.

6. (a) Fier, P. S.; Hartwig, J. F., Selective C-H Fluorination of Pyridines and Diazines Inspired by a Classic Amination Reaction. *Science* **2013**, *342* (6161), 956-960; (b) Wang, K.-P.; Yun, S. Y.; Mamidipalli, P.; Lee, D., Silver-Mediated Fluorination, Trifluoromethylation, and Trifluoromethylthiolation of Arynes. *Chemical Science* **2013**, *4* (8), 3205-3211; (c) Yin, F.; Wang, Z.; Li, Z.; Li, C., Silver-Catalyzed Decarboxylative Fluorination of Aliphatic Carboxylic Acids in Aqueous Solution. *Journal of the American Chemical Society* **2012**, *134* (25), 10401-10404; (d) Tang, P.; Furuya, T.; Ritter, T., Silver-Catalyzed Late-Stage Fluorination. *Journal of the American Chemical Society* **2010**, *132* (34), 12150-12154.
7. (a) Zhu, J.; Tsui, G. C.; Lautens, M., Rhodium-Catalyzed Enantioselective Nucleophilic Fluorination: Ring Opening of Oxabicyclic Alkenes. *Angewandte Chemie International Edition* **2012**, *51* (49), 12353-12356; (b) Bosman, A. W.; Vestberg, R.; Heumann, A.; Fréchet, J. M. J.; Hawker, C. J., A Modular Approach toward Functionalized Three-Dimensional Macromolecules: From Synthetic Concepts to Practical Applications. *Journal of the American Chemical Society* **2003**, *125* (3), 715-728.
8. (a) Ball, N. D.; Kampf, J. W.; Sanford, M. S., Synthesis and Reactivity of Palladium(II) Fluoride Complexes Containing Nitrogen-Donor Ligands. *Dalton Transactions* **2010**, *39* (2), 632-640; (b) Huacuja, R.; Herbert, D. E.; Fafard, C. M.; Ozerov, O. V., A Terminal Palladium Fluoride Complex Supported by an Anionic PNP Pincer Ligand. *Journal of Fluorine Chemistry* **2010**, *131* (11), 1257-1261.
9. Rossin, A.; Peruzzini, M.; Zanobini, F., Nickel(II) Hydride and Fluoride Pincer Complexes and their Reactivity with Lewis Acids  $BX_3 \cdot L$  ( $X = H, L = THF; X = F, L = Et_2O$ ). *Dalton Transactions* **2011**, *40* (17), 4447-4452.
10. Martínez-Prieto, L. M.; Melero, C.; del Río, D.; Palma, P.; Cámpora, J.; Álvarez, E., Synthesis and Reactivity of Nickel and Palladium Fluoride Complexes with PCP Pincer Ligands. NMR-Based Assessment of Electron-Donating Properties of Fluoride and Other Monoanionic Ligands. *Organometallics* **2012**, *31* (4), 1425-1438.
11. Vabre, B.; Petiot, P.; Declercq, R.; Zargarian, D., Fluoro and Trifluoromethyl Derivatives of POCOP-Type Pincer Complexes of Nickel: Preparation and Reactivities in  $SN^2$  Fluorination and Direct Benzoylation of Unactivated Arenes. *Organometallics* **2014**, *33* (19), 5173-5184.
12. (a) Schaub, T.; Backes, M.; Radius, U., Square-Planar (Pentafluorophenyl)nickel(II) Complexes by Derivatization of a C-F Activation Product. *European Journal of Inorganic Chemistry* **2008**, *2008* (17), 2680-2690; (b) Fischer, P.; Götz, K.; Eichhorn, A.; Radius, U., Decisive Steps of the Hydrodefluorination of Fluoroaromatics using  $[Ni(NHC)_2]$ . *Organometallics* **2012**, *31* (4), 1374-1383.
13. (a) Chakraborty, S.; Krause, J. A.; Guan, H., Hydrosilylation of Aldehydes and Ketones Catalyzed by Nickel PCP-Pincer Hydride Complexes. *Organometallics* **2009**, *28* (2), 582-586; (b) Gómez-Benítez, V.; Baldovino-Pantaleón, O.; Herrera-Álvarez, C.; Toscano, R. A.; Morales-Morales, D., High Yield Thiolation of Iodobenzene Catalyzed by the Phosphinite Nickel PCP Pincer Complex:  $[NiCl\{C_6H_3-2,6-(OPPh_2)_2\}]$ . *Tetrahedron Letters* **2006**, *47* (29), 5059-5062.

# **Chapter 4**

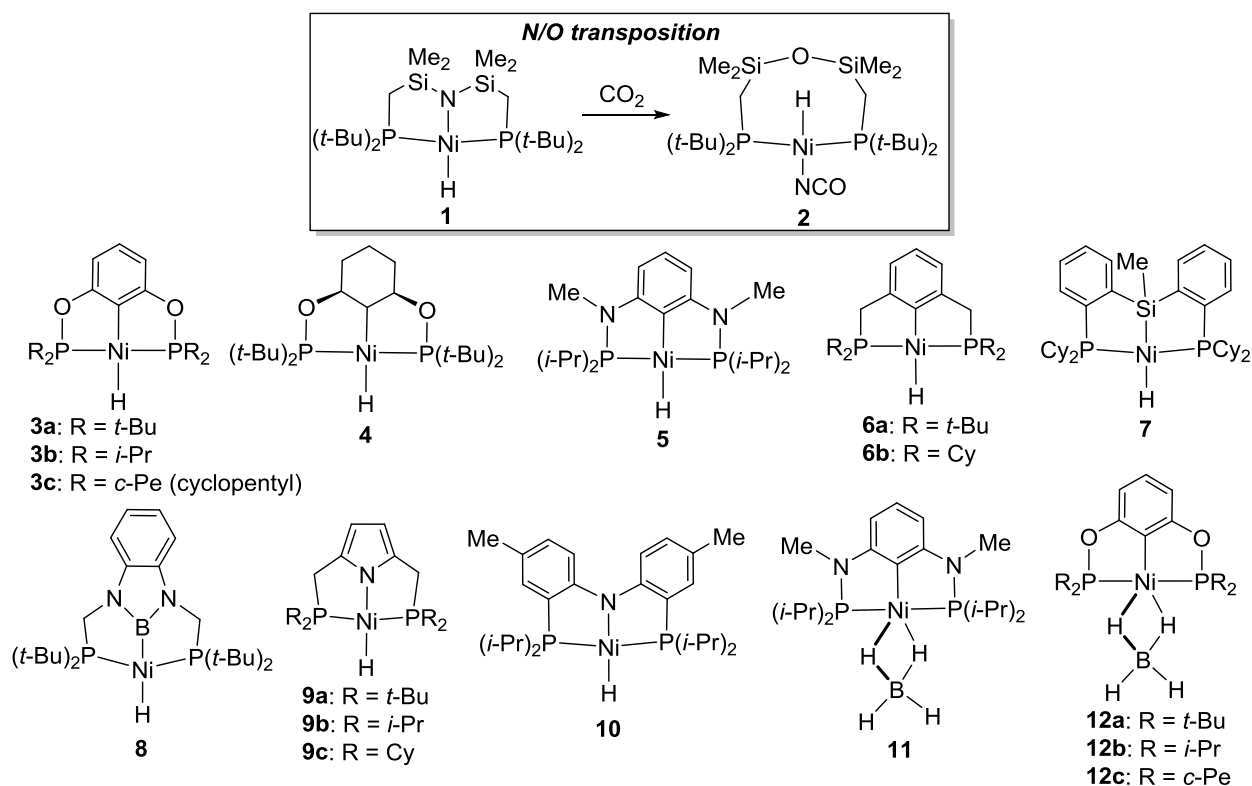
## **Relative Thermodynamic Favorability of CO<sub>2</sub> Reduction by Nickel Hydride Complexes**

## 4.1 Introduction

The reduction of CO<sub>2</sub> to formate or further is of utmost importance as previously stated (See Chapter 1). One method for this reduction is through the use of metal hydrides. In particular, many transition metal based hydride complexes, especially those supported by a pincer ligand, have been developed to reduce CO<sub>2</sub> to formate.<sup>1</sup> Pincer systems are preferred for this transformation because their relatively high thermal stability allows an easy access to metal hydride species and at the same time is amenable to heating which may be needed for CO<sub>2</sub> reduction. In addition, the reactivity is highly tunable due to the availability of a wide variety of pincer ligands. In fact, pincer complexes based on just about any late transition metal are now known to catalyze the reduction of CO<sub>2</sub> using a silane, borane or dihydrogen as the reducing agent. One metal of high interest is nickel due to its relatively low cost and high availability.

Catalytic reduction of CO<sub>2</sub> by nickel hydride species is relatively unexplored compared to the reduction catalyzed by iridium or ruthenium complexes. Recently in our group, a nickel hydride complex bearing a bisphosphinite-based (or POCOP) pincer ligand (**3a**, Scheme 4.1) was shown to be an effective catalyst for the reduction of CO<sub>2</sub> to a methanol derivative using a borane.<sup>2</sup> This process occurs first through the reversible reduction of CO<sub>2</sub> to make a nickel formate complex. One equivalent of borane then regenerates the hydride while producing a boroforate species. This particular formate can then undergo further reductions eventually to a methanol derivative. Replacing the pincer ligand with a sterically less bulky one (by reducing the size of phosphorous substituents) slows the reaction by trapping the nickel hydride species as a dihydridoborate species (analogous to **12**).<sup>3</sup> Additionally, changing the ligand system to a PSiP pincer ligand (i.e., **7** as a masked nickel hydride) and using HBpin as the reducing agent result in the reduction of CO<sub>2</sub> to a mixture consisting of pinBOCH<sub>2</sub>OBpin, pinBOBpin, and pinBOCH<sub>3</sub>.<sup>4</sup>

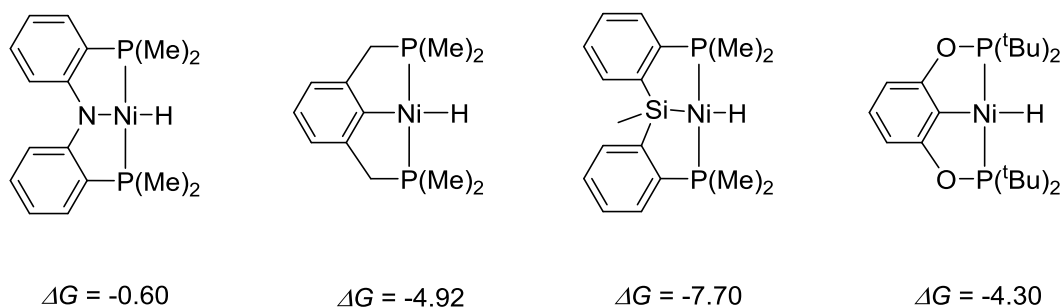
Other nickel hydride complexes that can catalytically reduce CO<sub>2</sub> include the PBP pincer complex **8** which can perform the Lewis acid assisted hydrosilylation of CO<sub>2</sub> where the previous complexes (**3**, **12**) have not yet been shown to catalyze this reaction.<sup>5</sup> The difference in selectivity highlights the importance of understanding how ligand modification impacts the reactivity of nickel hydride complexes towards CO<sub>2</sub>.



**Scheme 4.1.** Nickel hydride complexes studied for CO<sub>2</sub> reduction

Nickel hydride complexes have been found to be extremely efficient at reducing CO<sub>2</sub> to formate complex stoichiometrically, although very few systems have been developed into catalytic processes. A large number of nickel hydride complexes that reduce CO<sub>2</sub> to formate complexes are pincer based. This is largely because pincer complexes confer high thermal stability and, in a square planar geometry, force the anionic donor *trans* to the hydride to prevent decomposition via reductive elimination of the pincer ligand and the hydride. Several of these nickel hydride

complexes reduce CO<sub>2</sub> instantaneously and reversibly at room temperature under an atmospheric CO<sub>2</sub> pressure.<sup>6</sup> Some nickel hydride complexes have difficulty in reducing CO<sub>2</sub>, but can achieve the transformation at higher temperatures and/or under higher CO<sub>2</sub> pressures. Little is known about why specific complexes are better at reducing CO<sub>2</sub> than others. Empirical observations suggest that pincer complexes bearing a nitrogen donor *trans* to the hydride are particularly sluggish in CO<sub>2</sub> reduction. Hazari, Kemp, and coworkers have suggested that the natural bond orbital (NBO) of the donor ligand *trans* to the hydride correlates to the thermodynamics of CO<sub>2</sub> insertion.<sup>7</sup> They have provided computational and experimental evidence supporting the *trans* effect on the favorability of CO<sub>2</sub> reduction (Scheme 4.2); however, the computational methods are based on simplified models. Additional computational studies focusing on the <sup>t</sup>BuPOCOP nickel pincer complexes (**3a**) suggest that the insertion of CO<sub>2</sub> into the nickel hydride is thermodynamically downhill ( $\Delta G = -4.30$  kcal/mol).<sup>2b</sup>



**Scheme 4.2.** Computational thermodynamic data for the reduction of CO<sub>2</sub> in kcal/mol

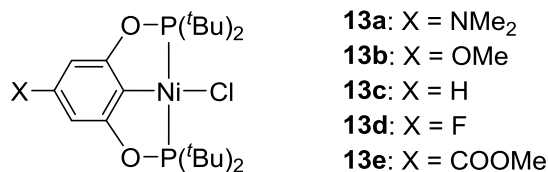
In this chapter, the synthesis of a series of POCOP pincer nickel hydride and formate compounds will be discussed. The equilibrium constant for the exchange of CO<sub>2</sub> between a formate complex and a hydride complex will be measured as a means to probe the relative thermodynamics of CO<sub>2</sub> reduction. This series of compounds will be compared against other



nickel and palladium complexes to help determine what factors influence the reduction of CO<sub>2</sub> to formate complexes.

#### 4.2 Synthesis of <sup>t</sup>BuPOCOP Nickel Pincer Hydride and Formate Complexes Bearing Different *para*-Substituents

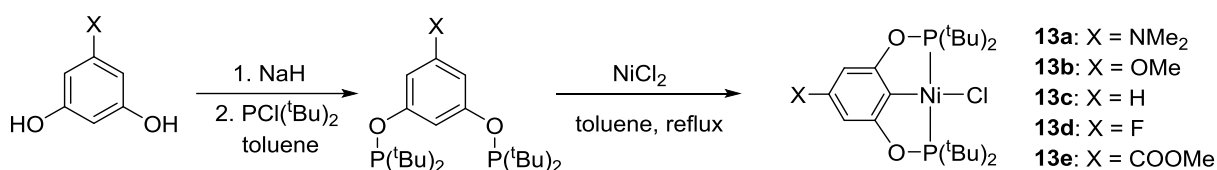
To study the electronic effects on the reduction of CO<sub>2</sub> by nickel hydride complexes, a series of complexes with varying substituents were needed. POCOP pincer ligands are ideal for this examination given their reported impact on the electronic properties at the metal center through the change of the substituent *para* to the metal.<sup>8</sup> Additionally, the previously reported complexes appear to have little impact on the steric environment around the metal center.<sup>9</sup> Furthermore, there is a vast collection of literature procedures that exist to make the starting substituted resorcinols.<sup>8c, 8d, 10</sup> The complexes with *tert*-butyl substituents on the phosphorous were targeted due to their increased stability and easier synthesis relative to the isopropyl analogs. Derivatives of resorcinol with dimethylamino (NMe<sub>2</sub>), methoxy (OMe), fluoro (F), and methyl ester (COOMe) substituted at the 5-position were chosen due to the ease of synthesis or their commercial availability (Scheme 4.3). Additionally, this range of substrates offers substantial electronic variation with molecules bearing electron-donating groups (NMe<sub>2</sub>, OMe) and those bearing electron-withdrawing groups (F, COOMe).<sup>11</sup> These substituted resorcinols could lead to the synthesis of the nickel chloride complexes, which in turn serve as stable precursors to the desired nickel hydride and formate complexes.



### Scheme 4.3 Target nickel chloride complexes

Synthesis of nickel chloride complexes was accomplished by following procedures adapted from the ones reported in the literature (Scheme 4.4).<sup>12</sup> The starting substituted resorcinols can either be purchased (H, OMe, COOMe) or synthesized (F, NMe<sub>2</sub>) following literature procedures.<sup>8c, 10a, 13</sup> The sodium hydride can then be added to deprotonate the resorcinols followed by the addition of di-*tert*-butylchlorophosphine. Nickel chloride and triethylamine were then added directly to the ligand solution to initiate the synthesis of the nickel chloride complexes. The one-pot method provides products in higher yields than the step-wise approach by minimizing the introduction of oxygen and moisture to the system, which are detrimental to the chlorophosphine and the pincer ligand. Following flash column chromatography or recrystallization, the complexes can be isolated in an analytically pure form. All the reported complexes gave characterization data consistent with those shown in the literature.<sup>8a, 8b, 12a</sup> For the new complexes (**13a** and **13d**) the <sup>31</sup>P{<sup>1</sup>H} NMR chemical shifts appear close to those of the other previously reported complexes (**13b**, **13c**, and **13e**) and do not present any obvious trend ( $\delta$  190.69 and 189.07 for the **13a** and **13d**, respectively). The <sup>1</sup>H NMR show triplets ( $J_{P-H} = 8.0$  Hz) at  $\delta = 1.40$  and 1.53, respectively, characteristic of virtual coupling resulted from the *trans* configuration for the phosphorus donors. The signal for the proton *meta* to the nickel center shows at  $\delta$  6.30 ( $J_{P-F} = 8.0$  Hz) for the fluorinated complex and  $\delta$  6.13 for the dimethylamino-substituted complex. This represents a trend where complexes with more electron-donating substituents have <sup>1</sup>H<sub>*meta*</sub> shifts further downfield from complexes with less electron-donating substituents. The <sup>31</sup>C{<sup>1</sup>H} NMR spectra also appear in

accordance with the analogous complexes reported in the literature.<sup>8a, 8b, 12a</sup> Complex **13d** shows characteristic CF coupling for the  $C_{para}$  ( $J_{C-F} = 243.4$  Hz),  $C_{meta}$  ( $J_{C-F} = 25.3$  Hz),  $C_{ortho}$  ( $J_{C-F} = 15.3$  Hz), and  $C_{ipso}$  ( $J_{C-F} = 3.0$  Hz) resonances. The X-ray structures (Figures 4.1 and 4.2) are consistent with the NMR results and show similar steric environments around nickel as previously reported *tert*-butyl-substituted POCOP nickel pincer complexes.<sup>8a, 8b, 12a</sup>



**Scheme 4.4** Synthesis of POCOP nickel chloride complexes

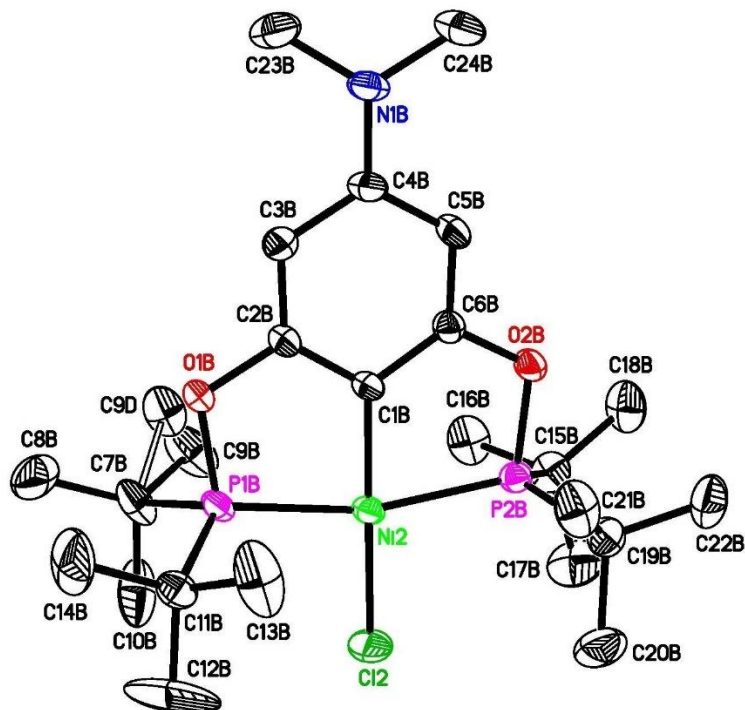


**Figure 4.1** ORTEP drawing of  $[2,6\text{-}(t\text{Bu}_2\text{PO})_2\text{C}_6\text{H}_2\text{NMe}_2]\text{NiCl}$  (**13a**) at the 50 % probability level. Selected bond lengths ( $\text{\AA}$ ) and angles ( $^\circ$ ): Ni–C (1) 1.8767(18), Ni–Cl(1) 2.1970(5), Ni–P(1) 2.1745(6), Ni–P(2) 2.1846(5), P(1)–Ni–P(2) 163.50(2), C(1)–Ni–Cl(1) 178.89(6).

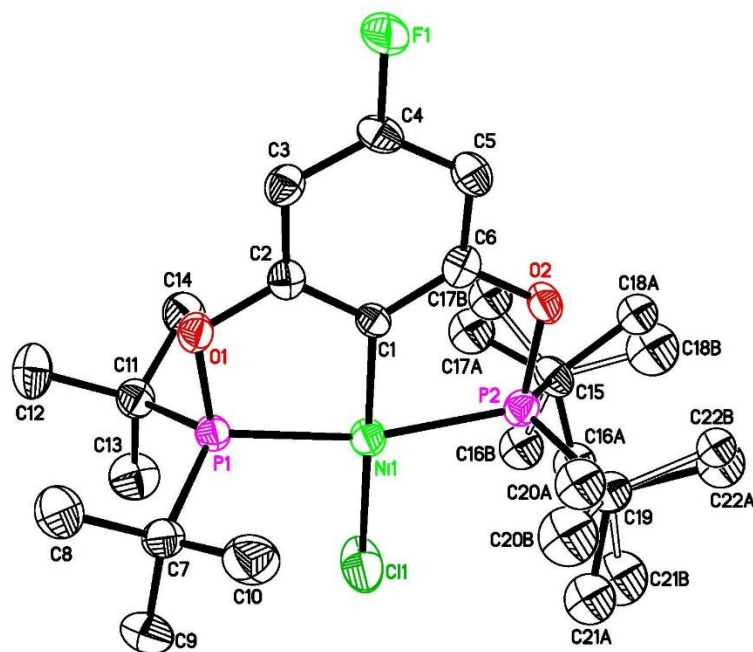
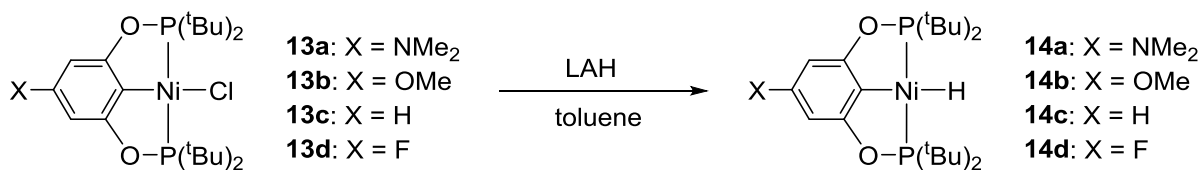


**Figure 4.2** ORTEP drawing of [2,6-(*t*Bu<sub>2</sub>PO)<sub>2</sub>C<sub>6</sub>H<sub>2</sub>F]NiCl (**13d**) at the 50 % probability level.

Selected bond lengths (Å) and angles (°): (Ni–C (1) 1.898(4), Ni–Cl(1) 2.2016(13), Ni–P(1) 2.1769(12), Ni–P(2) 2.1845(12), P(1)–Ni–P(2) 164.32(5), C(1)–Ni–Cl(1) 179.53(13).

Synthesis of nickel hydride complexes from their chloride derivatives can be accomplished from several different pathways.<sup>6</sup> The hydride donor lithium aluminum hydride (LAH) was chosen due to its high yielding procedure and relative ease of workup. For these reactions, 5-50 equivalents of LAH were required to prepare the desired nickel hydride complexes (Scheme 4.5). The need for larger amounts of LAH to make the *para*-fluoro substituted nickel hydride **14d** can be explained by the deactivation of LAH via fluoride-lithium interactions. All complexes were isolated in an analytically pure form. Nickel hydrides bearing OMe and H at the *para* position

(**14b** and **14c**) exhibited spectra that matched with those reported in the literature.<sup>8a, 12a</sup> Complexes containing NMe<sub>2</sub> and F substituents (**14a** and **14d**) showed characteristic hydride resonances as triplets ( $J_{\text{PH}} = 52.0$  Hz) at  $\delta = -7.97$  and  $-8.13$  ppm, respectively. Additionally, the <sup>31</sup>P{<sup>1</sup>H} NMR chemical shifts are around 30 ppm downfield ( $\delta = 221.8$ - $224.8$  ppm) from those of the corresponding chloride complexes ( $\delta = 189.1$ - $190.9$  ppm). The <sup>31</sup>C{<sup>1</sup>H} NMR spectra of these hydride complexes were similar to those of their chloride derivatives with the exception of the C<sub>ipso</sub> resonance which was shifted substantially more upfield ( $\sim 20$  ppm). This can be explained by the elongation of the C–Ni bond as observed from the crystal structures (e.g., Figure 4.3 for **14a**).



**Scheme 4.5.** Synthesis of nickel hydride complexes

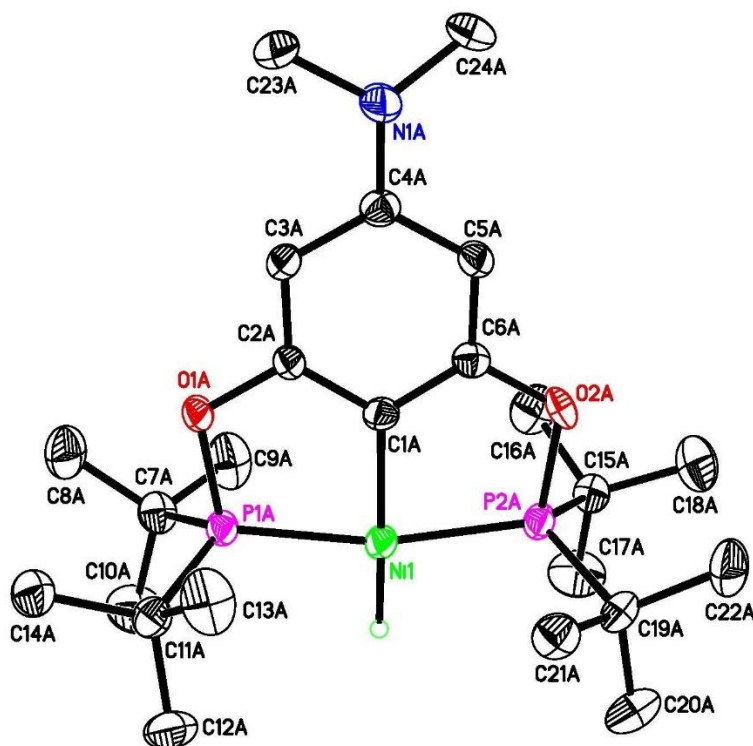
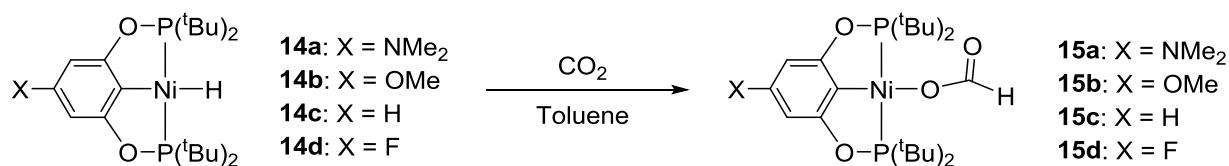


**Figure 4.3** ORTEP drawing of  $[2,6-(t\text{Bu}_2\text{PO})_2\text{C}_6\text{H}_2\text{NMe}_2]\text{NiH}$  (**14a**) at the 50 % probability level. Selected bond lengths (Å) and angles ( $^\circ$ ): Ni–C (1) 1.887(4), Ni–H(1) 1.43(5), Ni–P(1) 2.1281(13), Ni–P(2) 2.1274(14), P(1)–Ni–P(2) 165.21(5), C(1)–Ni–H(1) 174(2).

The synthesis of the nickel formate complexes from the nickel hydride complexes is a rather straightforward process. All complexes readily reduce  $\text{CO}_2$  in toluene at ambient temperature and under an atmospheric pressure (Scheme 4.6). The reaction appears to be instantaneous, achieving a full conversion before NMR spectra can be recorded (<10 min). Additionally, the reaction is so fast that pre-purified  $\text{CO}_2$  is not needed, allowing the use of a

multitude of CO<sub>2</sub> sources including dry ice and human breath. The nickel formate complexes can be readily isolated from the removal of solvent under vacuum; however, extended periods of time for evacuation lead to decarboxylation that revert the complexes back to the hydride species. The nickel formate complexes all exhibit characteristic formate signals in their <sup>1</sup>H NMR spectra as triplets ( $J_{\text{P-H}} = 4.0$  Hz) at  $\delta = 8.36$ - $8.49$  ppm due to a long-range proton-phosphorous coupling. The <sup>31</sup>P{<sup>1</sup>H} NMR spectra exhibit chemical shifts similar to the literature value for the unsubstituted formate complex (**15c**) ranging from 188.2 to 192.2 ppm.<sup>2a</sup> The <sup>31</sup>C{<sup>1</sup>H} NMR spectra show formate resonances at  $\delta = 167.5$  to  $167.7$  ppm, similar to the resonance for the unsubstituted pincer complex **15c**.<sup>2a</sup> The structures of complexes **15a**, **15b**, and **15d** have been studied by X-ray crystallography (Figures 4.4-4.6).



**Scheme 4.6.** Synthesis of nickel formate complexes



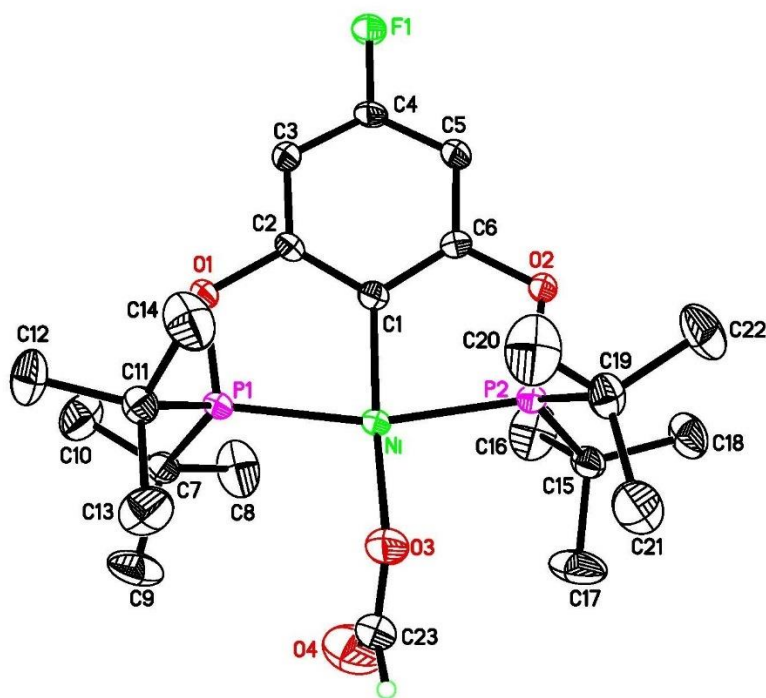


**Figure 4.4** ORTEP drawing of [2,6-(<sup>t</sup>Bu<sub>2</sub>PO)<sub>2</sub>C<sub>6</sub>H<sub>2</sub>F]NiOCOH (**15d**) at the 50 % probability level. Selected bond lengths (Å) and angles (°): Ni–C (1) 1.883(2), Ni–O(3) 1.9110(18), Ni–P(1) 2.2004(6), Ni–P(2) 2.1818(6), O(3)–C(23) 1.259(3), O(4)–C(23) 1.226(4), P(1)–Ni–P(2) 164.07(2), C(1)–Ni–O(3) 168.52(9).

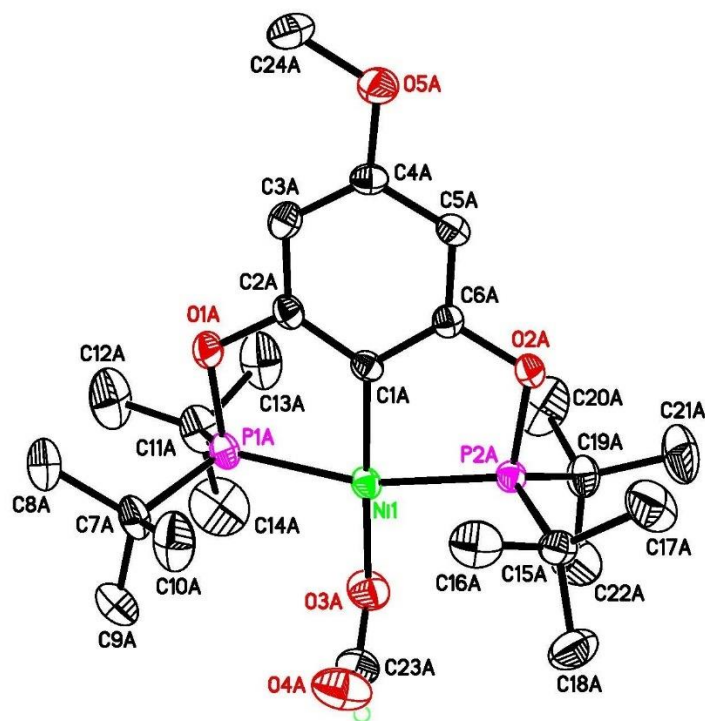


**Figure 4.5** ORTEP drawing of [2,6-(<sup>t</sup>Bu<sub>2</sub>PO)<sub>2</sub>C<sub>6</sub>H<sub>2</sub>OMe]NiOCOCH<sub>3</sub> (**15b**) at the 50 % probability level. One of two independent molecules in the crystal lattice is shown. Selected bond lengths (Å) and angles (°): Ni–C (1A) 1.873(4), Ni–O(3A) 1.907(3), Ni–P(1A) 2.1973(10), Ni–P(2A) 2.2018(10), O(3A)–C(23A) 1.278(6), O(4A)–C(23A) 1.209(6), P(1A)–Ni(1)–P(2A) 162.94(4), C(1)–Ni–O(3) 173.23(16).

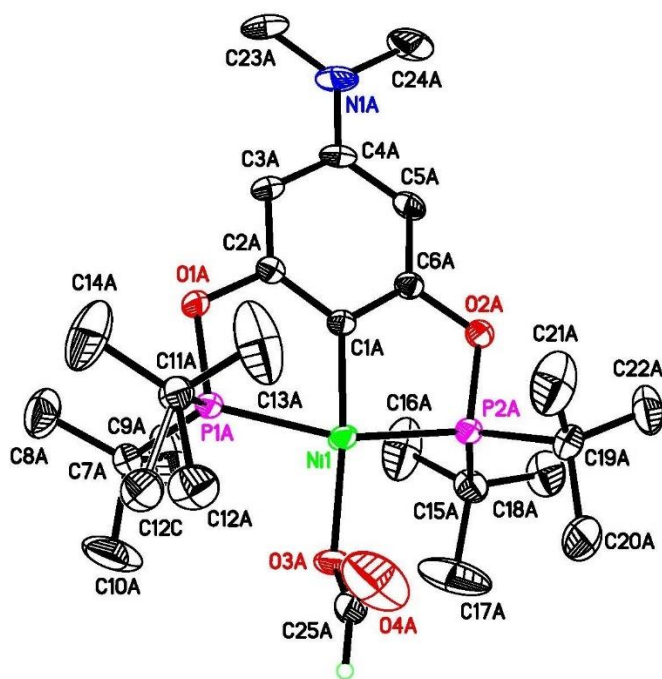
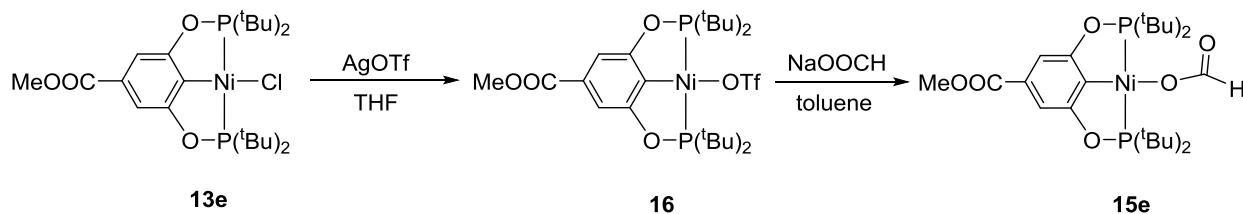


**Figure 4.6** ORTEP drawing of  $[2,6-(t\text{Bu}_2\text{PO})_2\text{C}_6\text{H}_2\text{NMe}_2]\text{NiOCOH}$  (**15a**) at the 50 % probability level. One of two independent molecules in the crystal lattice is shown. Selected bond lengths ( $\text{\AA}$ ) and angles ( $^\circ$ ): Ni–C (1A) 1.883(3), Ni–O(3A) 1.927(2), Ni–P(1A) 2.1827(8), Ni–P(2A) 2.1836(8), O(3A)–C(25A) 1.243(8), O(4A)–C(25A) 1.207(12), P(1A)–Ni(1)–P(2A) 162.75(3), C(1)–Ni–O(3) 168.58(11).

The COOMe-substituted complex presented several challenges in the synthesis of the hydride and formate complexes. Most known hydride donors either reduce the ester functionality (e.g., LAH,  $\text{NaNH}_2\text{BH}_2$ ) or were not successful in making a pure nickel hydride complex (e.g.,

NaBH<sub>4</sub>). Due to these limitations, synthesis of the formate complex without using the hydride was pursued. Direct substitution of chloride with sodium formate was unsuccessful resulting in a black precipitate with no evidence for the formation of the desired formate complex. As an alternative method, the chloride was first abstracted by silver triflate in THF kept in the dark (Scheme 4.7). The resulting triflate complex **16** was then treated with sodium formate in toluene to form an analytically pure formate complex **15e** (Scheme 4.7). The resulting formate complex gives spectral data and structural information (Figure 4.7) similar to other formate complexes mentioned above.



**Scheme 4.7.** Synthesis of nickel formate complex **15e** from nickel chloride complex **13e** via nickel triflate complex **16**

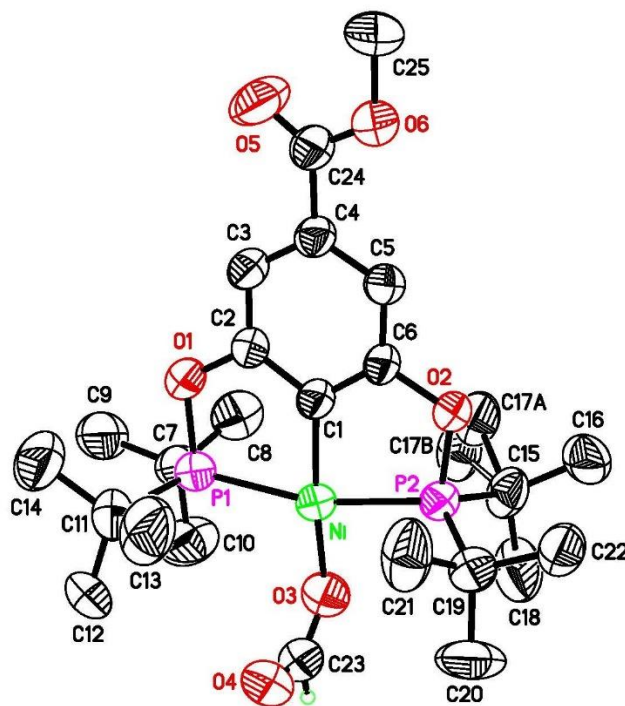


**Figure 4.7** ORTEP drawing of  $[2,6-(t\text{Bu}_2\text{PO})_2\text{C}_6\text{H}_2\text{NMe}_2]\text{NiOCOH}$  (**17**) at the 50 % probability level. Selected bond lengths (Å) and angles (°): Ni–C (1) 1.872(5), Ni–O(3) 1.897(4), Ni–P(1) 2.1996(17), Ni–P(2) 2.1912(16), O(3)–C(23) 1.236(8), O(4)–C(23) 1.224(10), P(1)–Ni(1)–P(2) 164.04(6), C(1)–Ni–O(3) 169.7(2).

The isolation of the COOMe-substituted hydride complex is significantly more challenging than the isolation of other hydride complexes. After many trials, it was found that the formate complex could be decarboxylated under high vacuum and mild heating (80 °C); however, this process is very slow (18-24 h). Due to the relative low stability of the resulting hydride complex,

most of the desired product proceeds through decomposition pathways before it can be isolated. It can be separated from decomposition products via sublimation at 120 °C to yield analytically pure crystals; however, the yield for this process is extremely low (8%). The  $^1\text{H}$  NMR and  $^{31}\text{P}\{^1\text{H}\}$  NMR spectra are similar to the analogous hydride species, showing peaks at  $\delta = -7.9$  and 221.79, respectively. With the synthesis of the COOMe-substituted complexes completed, five different POCOP pincer systems ( $\text{X} = \text{CO}_2\text{Me}$ , F, H, OMe, and  $\text{NMe}_2$ ) are now available for comparative studies of their ability to reduce  $\text{CO}_2$ .

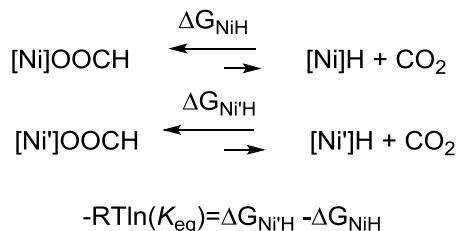
#### **4.3 Effects of *para*-Substituents on the Relative Thermodynamics for the Reduction of $\text{CO}_2$ by POCOP Nickel Pincer Hydride Complexes**

The change of Gibbs free energy ( $\Delta G$ ) for the direct reduction of  $\text{CO}_2$  to formate complex is difficult to measure. The reversibility of this reaction and the limited thermal stability of the starting hydride complexes are just some of the challenges in measuring these energies. The only published thermodynamic data on this transformation are computational in nature. All experimental data on this transformation are qualitative, providing information solely on whether or not the formate complex can be observed. To determine the ability of a nickel hydride complex to reduce  $\text{CO}_2$  in a *quantitative* manner, a competition experiment was designed to determine what factors can impact this reduction. Nickel complexes supported by POCOP ligands are extremely efficient at reducing  $\text{CO}_2$  to form their corresponding formate complexes. This suggests that as long as nickel hydrides are present, the amount of free  $\text{CO}_2$  is negligible. The reversibility of  $\text{CO}_2$  insertion into these hydride complexes has been demonstrated by  $^{13}\text{C}$  scrambling between a non-labeled nickel formate complex and  $^{13}\text{CO}_2$  as well as by the observation of hydride species when pure formate complexes are exposed to a dynamic vacuum for an extended period of time.<sup>2a</sup> Given these results, an equilibrium constant can be measured by mixing two complexes with different

pincer ligands in a closed system where both compete for the reduction of CO<sub>2</sub>. The measurement of the equilibrium constant can lead to the calculation in the difference in change of Gibbs free energy ( $\Delta\Delta G$ ) for each complex. The equilibrium constant can readily be measured from the ratio of concentrations as shown in eq. 4.1. From this measurement, the  $\Delta\Delta G$  value can be calculated according to eq. 4.2. This provides a reliable way to measure the relative thermodynamic favorability for a nickel hydride to reduce CO<sub>2</sub> to the formate complex.

$$K_{eq} = \frac{[\text{NiH}][\text{Ni}'\text{OOCH}]}{[\text{Ni}'\text{H}][\text{NiOOCH}]}$$

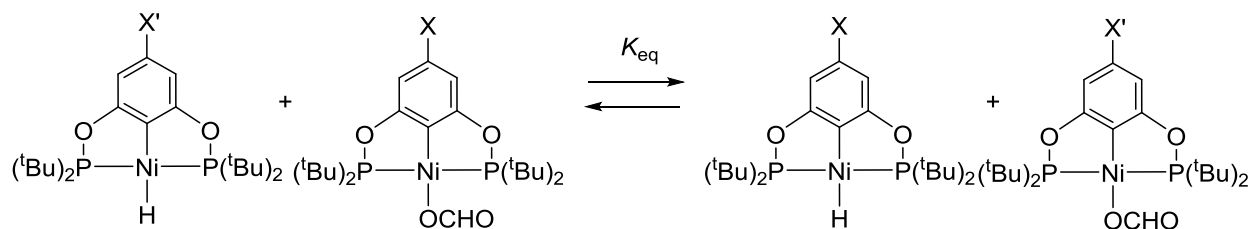
**Equation 4.1** Equilibrium constant measurement based on species concentration



**Equation 4.2**  $\Delta\Delta G$  calculation based on measured equilibrium constants

To calculate these  $\Delta\Delta G$  values, NMR experiments were performed in sealed J-Young NMR tubes using benzene-*d*<sub>6</sub> as the solvent. The equilibrium could be observed by <sup>1</sup>H and <sup>31</sup>P{<sup>1</sup>H} NMR spectroscopy. Nickel formate with X substituent at the *para* position of the POCOP pincer backbone was mixed with nickel hydride with X' substituent at the *para* position (Scheme 4.8). This mixture was monitored until the calculated  $K_{eq}$  value was unchanged for 3 consecutive days. The experiment was then repeated in the reverse direction to ensure that each mixture had indeed reached equilibrium. Each reaction was carried out at room temperature (23 °C) and typically took

5-14 days to achieve equilibrium. Increasing the temperature to 60 °C did not appear to change the  $\Delta\Delta G$  value of the reaction (within the margin of errors); however, it did appear to accelerate the decomposition of nickel complexes. Additionally, the reaction between complexes (**14a,c** and **15a,c**) (entry 1 in Table 4.1) was repeated with 0.75 mL of NMR solvent as opposed to the 0.25 mL typically used to confirm that CO<sub>2</sub>, if ever present in the headspace of the NMR tube, was not a factor in the measurement of the equilibrium constants.



**Scheme 4.8.**  $K_{\text{eq}}$  measurements of *para*-substituted nickel hydride and formate complexes

**Table 4.1** Relative thermodynamic measurements of POCOP complexes

Entry	X Group	X' Group	$K_{\text{eq}}$	$\Delta G_{\text{Ni}^{\text{I}}\text{H}} - \Delta G_{\text{Ni}^{\text{I}}\text{H}}$ (kcal/mol)
1	H	NMe <sub>2</sub>	3.08±0.11	0.65±0.03
2	H	OMe	1.34±0.11	0.17±0.05
3	F	H	2.64±0.2	0.57±0.04
4	OMe	NMe <sub>2</sub>	2.43±0.18	0.52±0.04
5	COOMe	NMe <sub>2</sub>	5.1±0.6	0.95±0.07
6	F	NMe <sub>2</sub>	7.3±0.7	1.16±0.07
7	F	OMe	2.97±0.10	0.63±0.03
8	COOMe	OMe	1.7±.2	0.31±0.07



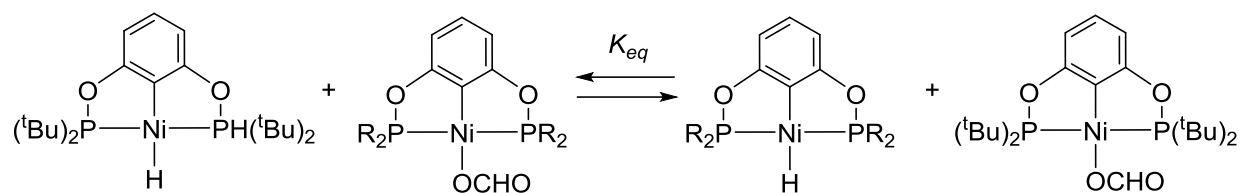
The measured equilibrium constants and  $\Delta\Delta G$  values for the reduction of CO<sub>2</sub> by different substituted nickel hydride complexes gave interesting results. The reduction of CO<sub>2</sub> by nickel complexes appears to be favored by nickel complexes with more electron-donating substituents on the pincer backbone. This suggests that the destabilization effect on the nickel hydride complex is more impactful than the destabilization effect on the nickel formate. The largest  $\Delta\Delta G$  (1.2 kcal/mol) was observed for the reaction between fluoro-substituted nickel hydride and dimethylamino-substituted nickel formate (entry 6). Differences of this large have been known to drastically impact reactivity and even mechanisms.<sup>14</sup> Given that all crystal structures show little variation around the coordination sphere, the reactivity differences observed here are due to electronic effects not from changes in structure or orientation. Mathematically, equilibrium constants should be multiples of each other (e.g., entry 1 = entry 2  $\times$  entry 4), which is observed in these measurements. The complexes appear to form a trend following their  $\sigma_p$  values, although the fluoro-substituted complex appears to be less favorable in the reduction of CO<sub>2</sub> than anticipated. This can possibly be explained by fluorine  $\pi$ -donation having a greater effect on the destabilization of the formate complex than on the hydride complex.

#### **4.4 Effects of *P*-Substituents on the Relative Thermodynamics for the Reduction of CO<sub>2</sub> by POCOP Nickel Pincer Hydride Complexes**

To further understand the structure-reactivity relationships, additional pincer ligand systems were examined. In addition to the modification to the pincer backbone, the POCOP ligand system could be altered through the change of the substituents on the phosphorous donor atoms. This change can be readily made by using different chlorophosphines when making the starting nickel chloride complexes. Complexes with isopropyl (<sup>i</sup>Pr) and cyclopentyl (<sup>c</sup>Pe) substituents on

the phosphorous centers were previously reported,<sup>3a,12a</sup> and those with cyclohexyl (Cy) substituents were prepared similarly. These changes to the phosphorous centers can have a slight change to the donor ability of the phosphorous atoms, but their largest impact is on the steric bulk that they create around the nickel center. The *tert*-butyl-substituted complexes are more sterically demanding around the nickel center whereas the isopropyl and cyclohexyl derivatives are sterically more accessible. The cyclopentyl-substituted complexes should be less sterically bulky compared to the isopropyl analog due to decreased C–P–C angles induced by the rings, although such a difference is relatively small.

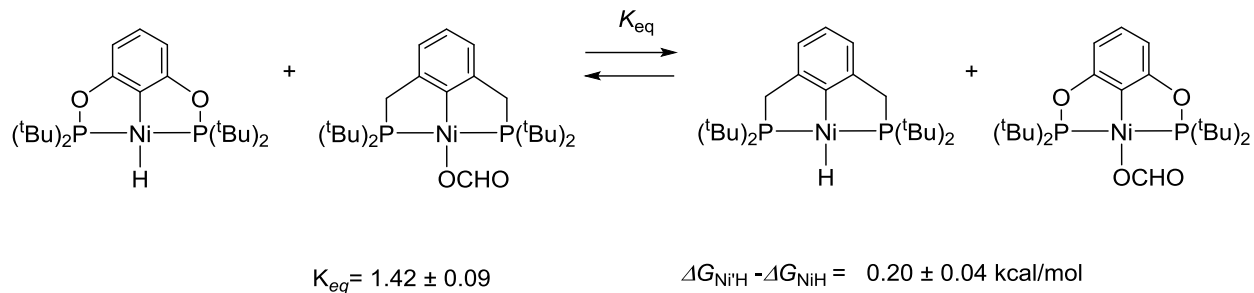
When comparing the  $\Delta\Delta G$  values measured for the POCOP complexes with different phosphorous substituents, the impact is noticeable. Using the *tert*-butyl-substituted complexes as the benchmark molecules, the  $\Delta\Delta G$  values range from 1.36 to 1.55 kcal/mol. This is an even greater impact than the previously discussed electronic effects induced by various substituents at the *para* position of the POCOP pincer ligand. The result here signifies that the steric environment affects the ability of the nickel complexes to reduce CO<sub>2</sub> more than the electronic effects, especially considering that *tert*-butyl groups are more electron donating than the isopropyl, cyclohexyl, and cyclopentyl groups. This is also significant because steric bulk is not thought to have a large impact on the reactivity of the hydride apart from preventing dimerization and decomposition pathways. This suggests that the major impact on these complexes comes from the stabilization of the formate complexes by creating less steric repulsion around the nickel center. The difference in the  $\Delta\Delta G$  values between the isopropyl-, cyclohexyl-, and cyclopentyl-substituted complexes appear to support this assertion; however, the error in measurements leads to uncertainty in this statement.



R = <sup>i</sup> Pr	$K_{eq} = .097 \pm 0.04$	$\Delta G_{Ni^iH} - \Delta G_{NiH} = 1.36 \pm 0.19$ kcal/mol
R = Cy	$K_{eq} = .08 \pm 0.03$	$\Delta G_{Ni^iH} - \Delta G_{NiH} = 1.45 \pm 0.15$ kcal/mol
R = <sup>o</sup> Pe	$K_{eq} = .07 \pm 0.01$	$\Delta G_{Ni^iH} - \Delta G_{NiH} = 1.55 \pm 0.06$ kcal/mol

**Scheme 4.9** Thermodynamic measurements of nickel hydride and formate complexes bearing different *P*-substituents

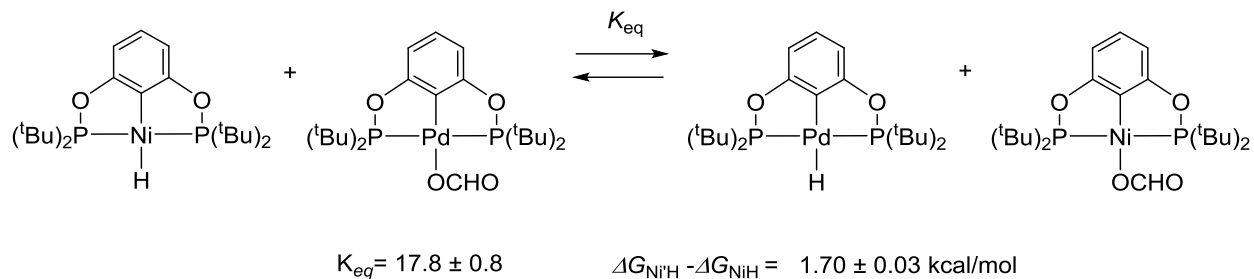
To further probe the relative thermodynamics of CO<sub>2</sub> reduction by nickel hydride complexes, pincer systems other than the aforementioned POCOP system could be examined. One attractive ligand system is the related PCP ligand system because of its similarity and the relative ease of synthesis. The main difference in POCOP and PCP ligand systems is that PCP pincer ligands have been found to be slightly more electron donating while also having slightly larger bite angles leading to more sterically hindered nickel center. Given these factors, it was unsurprising that the reduction of CO<sub>2</sub> was more favorable with a POCOP pincer ligand, although the difference is small ( $\Delta\Delta G = 0.2$  kcal/mol) (Scheme 4.10). This difference further confirms that the steric effects are more dominating than the electronic ones.



**Scheme 4.10** Thermodynamic measurements of nickel hydride and formate complexes bearing POCOP and PCP pincer ligands

#### 4.5 Comparison of Nickel and Palladium Complexes

We also sought out to determine what effects the metal might have on the reactivity towards CO<sub>2</sub> reduction. Palladium POCOP pincer complexes were chosen for this study due to their square planar geometry that is similar to all of the tested nickel complexes. Additionally, it would provide some insight into periodic trends in the reduction of CO<sub>2</sub>. The literature has several examples of catalytic CO<sub>2</sub> reduction with palladium pincer complexes that are analogous to nickel systems; however, it is not known whether the differences in efficiency are due to the stoichiometric reduction of CO<sub>2</sub> or the regeneration of the palladium hydride complexes. The <sup>t</sup>BuPOCOP palladium hydride and formate complexes were thus made as reported in the literature.<sup>15,16</sup> The measured  $K_{eq}$  (17.8) and the calculated  $\Delta\Delta G$  value (1.70 kcal/mol) showed that the nickel system was significantly more favorable in the reduction of CO<sub>2</sub> to the formate complex (Scheme 4.11). This can be explained by the better Lewis acid/base pair formed with the nickel-oxygen bond than the palladium-oxygen bond.



**Scheme 4.11** Thermodynamic measurements of nickel and palladium hydride and formate POCOP complexes

## 4.6 Conclusions

In conclusion, a series of nickel POCOP pincer hydride and formate complexes have been synthesized. These complexes were used to measure the  $\Delta\Delta G$  values for the reduction of  $\text{CO}_2$  by the hydride complexes to the formate complexes. It was found that the nickel complexes with more electron-donating ligands were thermodynamically more favorable for the reduction process. Ligands with less steric bulk around the nickel center were also found to promote  $\text{CO}_2$  reduction by nickel hydride complexes, either using less bulky phosphorus substituents ( $i\text{Pr}$ ,  $^o\text{Pe}$ , and  $\text{Cy}$  vs.  $t\text{Bu}$ ) or by using the POCOP ligand system (vs. the PCP ligand system). Also found was that palladium was less efficient than nickel in promoting the reduction of  $\text{CO}_2$  to a formate complex. Future work includes extending our method to other pincer and non-pincer ligand systems as well as other metal systems (square planar or other geometries).

## 4.7 Experimental Section

**Materials and Methods.** Unless otherwise mentioned, all the organometallic compounds were prepared and handled under an argon atmosphere using Schlenk and glovebox techniques. Dry

and oxygen-free solvents (THF, pentane, and toluene) were collected from an Innovative Technology solvent purification system. Benzene-*d*<sub>6</sub> was distilled over sodium benzophenone. THF, toluene, and resorcinol were purchased from Fisher scientific. Deuterated solvents were purchased from Cambridge Isotope Labs. All other chemicals were purchased from Sigma Aldrich and were used without further purification. Fluoro- and dimethylamino-substituted resorcinol were prepared according to literature procedures.<sup>8c, 10a</sup> Nickel complexes **13b**, **13c**, **12e**, **14b**, **14c**, and **15c** were prepared using the literature procedures.<sup>2a, 8b, 12a</sup> <sup>1</sup>H, <sup>13</sup>C {<sup>1</sup>H} and <sup>31</sup>P {<sup>1</sup>H} NMR spectra were recorded on a Bruker Avance-400 MHz spectrometer. Chemical shifts in NMR were referenced to residual solvents or TMS (0 ppm) present in CDCl<sub>3</sub>. <sup>31</sup>P {<sup>1</sup>H} NMR spectrum were referenced externally to 85% H<sub>3</sub>PO<sub>4</sub> (0 ppm).

**General Procedure for the Synthesis of [2,6-(<sup>t</sup>Bu<sub>2</sub>PO)<sub>2</sub>C<sub>6</sub>H<sub>2</sub>X]NiCl (X = F, NMe<sub>2</sub>).** To a flame dried Schlenk flask, a solution of resorcinol derivative (4.5 mmol) was made in toluene (100 mL). To the solution, NaH (10 mmol, 0.240 g) was added slowly (15 min). The mixture was then heated to reflux for 3 h. The reaction mixture was then cooled to room temperature and <sup>t</sup>Bu<sub>2</sub>PCl (10mmol, 1.90 mL) was added dropwise. The mixture was then refluxed for 1 h. After cooling to room temperature, nickel chloride (4.5 mmol, 0.583 g) and NEt<sub>3</sub> (11 mmol, 1.54 mL) were added to the suspension, followed by refluxing for 18 h. The green-orange suspension was then cooled to room temperature and gravity filtered. The resulting solution was pumped to dryness to yield a sticky yellow solid, which was purified through washing with MeOH or by column chromatography.

**Synthesis of [2,6-(<sup>t</sup>Bu<sub>2</sub>PO)<sub>2</sub>C<sub>6</sub>H<sub>2</sub>F]NiCl.** A solution of 5-fluororesorcinol (0.576 g, 4.5 mmol) was prepared by dissolving in 100 mL of toluene. Following the general procedure described above, a sticky yellow solid was obtained. Flash column chromatography was run by eluting the product with pentane/CH<sub>2</sub>Cl<sub>2</sub> (first 9 : 1 and then 1 : 1). After removal of the solvent, the product

was obtained as a crystalline solid (81% yield, NE225).  $^1\text{H}$  NMR (400 MHz,  $\text{C}_6\text{D}_6$ ,  $\delta$ ): 1.40 (vt,  $J_{\text{P-H}} = 8$  Hz,  $\text{CH}_3$ , 36H), 6.30 (d,  $J_{\text{F-H}} = 8$  Hz, Ar, 2H).  $^{13}\text{C}\{^1\text{H}\}$  NMR (101 MHz,  $\text{C}_6\text{D}_6$ ,  $\delta$ ): 27.82 (t,  $J_{\text{P-C}} = 3.0$  Hz,  $\text{CH}_3$ ), 39.21 (t,  $J_{\text{P-C}} = 6.0$  Hz,  $\text{CCH}_3$ ), 93.81 (dt,  $J_{\text{F-C}} = 25.3$  Hz,  $J_{\text{P-C}} = 6.1$  Hz,  $\text{C}_{\text{meta}}$ ), 119.54 (td,  $J_{\text{P-C}} = 21.2$  Hz,  $J_{\text{F-C}} = 3.0$  Hz,  $\text{C}_{\text{ipso}}$ ), 164.20 (d,  $J_{\text{F-C}} = 242.4$  Hz,  $\text{C}_{\text{para}}$ ), 169.33 (dt,  $J_{\text{F-C}} = 15.15$  Hz,  $J_{\text{P-C}} = 10.1$  Hz,  $\text{C}_{\text{ortho}}$ ).  $^{31}\text{P}\{^1\text{H}\}$  NMR (162 MHz,  $\text{C}_6\text{D}_6$ ,  $\delta$ ): 190.96 (s). Anal. Calcd for  $\text{C}_{22}\text{H}_{38}\text{O}_2\text{P}_2\text{NiClF}$ : C, 51.85; H, 7.52. Found: C, 52.05; H, 7.60.

**Synthesis of [2,6-( $^t\text{Bu}_2\text{PO}$ ) $_2\text{C}_6\text{H}_2\text{NMe}_2$ ]NiCl.** A solution of 5-dimethylaminoresorcinol (0.690 g, 4.5 mmol) was prepared by dissolving in 100 mL of toluene. Following the general procedure described above, a sticky red-orange solid was obtained. The solid was washed with 15 consecutive portions of cold MeOH (0  $^\circ\text{C}$ , 0.5 mL each time). After drying under vacuum, the product was isolated as an orange crystalline solid (88% yield, NE212).  $^1\text{H}$  NMR (400 MHz,  $\text{C}_6\text{D}_6$ ,  $\delta$ ): 1.53 (vt,  $J_{\text{P-H}} = 8$  Hz,  $\text{CH}_3$ , 36H), 2.44 (s,  $\text{CH}_3$ , 6H) 6.13 (s, Ar, 2H).  $^{13}\text{C}\{^1\text{H}\}$  NMR (101 MHz,  $\text{C}_6\text{D}_6$ ,  $\delta$ ): 28.05 (t,  $J_{\text{P-C}} = 3.0$  Hz,  $\text{CH}_3$ ), 39.09 (t,  $J_{\text{P-C}} = 7.0$  Hz,  $\text{CCH}_3$ ), 40.16 (s,  $\text{CH}_3$ ), 91.02 (t,  $J_{\text{P-C}} = 6.1$  Hz,  $\text{C}_{\text{meta}}$ ), 110.16 (t,  $J_{\text{P-C}} = 22.2$  Hz,  $\text{C}_{\text{ipso}}$ ), 152.84 (s,  $\text{C}_{\text{para}}$ ), 170.63 (t,  $J_{\text{P-C}} = 10.1$  Hz,  $\text{C}_{\text{ortho}}$ ).  $^{31}\text{P}\{^1\text{H}\}$  NMR (162 MHz,  $\text{C}_6\text{D}_6$ ,  $\delta$ ): 189.07 (s). Anal. Calcd for  $\text{C}_{24}\text{H}_{44}\text{O}_2\text{P}_2\text{NiClN}$ : C, 53.91; H, 8.29. Found: C, 54.20; H, 8.36.

**General Procedure for the Synthesis of [2,6-( $^t\text{Bu}_2\text{PO}$ ) $_2\text{C}_6\text{H}_2\text{X}$ ]NiH.** To a flame dried Schlenk flask was added a solution of nickel chloride complex (0.45-0.49 mmol) in toluene (25mL). Fresh  $\text{LiAlH}_4$  (45-100 mmol) was added to the solution. The green suspension was rigorously stirred for 18 h or until the in-situ  $^{31}\text{P}\{^1\text{H}\}$  NMR showed no chloride complex remaining. The suspension was then filtered over a pad of Celite, which was eluted with an additional 75mL of toluene. The solution was then evaporated to dryness. The remaining powder was washed with cold MeOH (0  $^\circ\text{C}$ ) to yield an analytically pure sample.

**Synthesis of [2,6-(<sup>t</sup>Bu<sub>2</sub>PO)<sub>2</sub>C<sub>6</sub>H<sub>2</sub>F]NiH.** A solution of [2,6-(<sup>t</sup>Bu<sub>2</sub>PO)<sub>2</sub>C<sub>6</sub>H<sub>2</sub>F]NiCl (0.250 g, 0.49 mmol) was prepared by dissolving in 25 mL of toluene. Following the general procedure with 0.970 g of LiAlH<sub>4</sub> (2.5mmol), a yellow-brown solid was obtained. Washing the crude product with 3 portions of cold MeOH (0 °C, 1 mL each time) followed by drying under vacuum yielded an analytically pure pale yellow solid (48% yield, NE238). <sup>1</sup>H NMR (400 MHz, C<sub>6</sub>D<sub>6</sub>, δ): 1.26 (vt, *J*<sub>P-H</sub> = 8 Hz, CH<sub>3</sub>, 36H), 6.64 (d, *J*<sub>F-H</sub> = 12 Hz, Ar, 2H), -8.13 (t, *J*<sub>P-H</sub> = 92 Hz, NiH, 1H). <sup>13</sup>C {<sup>1</sup>H} NMR (101 MHz, C<sub>6</sub>D<sub>6</sub>, δ): 28.26 (t, *J*<sub>P-C</sub> = 3.0 Hz, CH<sub>3</sub>), 37.76 (t, *J*<sub>P-C</sub> = 9.1 Hz, CCH<sub>3</sub>), 93.21 (dt, *J*<sub>F-C</sub> = 25.76 Hz, *J*<sub>P-C</sub> = 6.1 Hz, *C*<sub>meta</sub>), 136.86 (t, *J*<sub>P-C</sub> = 17.2 Hz, *C*<sub>ipso</sub>), 164.57 (d, *J*<sub>F-C</sub> = 240.4 Hz, *C*<sub>para</sub>), 168.19 (dt, *J*<sub>F-C</sub> = 14.1 Hz, *J*<sub>P-C</sub> = 10.1 Hz, *C*<sub>ortho</sub>). <sup>31</sup>P {<sup>1</sup>H} NMR (162 MHz, C<sub>6</sub>D<sub>6</sub>, δ): 224.74 (s). Anal. Calcd for C<sub>22</sub>H<sub>39</sub>O<sub>2</sub>P<sub>2</sub>NiF: C, 55.61; H, 8.27. Found: C, 55.37; H, 8.26.

**Synthesis of [2,6-(<sup>t</sup>Bu<sub>2</sub>PO)<sub>2</sub>C<sub>6</sub>H<sub>2</sub>NMe<sub>2</sub>]NiH.** A solution of [2,6-(<sup>t</sup>Bu<sub>2</sub>PO)<sub>2</sub>C<sub>6</sub>H<sub>2</sub>NMe<sub>2</sub>]NiCl (0.250 g, 0.47 mmol) was prepared by dissolving in 25 mL of toluene. Following the general procedure with 0.178 g of LiAlH<sub>4</sub> (4.7 mmol), a yellow-orange solid was obtained. Washing the crud product with 5 portions of cold MeOH (0 °C, 1 mL each time) followed by drying under vacuum yielded an analytically pure pale yellow solid (55% yield, NE237). <sup>1</sup>H NMR (400 MHz, C<sub>6</sub>D<sub>6</sub>, δ): 1.38 (vt, *J*<sub>P-H</sub> = 8 Hz, CH<sub>3</sub>, 36H), 2.57 (s, CH<sub>3</sub>, 6H) 6.39 (s, Ar, 2H), -7.97 (t, *J*<sub>P-H</sub> = 52 Hz, NiH, 1H). <sup>13</sup>C {<sup>1</sup>H} NMR (101 MHz, C<sub>6</sub>D<sub>6</sub>, δ): 28.52 (t, *J*<sub>P-C</sub> = 4.0 Hz, CH<sub>3</sub>), 37.37 (t, *J*<sub>P-C</sub> = 9.1 Hz, CCH<sub>3</sub>), 40.67 (s, CH<sub>3</sub>), 90.70 (t, *J*<sub>P-C</sub> = 6.1 Hz, *C*<sub>meta</sub>), 129.34 (t, *J*<sub>P-C</sub> = 19.19 Hz, *C*<sub>ipso</sub>), 153.30 (s, *C*<sub>para</sub>), 169.62 (t, *J*<sub>P-C</sub> = 10.1 Hz, *C*<sub>ortho</sub>). <sup>31</sup>P {<sup>1</sup>H} NMR (162 MHz, C<sub>6</sub>D<sub>6</sub>, δ): 221.76 (s). Anal. Calcd for C<sub>24</sub>H<sub>45</sub>O<sub>2</sub>P<sub>2</sub>NiN: C, 57.62; H, 9.07. Found: C, 55.49; H, 8.67.

**General Procedure for the Synthesis of [2,6-(<sup>t</sup>Bu<sub>2</sub>PO)<sub>2</sub>C<sub>6</sub>H<sub>2</sub>X]NiOCOH.** To a flame dried Schlenk flask, nickel hydride complex (0.50-0.55 mmol) was dissolved in 10 mL of toluene. The



resulting solution was exposed to a stream of CO<sub>2</sub>. After allowing the solution to stir for 15 min, the solvent was evaporated to generate analytically pure samples.

**Synthesis of [2,6-(<sup>t</sup>Bu<sub>2</sub>PO)<sub>2</sub>C<sub>6</sub>H<sub>2</sub>F]NiOCOH.** A solution of [2,6-(<sup>t</sup>Bu<sub>2</sub>PO)<sub>2</sub>C<sub>6</sub>H<sub>2</sub>F]NiH (0.100 g, 0.21 mmol) was prepared by dissolving in 5 mL of toluene. Following the general procedure described above, a yellow solid was obtained (81% yield, NE473). <sup>1</sup>H NMR (400 MHz, C<sub>6</sub>D<sub>6</sub>, δ): 1.48 (vt, *J*<sub>P-H</sub> = 8.0 Hz, CH<sub>3</sub>, 36H), 6.37 (d, *J*<sub>F-H</sub> = 4 Hz, Ar, 2H), 8.45 (s, OCOH, 1H). <sup>13</sup>C {<sup>1</sup>H} NMR (101 MHz, C<sub>6</sub>D<sub>6</sub>, δ): 27.48 (s, CH<sub>3</sub>), 39.08 (t, *J*<sub>P-C</sub> = 6.1 Hz, CCH<sub>3</sub>), 93.98 (d t, *J*<sub>F-C</sub> = 25.25 Hz, *J*<sub>P-C</sub> = 6.1 Hz, C<sub>meta</sub>), 114.77 (t d, *J*<sub>P-C</sub> = 40.4 Hz, *J*<sub>F-C</sub> = 3.0 Hz C<sub>ipso</sub>), 164.46 (d, *J*<sub>F-C</sub> = 242.4 Hz, C<sub>para</sub>), 169.58 (s, OCOH), 169.59 (dt, *J*<sub>F-C</sub> = 14.1 Hz, *J*<sub>P-C</sub> = 5.1 Hz, C<sub>ortho</sub>). <sup>31</sup>P {<sup>1</sup>H} NMR (162 MHz, C<sub>6</sub>D<sub>6</sub>, δ): 190.93 (s). Anal. Calcd for C<sub>23</sub>H<sub>39</sub>O<sub>4</sub>P<sub>2</sub>NiF: C, 53.21; H, 7.57. Found: C, 52.93; H, 7.67.

**Synthesis of [2,6-(<sup>t</sup>Bu<sub>2</sub>PO)<sub>2</sub>C<sub>6</sub>H<sub>2</sub>NMe<sub>2</sub>]NiOCOH.** A solution of [2,6-(<sup>t</sup>Bu<sub>2</sub>PO)<sub>2</sub>C<sub>6</sub>H<sub>2</sub>NMe<sub>2</sub>]NiH (0.150 g, 0.30 mmol) was prepared by dissolving in 10 mL of toluene. Following the general procedure described above, an orange-brown solid was obtained (91% yield, NE216). <sup>1</sup>H NMR (400 MHz, C<sub>6</sub>D<sub>6</sub>, δ): 1.47 (vt, *J*<sub>P-H</sub> = 8 Hz, CH<sub>3</sub>, 36H), 2.42 (s, CH<sub>3</sub>, 6H) 6.06 (s, Ar, 2H), 8.49 (t, *J*<sub>P-H</sub> = 4 Hz, OCOH, 1H). <sup>13</sup>C {<sup>1</sup>H} NMR (101 MHz, C<sub>6</sub>D<sub>6</sub>, δ): 27.61 (t, *J*<sub>P-C</sub> = 3.0 Hz, CH<sub>3</sub>), 38.80 (t, *J*<sub>P-C</sub> = 7.1 Hz, CCH<sub>3</sub>), 40.08 (s, CH<sub>3</sub>), 91.10 (t, *J*<sub>P-C</sub> = 6.1 Hz, C<sub>meta</sub>), 104.63 (t, *J*<sub>P-C</sub> = 24.2 Hz, C<sub>ipso</sub>), 152.95 (s, C<sub>para</sub>), 167.68 (s, OCOH), 170.72 (t, *J*<sub>P-C</sub> = 9.1 Hz, C<sub>ortho</sub>). <sup>31</sup>P {<sup>1</sup>H} NMR (162 MHz, C<sub>6</sub>D<sub>6</sub>, δ): 188.19 (s). Anal. Calcd for C<sub>25</sub>H<sub>45</sub>O<sub>4</sub>P<sub>2</sub>NiN: C, 55.17; H, 8.33. Found: C, 54.89; H, 8.52.

**Synthesis of [2,6-(<sup>t</sup>Bu<sub>2</sub>PO)<sub>2</sub>C<sub>6</sub>H<sub>2</sub>OMe]NiOCOH.** A solution of [2,6-(<sup>t</sup>Bu<sub>2</sub>PO)<sub>2</sub>C<sub>6</sub>H<sub>2</sub>OMe]NiH (0.100 g, 0.21 mmol) was prepared by dissolving in 10 mL of toluene. Following the general procedure described above, a brown solid was obtained (88% yield, NE258). <sup>1</sup>H NMR (400 MHz,

C<sub>6</sub>D<sub>6</sub>, δ): 1.44 (vt,  $J_{P-H} = 8$  Hz, CH<sub>3</sub>, 36H), 3.24 (s, CH<sub>3</sub>, 3H) 6.29 (s, Ar, 2H), 8.45 (t,  $J_{P-H} = 4$  Hz, OCOH, 1H). <sup>13</sup>C{<sup>1</sup>H} NMR (101 MHz, C<sub>6</sub>D<sub>6</sub>, δ): 27.63 (t,  $J_{P-C} = 3.0$  Hz, CH<sub>3</sub>), 38.99 (t,  $J_{P-C} = 6.1$  Hz, CCH<sub>3</sub>), 54.94 (s, CH<sub>3</sub>), 92.74 (t,  $J_{P-C} = 5.1$  Hz,  $C_{meta}$ ), 110.03 (t,  $J_{P-C} = 22.2$  Hz,  $C_{ipso}$ ), 162.35 (s,  $C_{para}$ ), 167.68 (s, OCOH), 170.23 (t,  $J_{P-C} = 9.1$  Hz,  $C_{ortho}$ ). <sup>31</sup>P{<sup>1</sup>H} NMR (162 MHz, C<sub>6</sub>D<sub>6</sub>, δ): 192.35 (s). Anal. Calcd for C<sub>24</sub>H<sub>42</sub>O<sub>5</sub>P<sub>2</sub>Ni: C, 54.26; H, 7.97. Found: C, 54.56; H, 8.09.

**Synthesis of [2,6-(<sup>t</sup>Bu<sub>2</sub>PO)<sub>2</sub>C<sub>6</sub>H<sub>2</sub>COOMe]NiOCOH.** To a flame dried Schlenk flask was added [2,6-(<sup>t</sup>Bu<sub>2</sub>PO)<sub>2</sub>C<sub>6</sub>H<sub>2</sub>COOMe]NiCl (0.500g, 0.91 mmol) and 25 mL of THF. Silver triflate (1.0 mmol) was then added to the solution and the suspension was stirred under dark conditions for 6 h. The mixture was then filtered through a short plug of Celite and the collected solution was evaporated to dryness. The resulting orange solid was used without further purification. Crystal structure (Figure 4.8) suggests that the triflate complex is highly moisture sensitive and should be treated as such.

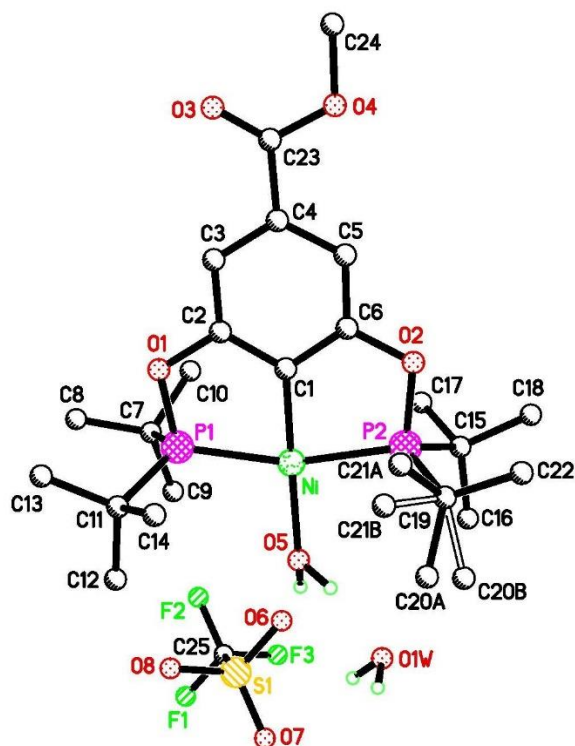


**Figure 4.8** ORTEP drawing of  $[\{2,6\text{-}(t\text{Bu}_2\text{PO})_2\text{C}_6\text{H}_2\text{COOMe}\}\text{Ni}(\text{H}_2\text{O})]\text{OTf}\cdot\text{H}_2\text{O}$  at the 50 % probability level. Selected bond lengths (Å) and angles ( $^\circ$ ): Ni–C (1) 1.872(2), Ni–O(5) 1.927(2), Ni–P(1) 2.1992(6), Ni–P(2) 2.1961(6), P(1)–Ni(1)–P(2) 163.50(3), C(1)–Ni–O(5) 176.40(10).

A solution of the crude triflate complex was dissolved in 10 mL of benzene, followed by the addition of sodium formate (1.0 mmol, 0.068 g). The reaction mixture turned from orange to brown and then dark, which was filtered through a pad of Celite. The collected solution was evaporated to dryness. The resulting brown powder was washed with pentane ( $3 \times 5$  mL) to yield

a brown crystalline solid 79% yield, NE299).  $^1\text{H}$  NMR (400 MHz,  $\text{C}_6\text{D}_6$ ,  $\delta$ ): 1.36 (vt,  $J_{\text{P-H}} = 8$  Hz,  $\text{CH}_3$ , 36H), 3.47 (s,  $\text{CH}_3$ , 3H) 7.49 (s, Ar, 2H), 8.36 (t,  $J_{\text{P-H}} = 4$  Hz, OCOH, 1H).  $^{13}\text{C}\{^1\text{H}\}$  NMR (101 MHz,  $\text{C}_6\text{D}_6$ ,  $\delta$ ): 27.35 (t,  $J_{\text{P-C}} = 3.0$  Hz,  $\text{CH}_3$ ), 39.09 (t,  $J_{\text{P-C}} = 7.1$  Hz,  $\text{CCH}_3$ ), 51.42 (s,  $\text{CH}_3$ ), 106.74 (t,  $J_{\text{P-C}} = 6.1$  Hz,  $\text{C}_{\text{meta}}$ ), 130.15 (t,  $J_{\text{P-C}} = 21.2$  Hz,  $\text{C}_{\text{ipso}}$ ), 131.54 (s,  $\text{C}_{\text{para}}$ ), 166.39 (s, COOMe), 167.45 (s, OCOH), 169.72 (t,  $J_{\text{P-C}} = 9.1$  Hz,  $\text{C}_{\text{ortho}}$ ).  $^{31}\text{P}\{^1\text{H}\}$  NMR (162 MHz,  $\text{C}_6\text{D}_6$ ,  $\delta$ ): 192.05 (s). Anal. Calcd for  $\text{C}_{24}\text{H}_{42}\text{O}_5\text{P}_2\text{Ni}$ : C, 54.26; H, 7.97. Found: C, 55.47; H, 7.45.

**Synthesis of  $[2,6\text{-}(\text{tBu}_2\text{PO})_2\text{C}_6\text{H}_2\text{COOMe}]_2\text{NiH}$ .**  $[2,6\text{-}(\text{tBu}_2\text{PO})_2\text{C}_6\text{H}_2\text{COOMe}]_2\text{NiOCOH}$  complex (0.150 g, 0.94 mmol) was placed in a sublimation apparatus under an inert atmosphere with a chilled water collection vessel. The apparatus was placed under high vacuum while slowly heated to 170 °C using an oil bath. The complex was allowed to decarboxylate and sublime for 18 h. A pale yellow crystalline material was collected (9% yield, NE366).  $^1\text{H}$  NMR (400 MHz,  $\text{C}_6\text{D}_6$ ,  $\delta$ ): 1.25 (vt,  $J_{\text{P-H}} = 8$  Hz,  $\text{CH}_3$ , 36H), 3.51 (s,  $\text{CH}_3$ , 3H) 7.80 (s, Ar, 2H), -7.90 (t,  $J_{\text{P-H}} = 52$  Hz, NiH, 1H).  $^{13}\text{C}\{^1\text{H}\}$  NMR (101 MHz,  $\text{C}_6\text{D}_6$ ,  $\delta$ ): 28.55 (t,  $J_{\text{P-C}} = 3.0$  Hz,  $\text{CH}_3$ ), 38.18 (t,  $J_{\text{P-C}} = 8.1$  Hz,  $\text{CCH}_3$ ), 51.59 (s,  $\text{CH}_3$ ), 106.46 (t,  $J_{\text{P-C}} = 6.1$  Hz,  $\text{C}_{\text{meta}}$ ) 151.29 (t,  $J_{\text{P-C}} = 14.1$  Hz,  $\text{C}_{\text{ipso}}$ ), 131.48 (s,  $\text{C}_{\text{para}}$ ), 167.52 (s, COOMe), 168.82 (t,  $J_{\text{P-C}} = 9.1$  Hz,  $\text{C}_{\text{ortho}}$ ).  $^{31}\text{P}\{^1\text{H}\}$  NMR (162 MHz,  $\text{C}_6\text{D}_6$ ,  $\delta$ ): 221.79 (s). Anal. Calcd for  $\text{C}_{24}\text{H}_{42}\text{O}_4\text{P}_2\text{Ni}$ : C, 55.95; H, 8.22. Found C, 53.79; H, 8.77.

**General Procedure for the Thermodynamic Measurements.** 10 mg of a hydride complex and 10 mg of a formate complex were added to a J-Young NMR tube, followed by the addition of 0.25 mL of benzene- $d_6$ . The solution was kept at 23 °C until a consistent equilibrium constant was measured for 3 consecutive days. The experiment was repeated by approaching the equilibrium from the reverse direction.

## 4.8 References Cited

- (a) Wang, W.-H.; Himeda, Y.; Muckerman, J. T.; Manbeck, G. F.; Fujita, E., CO<sub>2</sub> Hydrogenation to Formate and Methanol as an Alternative to Photo- and Electrochemical CO<sub>2</sub> Reduction. *Chemical Reviews* **2015**, *115* (23), 12936-12973; (b) Rakowski Dubois, M.; Dubois, D. L., Development of Molecular Electrocatalysts for CO<sub>2</sub> Reduction and H<sub>2</sub> Production/Oxidation. *Accounts of Chemical Research* **2009**, *42* (12), 1974-1982.
- (a) Chakraborty, S.; Zhang, J.; Krause, J. A.; Guan, H., An Efficient Nickel Catalyst for the Reduction of Carbon Dioxide with a Borane. *Journal of the American Chemical Society* **2010**, *132* (26), 8872-8873; (b) Huang, F.; Zhang, C.; Jiang, J.; Wang, Z.-X.; Guan, H., How Does the Nickel Pincer Complex Catalyze the Conversion of CO<sub>2</sub> to a Methanol Derivative? A Computational Mechanistic Study. *Inorganic Chemistry* **2011**, *50* (8), 3816-3825.
- (a) Chakraborty, S.; Patel, Y. J.; Krause, J. A.; Guan, H., Catalytic Properties of Nickel Bis(phosphinite) Pincer Complexes in the Reduction of CO<sub>2</sub> to Methanol Derivatives. *Polyhedron* **2012**, *32* (1), 30-34; (b) Chakraborty, S.; Zhang, J.; Patel, Y. J.; Krause, J. A.; Guan, H., Pincer-Ligated Nickel Hydridoborate Complexes: the Dormant Species in Catalytic Reduction of Carbon Dioxide with Boranes. *Inorganic Chemistry* **2013**, *52* (1), 37-47.
- Suh, H.-W.; Guard, L. M.; Hazari, N., Synthesis and Reactivity of a Masked PSiP Pincer Supported Nickel Hydride. *Polyhedron* **2014**, *84*, 37-43.
- Rios, P.; Curado, N.; Lopez-Serrano, J.; Rodriguez, A., Selective Reduction of Carbon Dioxide to Bis(silyl)acetal Catalyzed by a PBP-Supported Nickel Complex. *Chemical Communications* **2016**, *52* (10), 2114-2117.
- Eberhardt, N. A.; Guan, H., Nickel Hydride Complexes. *Chemical Reviews* **2016**, *116* (15), 8373-8426.
- Suh, H.-W.; Schmeier, T. J.; Hazari, N.; Kemp, R. A.; Takase, M. K., Experimental and Computational Studies of the Reaction of Carbon Dioxide with Pincer-Supported Nickel and Palladium Hydrides. *Organometallics* **2012**, *31* (23), 8225-8236.
- (a) Ramakrishnan, S.; Chakraborty, S.; Brennessel, W. W.; Chidsey, C. E. D.; Jones, W. D., Rapid Oxidative Hydrogen Evolution from a Family of Square-Planar Nickel Hydride Complexes. *Chemical Science* **2016**, *7* (1), 117-127; (b) Li, H.; Meng, W.; Adhikary, A.; Li, S.; Ma, N.; Zhao, Q.; Yang, Q.; Eberhardt, N. A.; Leahy, K. M.; Krause, J. A.; Zhang, J.; Chen, X.; Guan, H., Metathesis Reactivity of Bis(phosphinite) Pincer Ligated Nickel Chloride, Isothiocyanate and Azide Complexes. *Journal of Organometallic Chemistry* **2016**, *804*, 132-141; (c) Göttker-Schnetmann, I.; White, P.; Brookhart, M., Iridium Bis(phosphinite) *p*-XPCP Pincer Complexes: Highly Active Catalysts for the Transfer Dehydrogenation of Alkanes. *Journal of the American Chemical Society* **2004**, *126* (6), 1804-1811; (d) Göttker-Schnetmann, I.; White, P. S.; Brookhart, M., Synthesis and Properties of Iridium Bis(phosphinite) Pincer Complexes (*p*-XPCP)IrH<sub>2</sub>, (*p*-XPCP)Ir(CO), (*p*-XPCP)Ir(H)(aryl), and {(*p*-XPCP)Ir}<sub>2</sub>{μ-N<sub>2</sub>} and Their Relevance in Alkane Transfer Dehydrogenation. *Organometallics* **2004**, *23* (8), 1766-1776.
- Vabre, B.; Spasyuk, D. M.; Zargarian, D., Impact of Backbone Substituents on POCOP-Ni Pincer Complexes: A Structural, Spectroscopic, and Electrochemical Study. *Organometallics* **2012**, *31* (24), 8561-8570.
- (a) Lao, D. B.; Owens, A. C. E.; Heinekey, D. M.; Goldberg, K. I., Partial Deoxygenation of Glycerol Catalyzed by Iridium Pincer Complexes. *ACS Catalysis* **2013**, *3* (10), 2391-2396; (b) Kang, P.; Meyer, T. J.; Brookhart, M., Selective Electrocatalytic Reduction of Carbon Dioxide to Formate by a Water-Soluble Iridium Pincer Catalyst. *Chemical Science* **2013**, *4* (9), 3497-3502.

11. Hansch, C.; Leo, A.; Taft, R. W., A Survey of Hammett Substituent Constants and Resonance and Field Parameters. *Chemical Reviews* **1991**, *91* (2), 165-195.
12. (a) Chakraborty, S.; Krause, J. A.; Guan, H., Hydrosilylation of Aldehydes and Ketones Catalyzed by Nickel PCP-Pincer Hydride Complexes. *Organometallics* **2009**, *28* (2), 582-586; (b) Pandarus, V.; Zargarian, D., New Pincer-Type Diphosphinito (POCOP) Complexes of Nickel. *Organometallics* **2007**, *26* (17), 4321-4334; (c) Gómez-Benítez, V.; Baldovino-Pantaleón, O.; Herrera-Álvarez, C.; Toscano, R. A.; Morales-Morales, D., High Yield Thiolation of Iodobenzene Catalyzed by the Phosphinite Nickel PCP Pincer Complex:  $[\text{NiCl}\{\text{C}_6\text{H}_3\text{-2,6-(OPPh}_2)_2\}]$ . *Tetrahedron Letters* **2006**, *47* (29), 5059-5062.
13. Brooks, P. R.; Wirtz, M. C.; Vetelino, M. G.; Rescek, D. M.; Woodworth, G. F.; Morgan, B. P.; Coe, J. W., Boron Trichloride/Tetra-n-Butylammonium Iodide: A Mild, Selective Combination Reagent for the Cleavage of Primary Alkyl Aryl Ethers. *The Journal of Organic Chemistry* **1999**, *64* (26), 9719-9721.
14. (a) Huang, G.; Kalek, M.; Liao, R.-Z.; Himo, F., Mechanism, Reactivity, and Selectivity of the Iridium-Catalyzed C(sp<sup>3</sup>)-H Borylation of Chlorosilanes. *Chemical Science* **2015**, *6* (3), 1735-1746; (b) Xu, L.; Hilton, M. J.; Zhang, X.; Norrby, P.-O.; Wu, Y.-D.; Sigman, M. S.; Wiest, O., Mechanism, Reactivity, and Selectivity in Palladium-Catalyzed Redox-Relay Heck Arylations of Alkenyl Alcohols. *Journal of the American Chemical Society* **2014**, *136* (5), 1960-1967.
15. Adhikary, A.; Schwartz, J. R.; Meadows, L. M.; Krause, J. A.; Guan, H., Interaction of Alkynes with Palladium POCOP-Pincer Hydride Complexes and its Unexpected Relation to Palladium-Catalyzed Hydrogenation of Alkynes. *Inorganic Chemistry Frontiers* **2014**, *1* (1), 71-82.
16. Adhikary, A. *Synthesis and Catalytic Applications of Nickel and Palladium Pincer Complexes*. Ph.D. Dissertation, University of Cincinnati: Cincinnati, OH 2015.

**Chapter 5**

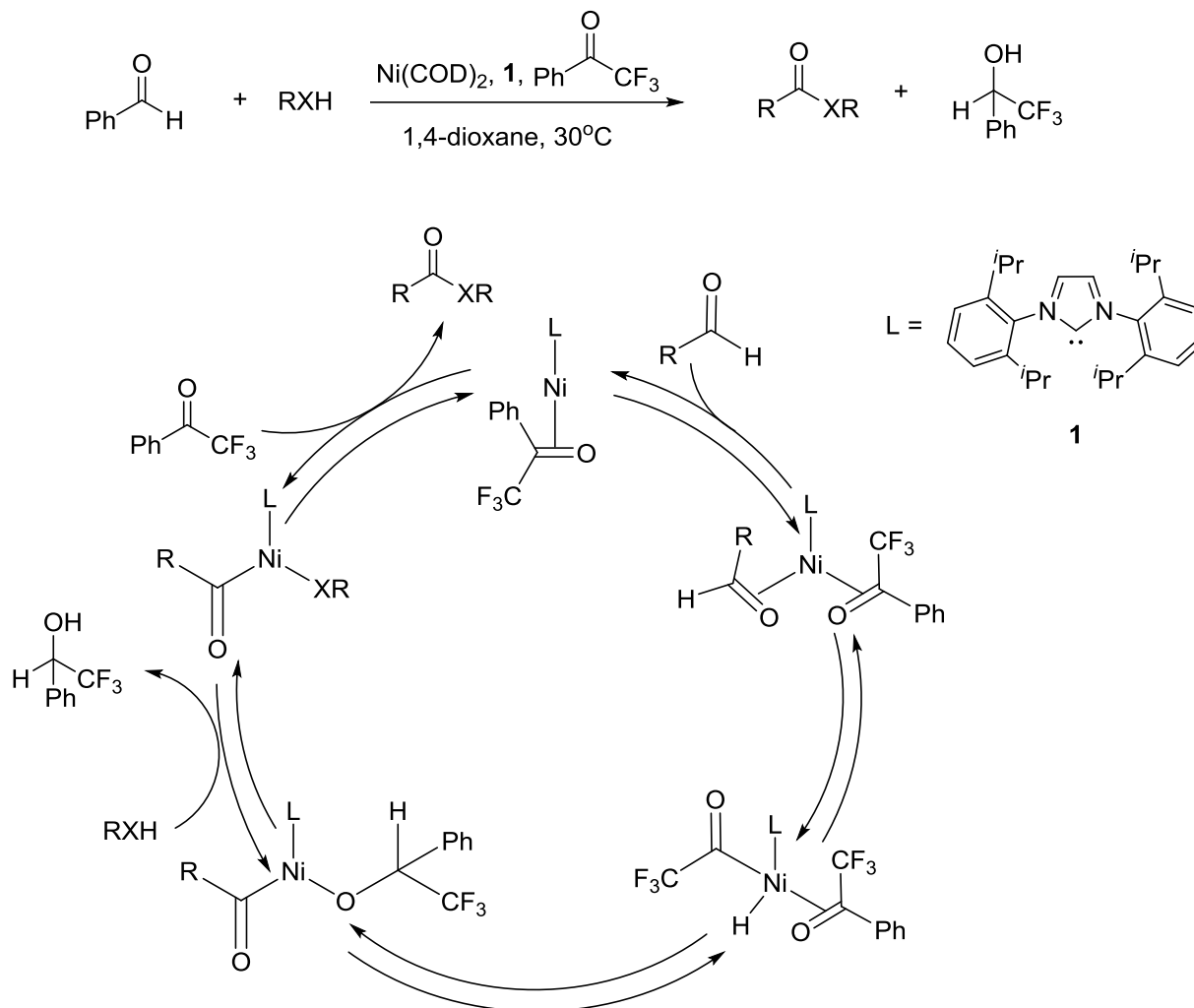
**Oxidative Esterification of Aldehydes with  
Alcohols Catalyzed by a POCOP Pincer  
Hydride Complex**

## 5.1 Introduction

Reductive processes catalyzed by nickel are of high interest to the catalysis community. Reductions of aldehydes belong to a specific subset of reductions that are useful synthetic tools for the production of alcohols. Additionally, they provide excellent models for the studies of the reduction of other carbonyl compounds.

Nickel pincer complexes have been known to catalyze a number of different transformations involving aldehydes. Two of these transformations developed by our group are the catalytic hydrosilylation and cyanomethylation reactions.<sup>1</sup> The hydrosilylation of aldehydes occurs when an aldehyde inserts into the nickel hydride complex to make a nickel alkoxide species. The nickel hydride is then regenerated with a silane to complete the catalytic cycle.<sup>1a</sup> In the case of cyanomethylation of aldehydes, an aldehyde inserts into a nickel cyanomethyl species to also generate a nickel alkoxide species.<sup>1b</sup> Here the strong  $\pi\pi$ - $d\pi$  repulsion helps to activate an acetonitrile molecule to regenerate the catalyst while releasing the cyanomethylation product. One additional reductive process of interest is the oxidative esterification of aldehydes with alcohols, where one equivalent of aldehyde serves as a hydrogen acceptor (hence a reduction process for that aldehyde).

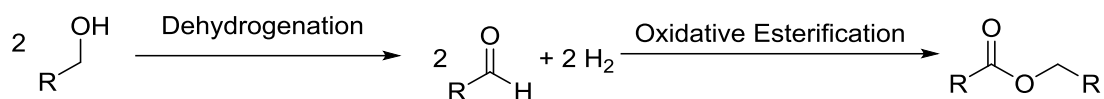




**Scheme 5.1.** Oxidative esterification of aldehydes catalyzed by Ni(COD)<sub>2</sub> and IPr (**1**)

Very few homogeneous organometallic catalysts are known for the oxidative esterification of aldehydes. Dong and co-workers used nickel (0) compounds supported by the *N*-heterocyclic carbene ligand **1** to catalyze the reaction, which was proposed to proceed via oxidative addition of an aldehyde C–H bond.<sup>2</sup> The catalytic cycle is complicated but this reaction is notable for being able to incorporate both alcohols and amines into the products (Scheme 5.1). A more recent study used actinide metals to catalyze the oxidative esterification reactions.<sup>3</sup> Another example of

oxidative esterification is in the acceptorless dehydrogenation of alcohols to form esters, in which case no aldehyde is needed as the hydrogen acceptor (Scheme 5.2).<sup>4</sup> Here after one dehydrogenation event, the aldehyde generated can undergo the oxidative esterification with its starting alcohol. The key feature of these processes is that they either use a hydrogen acceptor or generate H<sub>2</sub> directly in the process. In the former scenario, the hydrogens produced, either as free H<sub>2</sub> or as MH<sub>2</sub>, reduces the sacrificial hydrogen acceptor.



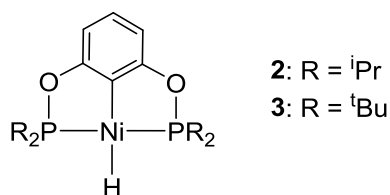
**Scheme 5.2.** General process for the acceptorless dehydrogenation of alcohols to form esters

In this chapter, the development of a new catalytic system for the oxidative esterification of aldehydes with alcohols will be described. The catalytic reactions will be optimized and the substrate scope will be studied to demonstrate the synthetic utility of this process. The mechanism will be elucidated and the decomposition products will be identified.

## 5.2 Optimization of Catalytic Oxidative Esterification of Benzaldehyde with Short-Chain Alcohols

Our group has been interested in developing reduction processes catalyzed by nickel hydride complexes. In an attempt to optimize the conditions for the catalytic hydrogenation of aldehydes to alcohols, it was discovered that in methanol, nickel hydride complex **2** could catalyze the oxidative esterification of benzaldehyde to methyl benzoate (Scheme 5.3). This process consumes two equivalents of benzaldehyde where one equivalent serves as a hydrogen acceptor while the second equivalent of benzaldehyde is formally oxidized to the ester. It should be mentioned that the disproportionation of benzaldehyde, also known as the Tishchenko reaction,

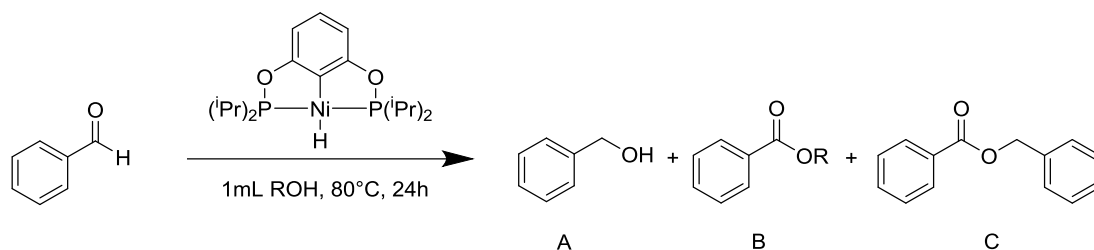
could lead to the homo-ester benzyl benzoate. In our system, the Tishchenko product is not observed in large quantities and the hetero-ester arising from benzaldehyde and methanol is the predominant ester product. The amount of benzyl alcohol generated is usually equal to the amount of methyl ester produced when the reaction goes to completion; however, when benzaldehyde is left unreacted, there is an excess of benzyl alcohol generated. This amount of surplus benzyl alcohol equals to the amount of catalyst present in the reaction. This, along with the literature precedents,<sup>1a</sup> suggests that the reduction of benzaldehyde occurs first during the reaction.



**Scheme 5.3.** Nickel hydride complexes used for the oxidative esterification of benzaldehyde and methanol

The oxidative esterification reaction (Table 5.1) proceeds at room temperature although the rate is greatly improved through mild heating (80 °C). Temperatures beyond 80 °C were not attempted due to pressure buildup concerns (methanol has a boiling point of 64.7 °C). The catalyst can be used with relatively low loadings (0.1 mol%) and can achieve high turnovers for this process (TON = 930). Additionally, the catalyst can be used under neat conditions with very little side reactions such as the Tishchenko product being formed. When a sterically more bulky nickel hydride complex **3** is employed as the catalyst, the reaction still occurs under the same conditions albeit with a much lower conversion (56%). This is possibly due to the slower initial reduction of benzaldehyde to nickel benzyloxide, as reported previously.<sup>1a</sup>

**Table 5.1.** Optimization of the oxidative esterification of benzaldehyde and short chain alcohols



Entry	Alcohol	Cat(Mol%)	Temperature	% Conversion	%A	%B	%C
1	MeOH	10	RT	65	54	46	0
2	EtOH	10	RT	20	75	25	0
3	MeOH	10	80	100	50	50	0
4	EtOH	10	80	100	50	50	0
5	MeOH	1	80	100	50	50	trace
6	EtOH	1	80	99	50	50	0
7 <sup>a</sup>	MeOH	0.1	80	93	48	48	2
8 <sup>a</sup>	MeOH	0.1	60	8	50	50	0

For all reactions 0.02 mmol catalyst was used. % conversion and product ratios are measured by <sup>1</sup>HNMR integrations of crude samples. <sup>a</sup>0.1 mol% reactions are performed neat.

The reactions were initially performed using the substrate alcohol as the solvent. An attempt was made to determine if a non-alcoholic solvent could be used for the reaction. Unfortunately, changing the solvent to common organic solvents such as THF and toluene led to limited conversion of benzaldehyde. To ensure the lack of reactivity was not due to a decrease in the polarity of the solvent, highly polar solvents such as DMSO, glyme, and diglyme were used. All solvents proved inferior to the short chain alcohols (methanol and ethanol) for these reactions

although the solvents could be ineffective due to the difficulty in removing residual water (see Section 5.6). One explanation for this is the decrease in concentration for the catalytically active nickel alkoxide species, which will be discussed in detail in the next section.

### 5.3 Reaction Profile and Mechanistic Elucidation

To further understand the details of the reaction, mechanistic studies were carried out. Our catalyst makes the oxidative esterification mechanism discussed in Scheme 5.1 unlikely so other mechanisms were considered. One possibility is a nickel-mediated Tishchenko-type reaction followed by a trans-esterification process. To discern this mechanism, a reaction profile using benzaldehyde and ethanol was examined. As demonstrated in Figure 5.1, the major pathway seems to be the direct formation of benzyl alcohol and ethyl benzoate. This suggests that the pathway involving trans-esterification of the Tishchenko product is unlikely to be operative. To further rule out the trans-esterification pathway, nickel hydride complex **2** was mixed to one equivalent of benzyl benzoate in ethanol and then heated at 80 °C for 24 h (Scheme 5.4). Under these conditions the nickel hydride does promote the trans-esterification process; however, it is an incredibly inefficient “catalyst” only converting 3% of benzyl benzoate to ethyl benzoate.

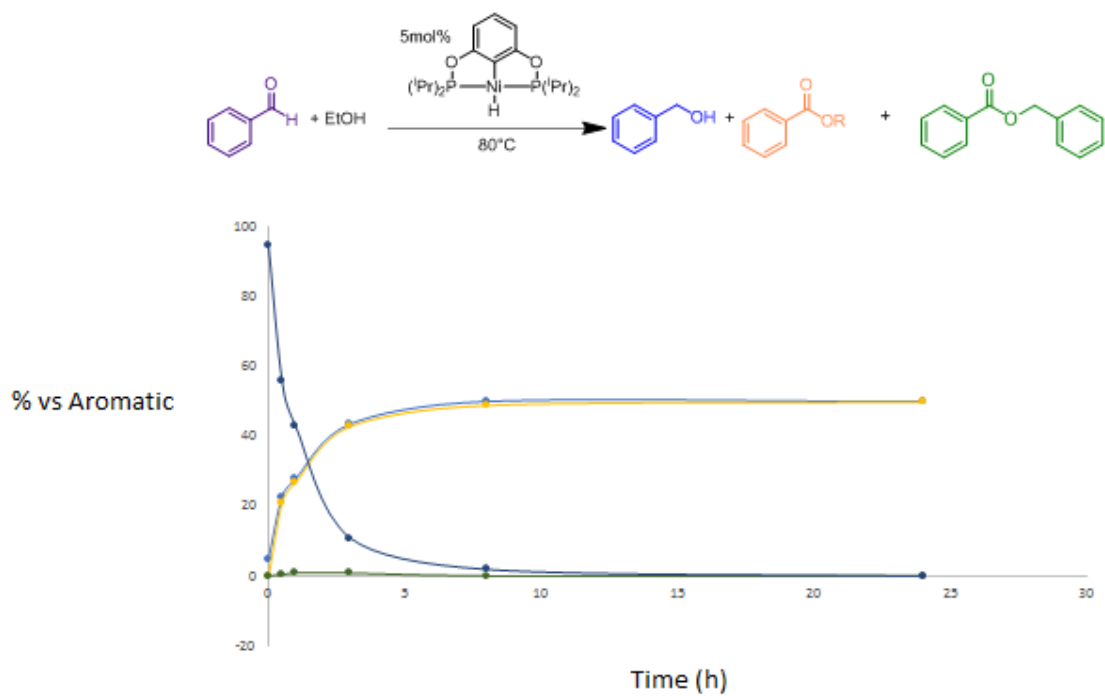
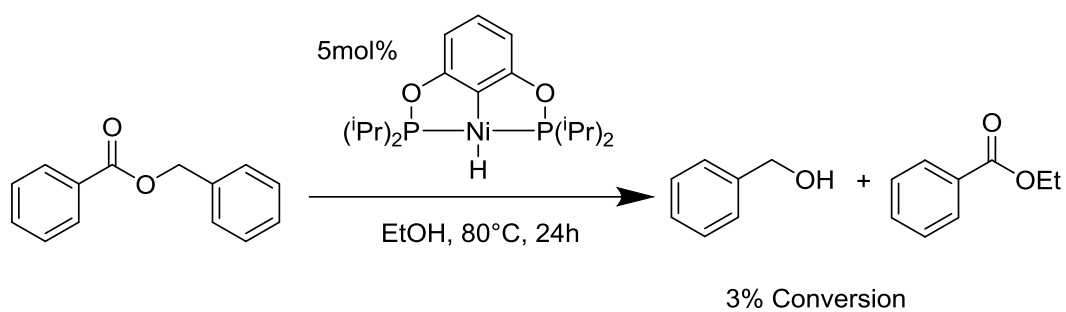


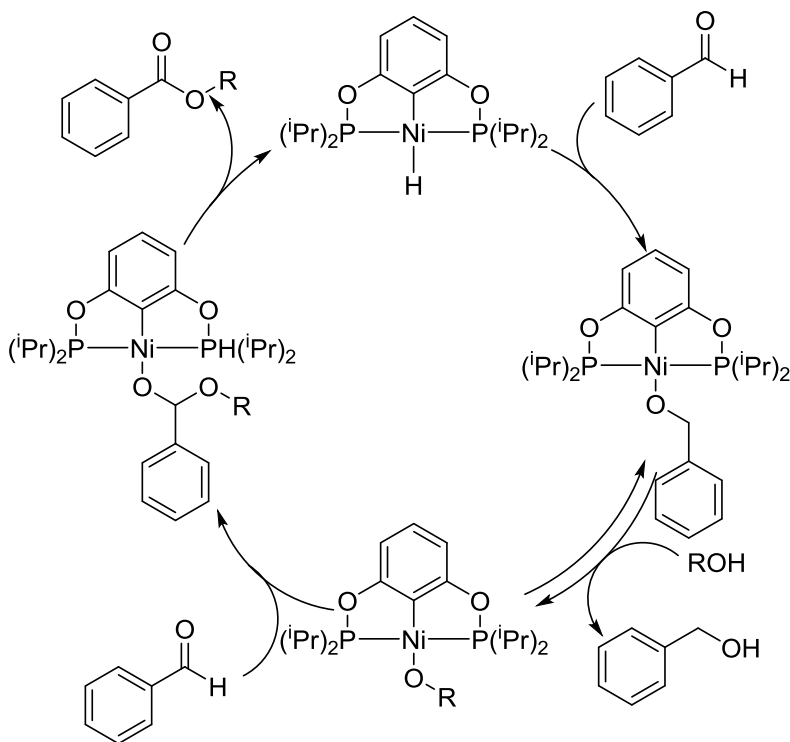
**Figure 5.1.** Reaction profile for the oxidative esterification of benzaldehyde and ethanol



**Scheme 5.4.** Trans-esterification reaction of benzyl benzoate in ethanol promoted by **2**

Having ruled out the possibility of a Tishchenko reaction followed by a trans-esterification process, we focus on the mechanism of direct oxidative esterification. Metal hydride complexes

of iridium and ruthenium are known to catalyze acceptorless dehydrogenation of primary alcohols to esters at high temperatures in open systems.<sup>4</sup> These catalysts operate by first performing a single acceptorless dehydrogenation event to form an aldehyde intermediate. The aldehyde can then disproportionate to form the homo-ester, although the mechanism for the disproportionation process is unclear. Some have suggested that it proceeds via dehydrogenation of a hemiacetal formed by reacting the alcohol with the aldehyde.<sup>5</sup> Another proposed pathway involves the insertion of the aldehyde carbonyl bond into a metal alkoxide species (Scheme 5.5). A  $\beta$ -hydride elimination event from the resulting hemiacetal provides the ester while regenerating the metal hydride. We think the latter pathway is more likely to operate here due to the reported instability of the nickel alkoxide complexes.<sup>1</sup>

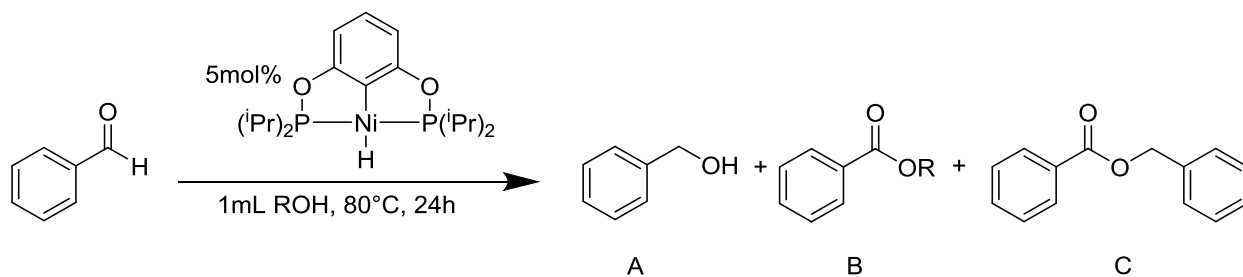


**Scheme 5.5.** Proposed catalytic cycle for the oxidative esterification of benzaldehyde with an alcohol

## 5.4 Substrate Scope

The scope of alcohols for this reaction was studied using 5 mol% of nickel hydride complex **2** as the catalyst and benzaldehyde as the aldehyde substrate. As shown in Table 5.2 (entries 1 and 2), methanol and ethanol work well with this transformation. With *n*-propanol (entry 3), the catalytic efficiency drops significantly, suggesting that the reaction is more efficient with short chain alcohols. Additionally, branched alcohols (entries 4 and 5) prove to be problematic due to the competing transfer hydrogenation pathways. A more bulky alcohol, <sup>t</sup>BuOH, completely shuts down the oxidative esterification reaction, providing only 5 mol% of PhCH<sub>2</sub>OH as a result of the initial reduction of the benzaldehyde (entry 6). This suggests the reaction pathway cannot be a simple transfer dehydrogenation of a hemiacetal that is generated in-situ. Additionally, this implies that the [Ni]O<sup>t</sup>Bu species (Scheme 5.5) is too bulky to further react with an aldehyde. Phenol also shuts down this reaction, suggesting that the phenoxide species cannot react with aldehydes either, possibly due to decreased pπ-dπ repulsion.

**Table 5.2.** Oxidative esterification of benzaldehyde and alcohols catalyzed by complex **2**





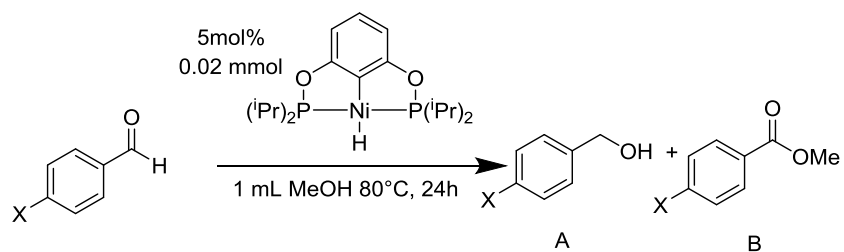
Entry	Alcohol	% Conversion	%A	%B	%C	Others
1	MeOH	100	50	50	0	0
2	EtOH	100	50	50	0	0
3	<sup>n</sup> PrOH	72	53	47	0	0
4 <sup>a</sup>	<sup>i</sup> PrOH	98	57	39	1	0
5 <sup>b</sup>	1-PhEtOH	84	81	19	0	0
6	<sup>t</sup> BuOH	5	100	0	0	0
7	PhOH	0	0	0	0	0

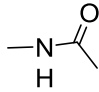
<sup>a</sup>excess benzyl alcohol from transfer hydrogenation <sup>b</sup>acceptorless dehydrogenation also present.

The scope of aldehydes for this reaction was studied with 5 mol% of nickel hydride catalyst using 1 mL of MeOH as both the solvent and the alcohol substrate. To examine the electronic effects on this reaction, benzaldehydes with varying substituents at the *para* position were chosen. Aldehydes with electron-withdrawing or electron-donating substituents are converted to the corresponding alcohols and methyl esters with 95-99% yield (Table 5.3). The dimethylamino-substituted benzaldehyde is problematic, only achieving 41% yield of the ester and the alcohol (entry 6). Also problematic is the phenol-type substrate (entry 7), which can protonate the nickel hydride species to form a catalytically inactive phenoxide species (see Section 5.6).

**Table 5.3.** Oxidative esterification of various *para*-substituted benzaldehydes with

methanol

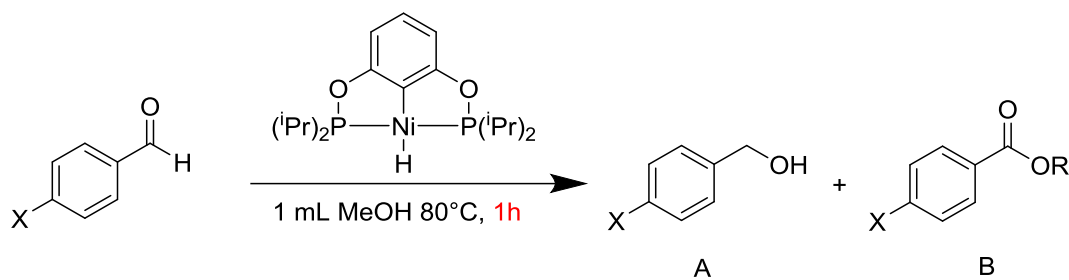


Entry	X	% Yield <sup>a</sup>	%A	%B
1	CF <sub>3</sub>	99	50	50
2	NO <sub>2</sub>	96	52	48
3	Cl	98	50	50
4	Br	95	51	49
5		97	50	50
6	NMe <sub>2</sub>	41	52	48
7	OH	5	100	0

<sup>a</sup> % Yield determined as sum of products vs a mesetylene internal standard.

To understand the electronic effects on the reaction rate, the catalytic reaction was stopped after 1 h rather than 24 h (Table 5.4). It became evident that aldehydes bearing electron-withdrawing groups reacted faster. This suggests that the turnover-determining step in this reaction is an insertion event. Because the insertion of the aldehydes is typically fast (>5 min), the slower step during the catalytic cycle must be the insertion of the aldehyde into the nickel alkoxide species.

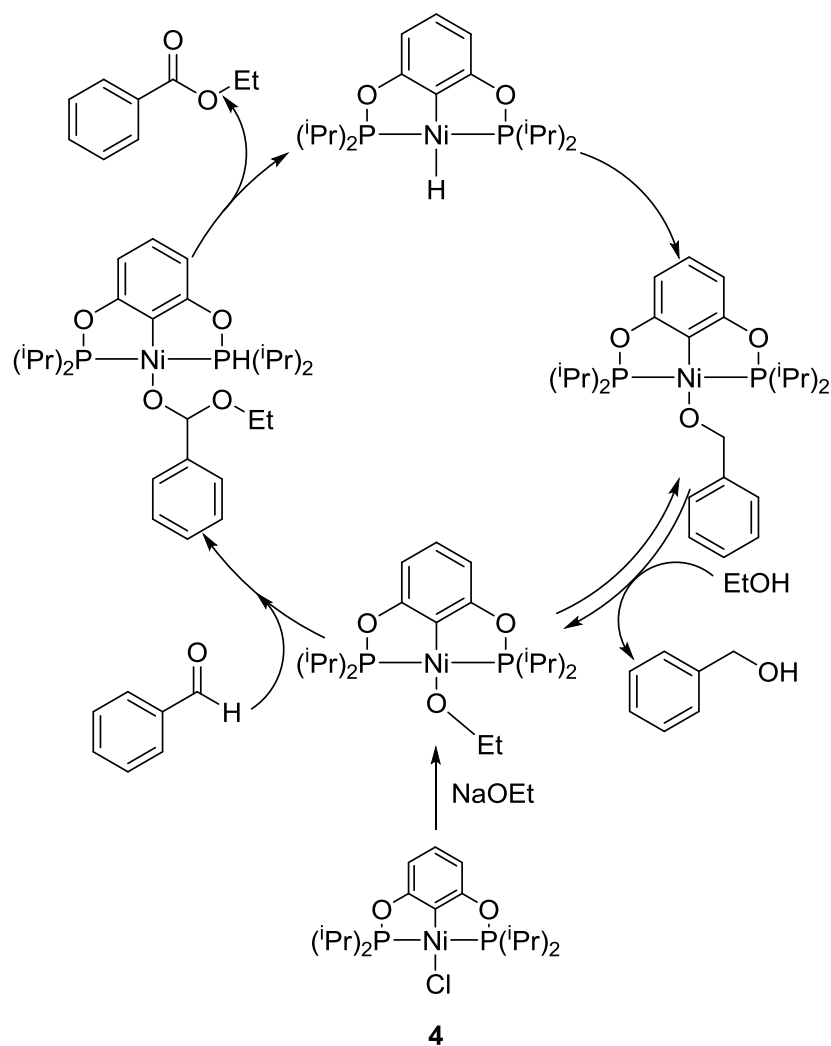
**Table 5.4** Oxidative esterification of various *para*-substituted benzaldehydes with methanol stopped at 1 h



Entry	X	% Conversion	%A	%B
1	CF <sub>3</sub>	93	50	50
2	NO <sub>2</sub>	57	55	45
3	Cl	40	58	42
4	Br	58	56	44
5		22	56	44
6	NMe <sub>2</sub>	9	70	30
7	OH	0	0	0
8	H	38	54	46

### 5.5 An Alternative Way to Enter into the Catalytic Cycle Using Nickel Chloride Complexes

The sensitivity of the starting nickel hydride complexes limits the synthetic utility. More specifically, the nickel hydrides are difficult to make and readily decompose when exposed to the air. Given these limitations, using easy-to-make and air-stable pre-catalysts would be desirable. The nickel chloride complexes that serve as the starting materials in the synthesis of nickel hydride complexes meet these requirements. Furthermore, procedures are available to convert the nickel chloride complexes to the nickel alkoxide complexes, which are the active species in the catalytic cycle.<sup>6</sup>

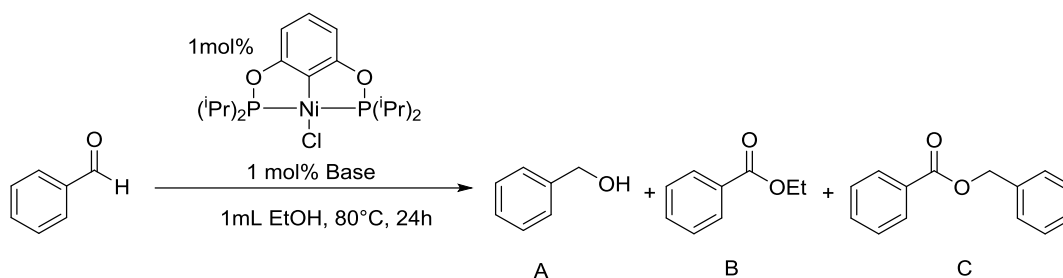


**Scheme 5.6.** Mechanism for the oxidative esterification of benzaldehyde and alcohols using pre-catalyst (**4**)

Nickel chloride complex **4** in conjunction with sodium methoxide catalyzes this reaction with no observable reduction in efficiency (Table 5.5). The reactions must be conducted under an inert atmosphere, possibly due to oxidation of nickel hydride active formed during the catalytic cycle (Scheme 5.6). When sodium hydroxide is used as the base, the reaction is almost completely shut down (8% conversion, entry 4). This can be explained by the presence of water, which proves to be detrimental to the catalytic reaction (Section 5.6). With the addition of a drying agent such

as sodium sulfate or 4 Å molecular sieves, the reaction becomes efficient, resulting in the conversion of benzaldehyde up to 95%. The study here demonstrates the possibility of using an air-stable pre-catalyst for this oxidative esterification process.

**Table 5.5** Oxidative esterification of benzaldehyde and alcohols using pre-catalyst (4)



Entry	Base	% Conversion	%A	%B	%C
1	NaOMe	99	49	49	2
2 <sup>a</sup>	NaOH	95	49	49	2
3 <sup>b</sup>	NaOH	92	47	45	13
4 <sup>c</sup>	NaOH	8	0	0	100

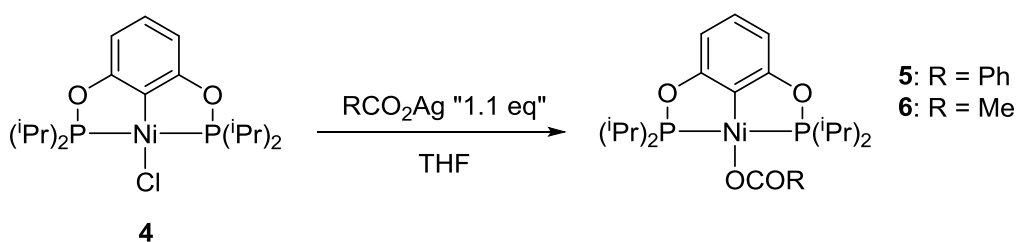
For all reactions base was added first and stirred. 0.1 mmol nickel complex and 0.1 mmol base were used. <sup>a</sup> 4Å Mol sievs used as drying agent. <sup>b</sup> Sodium sulfate used as drying agent. <sup>c</sup> No drying agent added.

## 5.6 Studies of Catalyst Decomposition Pathways

Throughout the chapter, a number of species including water, oxygen, impurity present in aldehydes, and phenols have been shown to retard the catalytic reactions. The main impurities in unpurified aldehydes are the oxidized carboxylic acids. These acids are sufficiently acidic to protonate the nickel hydride, resulting in nickel carboxylate species that are unlikely to catalyze

the oxidative esterification reactions. Water can also serve as a reagent to generate these carboxylate species. If water were to enter the catalytic cycle, the aldehyde could insert into nickel hydroxide to form a hemiacetal intermediate. Following  $\beta$ -hydride elimination, an acid is formed which in turn will protonate the hydride. Similarly, phenols could be acidic enough to protonate the hydride and form the catalytically inactive phenoxide species.

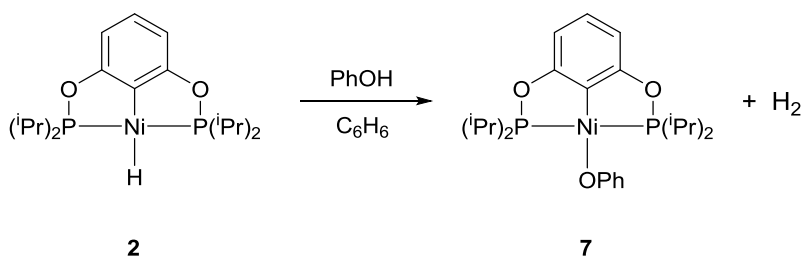
To demonstrate that these impurities were detrimental to the catalytic reaction, independent synthesis of the postulated decomposition products was pursued. Synthesis of the nickel benzoate complex proved surprisingly challenging. When benzoic acid was mixed with the nickel hydride, the desired nickel benzoate species was generated; however, large amounts of decomposition products were produced as well. These decomposition products may originate from the protonation of the oxygen atoms within the phosphinite pincer ligand. It was not possible to separate the benzoate complex from the impurities, so attention was turned to an alternative route.



**Scheme 5.7.** Synthesis of nickel carboxylate complexes from silver salts

The nickel acetate complex was chosen as a model for the synthesis of the nickel benzoate complex. Nickel acetate complex **6** was previously synthesized in our group; however, this complex was never fully characterized. This particular complex was found to be readily accessible by stirring silver acetate with the nickel chloride complex in the dark (Scheme 5.7). The resulting complex can be easily isolated and shows a characteristic  $^{31}\text{P}\{^1\text{H}\}$  NMR peak at  $\delta = 183.91$  ppm.

This synthesis is currently being extended to the nickel benzoate complex **5** with promising preliminary results. The reaction of silver benzoate and the nickel chloride complex yields a solution with an in situ  $^{31}\text{P}\{^1\text{H}\}$  NMR peak at  $\delta = 183.52$  ppm, signaling that the complex has been made. Efforts to purify this complex are currently underway. Another decomposition pathway that has been previously discussed is for the reactions with phenol-type substrates. It was previously speculated that these reactions fail to occur due to the protonation of the nickel hydride by the phenol to create a nickel phenoxide complex. The nickel phenoxide complex synthesis was attempted through the addition of phenol to the nickel hydride complex dissolved in benzene (Scheme 5.8). The reaction mixture immediately evolves gas and changes the color from pale yellow to red orange in <10 min. The resulting complex shows a characteristic peak of  $\delta = 179.72$  ppm in the  $^{31}\text{P}\{^1\text{H}\}$  NMR spectrum. Full characterization of this complex is currently underway.

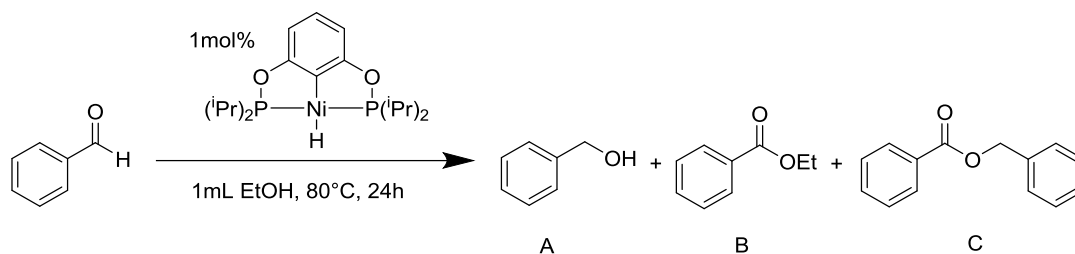


**Scheme 5.8.** Reaction of nickel hydride complex **2** with phenol

To demonstrate that the formation of the aforementioned complexes was detrimental to the oxidative esterification reaction, control experiments were performed using additives to accelerate catalyst deactivation (Table 5.6). When adding water directly to the reaction mixture, the reaction is limited to only 11% conversion of starting material with Tishchenko product being observed. Additionally, benzoic acid is observed from the product mixture. When benzoic acid is added

directly to the reaction, the conversion is limited to 11% and only the Tishchenko product is observed (entry 3). This suggests that benzoic acid not only deactivates the catalyst by shutting down the oxidative esterification cycle, but also forms decomposition products that catalyze the Tishchenko reaction. To further test this hypothesis, the nickel acetate complex was employed under the catalytic conditions for oxidative esterification (Scheme 5.9). Only the Tishchenko process was observed with 8% of benzaldehyde being converted. When nickel benzoate complex is fully characterized, it will be tested for these reactions.

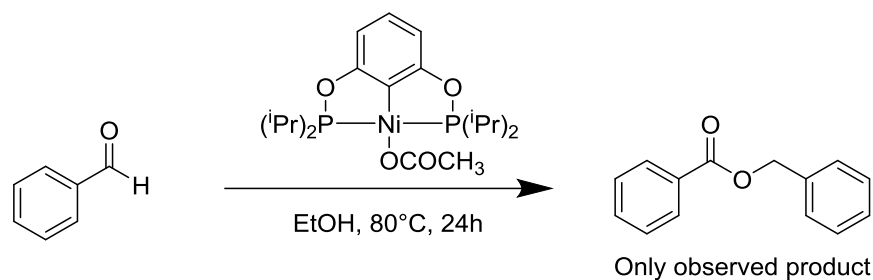
**Table 5.6.** Catalyst deactivation through the addition of common substrate impurities



	Solvent	% Conversion	%A	%B	%C	Others
1	EtOH	100	50	50	0	
2 <sup>a</sup>	Wet EtOH	11	50	48	2	<chem>c1ccccc1C(=O)O</chem>
3 <sup>b</sup>	EtOH	11	0	0	100	0

<sup>a</sup> 100 eq H<sub>2</sub>O added to reaction. <sup>b</sup> benzoic acid added directly to solution.





**Scheme 5.9.** Catalytic reaction using complex **6**

## 5.7 Conclusions

In conclusion, a new catalytic system for the oxidative esterification of aldehydes with alcohols has been developed. The catalytic system is compatible with various short chain alcohols for the synthesis of aryl esters. During the catalytic cycle, one equivalent of aldehyde is consumed as a sacrificial hydrogen acceptor. The mechanism appears to be different from those proposed for the previously reported oxidative esterification reactions; however, it does have several commonly proposed steps leading to the dehydrogenation of alcohols to homoesters. Several decomposition pathways have also been identified and the isolation of each decomposition product is currently underway.

## 5.8 Experimental Section

**Materials and Methods.** Unless otherwise mentioned, all the organometallic compounds were prepared and handled under an argon atmosphere using Schlenk and glovebox techniques. Dry and oxygen-free solvents (THF and toluene) were collected from an Innovative Technology solvent purification system. All alcohols were dried, distilled and stored over 4Å molecular sieves. All aldehydes were dried and distilled or recrystallized according to the appropriate literature

procedures.<sup>7</sup> Nickel chloride and hydride complexes were prepared according to the literature procedures.<sup>1a</sup>  $^1\text{H}$ ,  $^{13}\text{C}\{^1\text{H}\}$  and  $^{31}\text{P}\{^1\text{H}\}$  NMR spectra were recorded on a Bruker Avance-400 MHz spectrometer. Chemical shifts in NMR were referenced to residual solvents or TMS (0 ppm) present in  $\text{CDCl}_3$ .  $^{31}\text{P}\{^1\text{H}\}$  NMR spectrum were referenced externally to 85%  $\text{H}_3\text{PO}_4$  (0 ppm).

**General Procedure for Catalytic Oxidative Esterification of Benzaldehyde with Alcohols.** To a flame-dried 5 dram scintillation vial equipped with a stir bar, 1 mL of alcohol and aldehyde (2 mmol) were added. Nickel hydride complex (0.02 mmol, 1 mol% loading) was then added and the vial was capped and wrapped with parafilm to ensure it was sealed. The vial was then placed in an 80 °C oil bath and heated at this temperature. After a given period of time, the vial was removed from the oil bath and cooled to room temperature in a water bath. Mesitylene was then added as an internal standard. A aliquot of the reaction mixture was withdrawn and diluted in  $\text{CDCl}_3$  for NMR analysis. The reaction mixture was concentrated under vacuum and the crude ester product was purified by flash column chromatography (eluted by hexanes/ethyl acetate = 9 : 1).

**Synthesis of  $[2,6-(^i\text{Pr}_2\text{PO})_2\text{C}_6\text{H}_3]\text{NiOCOCH}_3$  (6).** To a solution of  $[2,6-(^i\text{Pr}_2\text{PO})_2\text{C}_6\text{H}_3]\text{NiCl}$  (0.100 g, 0.23 mmol) in 25mL of THF was added silver acetate (0.042 g, 0.27 mmol). The suspension was stirred under dark conditions for 6 h. The reaction mixture was then filtered through a short plug of Celite and the collected solution was evaporated to dryness. The resulting solid was washed with cold methanol (0 °C) and dried to yield an orange powder (0.051 g, 48% yield, NE590). X-ray quality crystals were grown from slow evaporation of a THF solution.

**Synthesis of  $[2,6-(^i\text{Pr}_2\text{PO})_2\text{C}_6\text{H}_3]\text{NiOCOPh}$  (5).** To a solution of  $[2,6-(^i\text{Pr}_2\text{PO})_2\text{C}_6\text{H}_3]\text{NiCl}$  (0.100 g, 0.23 mmol) in 25mL of THF was added silver benzoate (0.062 g, 0.27 mmol). The suspension was stirred under dark conditions for 6 h. The reaction mixture was then filtered through a short

plug of Celite and the collected solution was evaporated to dryness. The resulting solid was washed with *n*-pentane and dried to yield an orange powder (0.043 g, 36% yield, NE586). X-ray quality crystals were grown from slow evaporation of a concentrated solution in THF.

**Synthesis of [2,6-(*i*Pr<sub>2</sub>PO)<sub>2</sub>C<sub>6</sub>H<sub>3</sub>]NiOPh (7).** To a solution of [2,6-(*i*Pr<sub>2</sub>PO)<sub>2</sub>C<sub>6</sub>H<sub>3</sub>]NiH (0.050 g, 0.12 mmol) in 25mL of benzene was added phenol (0.012 g, 0.13 mmol). The pale-yellow solution immediately changed the color to orange, accompanied by a rapid gas evolution. The solution was then evaporated to dryness to yield an orange powder (0.022 g, 37% yield, NE583). X-ray quality crystals were grown from slow evaporation of a benzene solution.

## 5.9 References Cited

1. (a) Chakraborty, S.; Krause, J. A.; Guan, H., Hydrosilylation of Aldehydes and Ketones Catalyzed by Nickel PCP-Pincer Hydride Complexes. *Organometallics* **2009**, *28* (2), 582-586; (b) Chakraborty, S.; Patel, Y. J.; Krause, J. A.; Guan, H., A Robust Nickel Catalyst for Cyanomethylation of Aldehydes: Activation of Acetonitrile under Base-Free Conditions. *Angewandte Chemie International Edition* **2013**, *52* (29), 7523-7526.
2. Whittaker, A. M.; Dong, V. M., Nickel-Catalyzed Dehydrogenative Cross-Coupling: Direct Transformation of Aldehydes into Esters and Amides. *Angewandte Chemie International Edition* **2015**, *54* (4), 1312-1315.
3. Liu, H.; Eisen, M. S., Selective Actinide-Catalyzed Tandem Proton-Transfer Esterification of Aldehydes with Alcohols for the Production of Asymmetric Esters. *Organometallics* **2017**, *36* (8), 1461-1464.
4. Gunanathan, C.; Milstein, D., Applications of Acceptorless Dehydrogenation and Related Transformations in Chemical Synthesis. *Science* **2013**, *341* (6143) 1229712.
5. Nguyen, D. H.; Trivelli, X.; Capet, F.; Paul, J.-F.; Dumeignil, F.; Gauvin, R. M., Manganese Pincer Complexes for the Base-Free, Acceptorless Dehydrogenative Coupling of Alcohols to Esters: Development, Scope, and Understanding. *ACS Catalysis* **2017**, *7* (3), 2022-2032.
6. (a) Adhikary, A.; Krause, J. A.; Guan, H., Configurational Stability and Stereochemistry of P-Stereogenic Nickel POCOP-Pincer Complexes. *Organometallics* **2015**, *34* (14), 3603-3610; (b) Hao, J.; Vabre, B.; Zargarian, D., Reactions of Phenylhydrosilanes with Pincer-Nickel Complexes: Evidence for New Si-O and Si-C Bond Formation Pathways. *Journal of the American Chemical Society* **2015**, *137* (48), 15287-15298.
7. Armarego, W. L. F.; Chai, C. L. L., Chapter 4 - Purification of Organic Chemicals. In *Purification of Laboratory Chemicals (Sixth Edition)*, Butterworth-Heinemann: Oxford, 2009; pp 88-444.